Quantitative Model of Calcium/Calmodulin-Dependent Protein Kinase II Activation

Thesis by

Stefan Mihalas

California Institute of Technology

In Partial Fulfillment of the Requirements

for the Degree of

Doctor of Philosophy

California Institute of Technology

Pasadena, California, 91125

2006

(Defended May 24, 2006)

Doresc să dedic acestă teză faimilei mele: soţiei Anca, tatalui Gheorghe Ioan, mamei Georgeta si sorei Minodora. Dragostea voastră necondiţionată şi suportul vostru permanent m-au ajutat să ajung aici.

Acknowledgements

I am very very grateful to Dr. Mary B. Kennedy for her constant advisement, and her incredible persistence for biological realism, a trait which, I believe, was passed to all the members of the lab.

I am also very grateful to the members of my committee: Dr. Jerome Pine, Dr. Erik Winfree and Dr. Kip Thorne for their continuous support, their feedback on the research and the thesis.

I would like to thank all the members of the Kennedy lab, including Mee Choi, Tamara Ursem, Holly Beale, Eduardo Marcora, William Ford for the research-related discussions, reading and providing feedback for the thesis, technical support and providing a great working environment.

I would also like to thank my previous advisers and mentors, whom all shaped who I am today: Dr. James Bower, Dr. Ion Cotăescu, Dr. Dan Papuc, Dr. Doekele Stavenga, Prof. Rodica Bratu, Prof. Ioan Nedin, Dr. Sandu Golcea and Dr. Gheorghe Mihalaş. Thank you all for opening the window to science for me. I learned so many things from you all.

Abstract

Calcium/calmodulin-dependent protein kinase II (CaMKII) is a key element in the Ca^{2+} second messenger cascades that lead to long term potentiation (LTP) of synaptic strength. In this thesis, I have constructed kinetic models of activation of CaMKII and measured some of the unknown parameters of the model. I used the models to elucidate mechanisms of activation of CaMKII and to study the kinetics of its activation under conditions similar to those in dendritic spines.

In chapter 2, I developed a new experimental method to rapidly stop the autophosphorylation reaction. I used this method to measure the catalytic turnover number of CaMKII. To quantitatively characterize CaMKII atophosphorylation in nonsaturating Ca^{2+}, I also measured the autophosphorylation turnover number when CaMKII is activated by calmodulin mutants that can bind Ca^{2+} only in either the amino or the carboxyl lobes.

Previous models of CaMKII activation assumed that binding of calmodulins to individual CaMKII subunits is independent and that autophosphorylation occurs within a ring of 6 subunits. However, a recent structure of CaMKII suggests that pairs of subunits cooperate in binding calmodulin and raises the possibility that the autophosphorylation occurs within pairs of subunits. In chapter 3, I constructed a model in which CaMKII subunits cooperate in binding calmodulin. This model reconciled previous experimental results from the literature that appeared contradictory. In chapter 4, I constructed two models for CaMKII autophosphorylation, in which autophosphorylation can occur either in rings or pairs, and used them to design experiments aimed at differentiating between these possibilities. Previously published measurements and the measurements that I performed are more consistent

with autophosphorylation occurring within pairs.

In chapter 5, I constructed a model for simultaneous interactions among Ca^{2+}, calmodulin, and CaMKII, and I used an automatic parameter search algorithm to fit the parameters for this model. I used it to characterize which of the parameters of Ca^{2+} transients are critical for CaMKII activation.

This modeling work is part of a continuing effort to realistically model the spatial and temporal aspects of Ca^{2+} second messenger signaling in dendritic spines.

Contents

Chapter 1

Background

1.1 Neurons

The human central nervous system contains approximately 10^{11} neurons. In resting conditions, neurons have a negative membrane potential. When depolarized, if the depolarization reaches a threshold, the neuron continues to depolarize rapidly, and then returns to the resting membrane potential, a process which generates an action potential. Each neuron connects to a large number of other neurons via specialized structures called synapses. Most of the synapses are chemical and unidirectional. Synaptic strength is defined as the maximal current that enters the postsynaptic neuron when the presynaptic neuron fires an action potential. The synaptic strength is plastic and its change depends on past activity of the neurons. The change in synaptic strength as a result of neuronal activity has been hypothesized to be an underlying mechanism of memory formation.

1.2 Synapses

The hypothesis of functionally plastic synapses was first formulated by Hebb (1949) in his book The Organization of Behavior. Hebb proposed that a synapse becomes stronger if the firing of the presynaptic neuron contributes to the firing of the postsynaptic neuron. Long term potentiation (LTP) of synaptic strengths following electrical stimulation has been observed in many cortical areas and under several

stimulation protocols (Bliss and Lomo, 1973). To maintain a balance in neuronal activity, an opposite effect is necessary: long term depression (LTD) of synaptic strengths. LTD has been observed, and the stimulation protocols leading to LTD are qualitatively similar to those creating LTP. LTP is observed following high frequency (100 Hz) stimulation of afferent pathways while LTD is observed following low frequency (1 Hz) stimulation. More recently it has been observed that the exact timing of the firing of the pre- and postsynaptic neurons plays a role in synaptic plasticity. If the postsynaptic neuron fires immediately following the presynaptic neuron, in a time window similar to that required for the presynaptic neuron to contribute to the firing of the postsynaptic neuron, the synaptic strength is increased. If the postsynaptic neuron fires before the presynaptic neuron, the synaptic strength is decreased. This spike timing dependent plasticity (STDP) has been observed in neuronal cultures from cortex (Markram et al., 1997) and hippocampus (Bi and Poo, 1998).

Chemical synapses can be classified as excitatory, if the firing of the presynaptic neuron leads to depolarization of the postsynaptic neuron, and inhibitory, if the firing of the presynaptic neuron leads to either hyperpolarization or no depolarization coupled with a decrease in membrane resistance. In vertebrates, typical neurotransmitters used in excitatory synapses are glutamate (Glu) and acetylcholine (ACh). Inhibitory synapses of vertebrates use γ-aminobutiric acid (GABA) and glycine (Gly). In mammals, glutamate and GABA are used mainly in the central nervous system, while acetylcholine and glycine are used mainly in the peripheral nervous system (Shepherd, 1998, chapter 2). Each neuron receives both excitatory and inhibitory inputs; however, it typically has one type of excitatory or inhibitory neurotransmitter as output as well as a peptide or a biogenic amine cotransmitter with a modulatory role. Consequently, the neurons can be classified by the neurotransmitter they use in the output synapses. However, the neuronal populations using the same neurotransmitter are heterogeneous. One of the most prevalent and well-studied neuronal types found in cerebral cortex and hippocampus is the pyramidal neuron.

Pyramidal neurons are excitatory glutamatergic neurons which have a pyramidal-

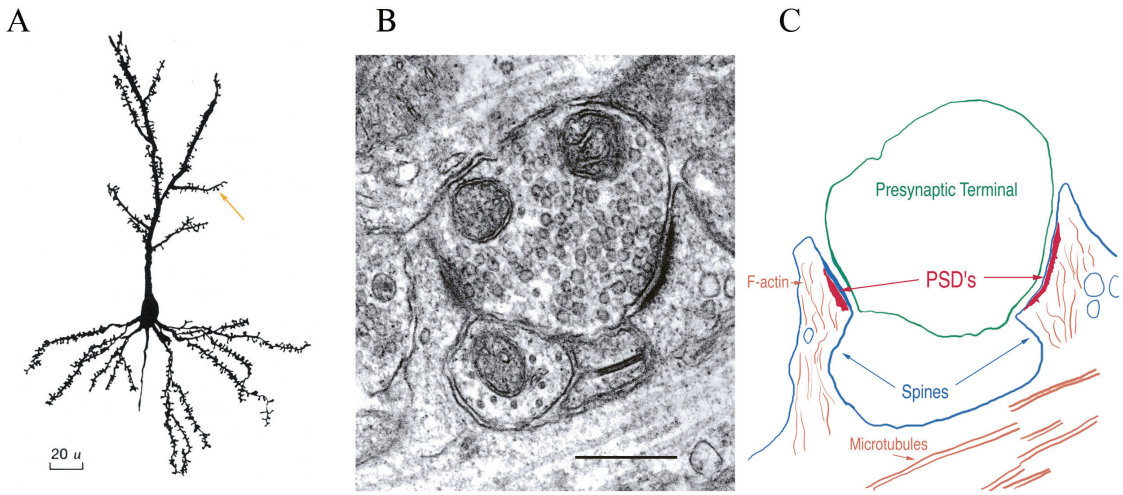

Figure 1.1. Spine Structure: **A** A Pyramidal neuron with arrows pointing at dendritic spines. **B** Electron micrograph of a presynaptic bouton forming synapses with two dendritic spines. The scale bar is 400 nm. **C** Tracing of B annotating the major synaptic structures. Reproduced from (Kennedy, 2000).

shaped cell body (soma). Pyramidal neurons form and receive, on average, 10^4 synapses. While the average number of synapses may differ from region to region it is estimated that pyramidal neurons from hippocampal area CA3 form 30,000−60,000 synapses in the ipsilateral CA1 hippocampus (Li et al., 1994). For a given neuron, the output synapses arise from one axon, while the input synapses are made onto several dendrites and onto the soma (figure 1.1, A).

1.3 Synaptic Transmission

Most excitatory synapses comprise three specialized structures: a presynaptic bouton and a postsynaptic spine separated by a thin synaptic cleft (figure 1.1, B and C). Arrival of an action potential at the presynaptic bouton opens up voltage gated calcium channels (VGCC). The subsequent rise in $[Ca^{2+}]$ initiates a Ca^{2+}-mediated biochemical cascade that leads to fusion of vesicles containing glutamate with the cell membrane. Most of the fusion events happen in a region called the active zone. Across from the active zone there is a proteinaceous thickening of the postsynaptic membrane called the postsynaptic density (PSD). The postsynaptic density consists

of a large number of protein types that form the signal transduction machinery for synaptic plasticity (Kennedy, 2000).

After glutamate is released into the synaptic cleft, it rapidly diffuses and binds to receptors found in the postsynaptic membrane. In the postsynaptic membrane there are 3 types of glutamate receptors: α-amino- 3-hydroxy- 5-methyl-4-isoxazolepropionic acid-type receptors (AMPARs), N-methyl-D-aspartic acid-type receptors (NMDARs) and G-protein coupled receptors. AMPARs and NMDARs are ligand-gated ion channels also called ionotropic receptors, whereas the G-protein coupled receptors are metabotropic receptors (mGluRs). Upon glutamate binding, AMPARs open and allow Na^+ influx which leads to a local depolarization of the postsynaptic membrane. AMPAR channels are responsible for most episodes of depolarization of the postsynaptic membrane, while NMDARs and mGluRs have mainly a modulatory role.

The depolarization of the postsynaptic neuron caused by release of glutamate from a presynaptic neuron is called the excitatory postsynaptic potential (EPSP). For a pyramidal neuron a large number of EPSPs are necessary to change the membrane potential from resting to the threshold for firing an action potential. The time required for transmission of an electrical signal from a pre- to a postsynaptic neuron is about 1 ms. This includes the time delays caused by Ca^{2+} cascades in the presynaptic bouton leading to vesicle fusion, glutamate diffusion across the cleft, glutamate binding to AMPARs and opening of the AMPARs after glutamate binding. The unbinding of glutamate and closing of the AMPARs occur on a time scale of 1 ms as well. The observed time for decay of EPSPs is $\sim$10 ms. The slow decay time is a consequence of the capacitive effects of the cellular membrane.

After its release into the synaptic cleft, glutamate binds to NMDARs as well. When the postsynaptic membrane is at resting potential the pore of the NMDA channel is almost completely blocked by the presence of a Mg^{2+} ion. When the postsynaptic membrane is depolarized the Mg^{2+} blocking the pore is removed leading to a more than 10 fold increase in conductance of an open NMDA channel (Nowak et al., 1984; Mayer et al., 1984; Ascher and Nowak, 1988). The NMDA channel

is permeable to both Na^+ and Ca^{2+}. Firing of the presynaptic neuron when the postsynaptic one remains near resting potential leads to a small Ca^{2+} influx through NMDAR. However, if the postsynaptic neuron depolarizes before glutamate unbinds from the NMDAR, the Ca^{2+} influx through the NMDAR is considerably larger. The unbinding of glutamate occurs on a time scale of ∼100 ms (Lester and Jahr, 1992).

Metabotropic glutamate receptors are found on the periphery of the postsynaptic density, in a gradient, decreasing towards the spine neck (Nusser et al., 1994). MGluRs have mainly a modulatory role. They contribute to the intracellular Ca^{2+} signaling via the inositol-1,3,4-trisphosphate (IP3) secondary messenger cascade. IP3 opens specific Ca^{2+} channels in the endoplasmic reticulum, a closed, tubular network of internal membranes. Electron microscopy studies show that approximately 50% of the dendritic spines on CA1 hippocampal pyramidal neurons contain extensions of endoplasmic reticulum called spine apparatus (Spacek and Harris, 1997). The probability of a spine having a spine apparatus is well correlated with the spine size. The apparatus is present in 80% of large mushroom-type spines and only in 20% of small thin spines (Harris, 1999). This suggests slightly different mechanisms for Ca^{2+} handling in different spine types. The physiological consequences of these differences have not yet been explored.

1.4 Calcium

Action potentials (APs) are usually initiated in the soma, near the axon hillock, and actively travel along the axon. Action potentials also backpropagate into the dendritic tree, depolarizing the membrane and opening voltage gated calcium channels (VGCC). Voltage gated calcium channels can be classified as high voltage activated (Vm > -30 mV) and low voltage activated (Vm > -70mv). The high voltage activated VGCC can be further classified as persistent (L-type) and inactivating (P/Q-, N- and R-type) channels. Persistent Ca^{2+} channels do not fully deactivate when the membrane potential is maintained depolarized. L-type VGCCs deactivate rapidly when the membrane potential returns to the resting value, so they are tuned

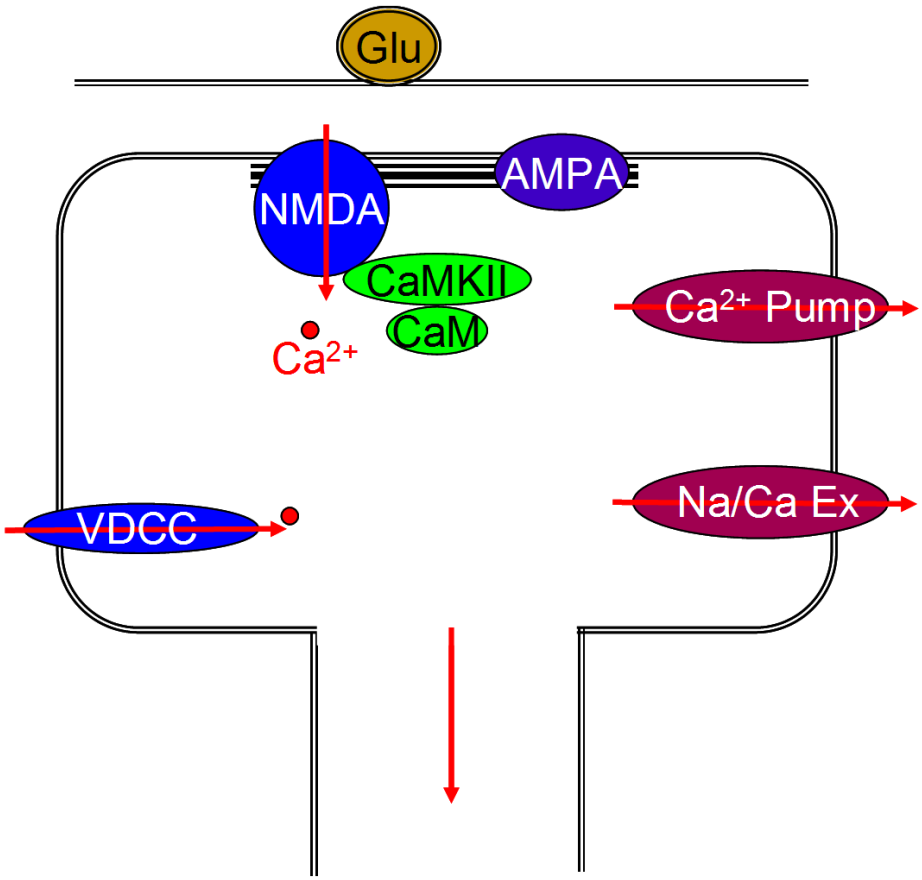

Figure 1.2. Ca^{2+} dynamics: Mechanisms for Ca^{2+} entry into, and extrusion from, spines. The main sources for Ca^{2+} influx are NMDAR and VGCC while the main extrusion mechanisms are Ca^{2+} pumps and Na^{+}/Ca^{2+} exchangers.

to respond to long depolarizations, while P/Q-, N- and R-type VGCCs deactivate slowly, so they are tuned to respond to short depolarizations (Tsien et al., 1988; Hille, 2001, Table 4.1). Dendritic spines have L- and R-type VGCC, however the L-type channels do not contribute significantly to the rise in $[Ca^{2+}]$ following an AP (Sabatini et al., 2002).

Proteins governing the dynamics of Ca^{2+} entry into, and extrusion from, spines are diagrammed in figure 1.2. After entry into the cytoplasm Ca^{2+} ions are quickly buffered by binding to a variety of proteins. The buffering process can be characterized by buffering capacity (κ_B): the ratio of total Ca^{2+} to free Ca^{2+}. The Ca^{2+} buffering capacity in the soma and proximal dendrites is 100 while in more distal dendrites and dendritic spines it has been estimated as 20 (Sabatini et al., 2002). Ca^{2+}

leaves the spine by diffusion through the spine neck and by extrusion through Ca^{2+} pumps and Na^{+}/Ca^{2+} exchangers. Free Ca^{2+} diffuses quite rapidly in the cytoplasm ($D = 0.22\mu m^2/ms$); however, due to buffering and tortuosity, the diffusion is slowed considerably (Klingauf and Neher, 1997).

By analyzing the correlations in the fluctuations of $[Ca^{2+}]$ in spines and parent dendrites, Sabatini et al. concluded that diffusion through the spine neck contributes little to Ca^{2+} extrusion from the spines.

The typical time constant for extrusion of Ca^{2+} from spines is ∼10ms (Sabatini et al., 2002). The openings of VGCCs resulting from a backpropagating action potential produces a short Ca^{2+} influx. This was assumed by Sabatini et al. to be shorter than the time scale of the extrusion mechanisms and approximated to be a δ function. These authors measured the change in $[Ca^{2+}]$ in a spine in response to a backpropagating action potential. Subsequently, they measured both the change in $[Ca^{2+}]$ resulting from a longer Ca^{2+} influx, and the Ca^{2+} current through NMDA channels. They concluded that physiological Ca^{2+} transients (e.g., NMDAR activation or generated by backpropagating action potentials) do not saturate the extrusion mechanisms. The extruded flux of Ca^{2+} increases almost linearly in response to a rise in $[Ca^{2+}]$ in spines. Consequently, $[Ca^{2+}]$ in spines produced by longer Ca^{2+} influxes can be calculated as the convolution of the current influx with a convolution kernel derived from the measurements of $[Ca^{2+}]$ produced by a backpropagating action potential.

$$[Ca^{2+}](t) = [Ca^{2+}]_{rest} + \int_{-\infty}^{t} \alpha e^{-\frac{t-t_1}{\tau}} J(t_1) dt_1 \tag{1.1}$$

- $[Ca^{2+}]_{rest}$ − resting Ca^{2+} concentration
- α − a constant which is different for different spines
- $e^{-\frac{t-t_1}{\tau}}$ − convolution kernel
- τ − a constant (time constant of extrusion mechanisms) which is similar for most spines

- $J(t)$ – Ca^{2+} influx in the spine at time t

This method provides a simple way to calculate the time dependence of the Ca^{2+} concentration in spines during physiologically realistic conditions. I used this method in chapter 5 to find the calcium dependence on time for which the calmodulin/CaMKII models have to be precise.

1.5 Calmodulin

Most of the Ca^{2+} signaling machinery is highly conserved across species. Calmodulin (CaM) is a ubiquitous Ca^{2+} binding protein which plays an important role in many Ca^{2+} messenger cascades (Cohen and Klee, 1988). Calmodulin has 4 Ca^{2+} binding sites situated in helix-loop-helix regions called EF hands (figure 1.3). Two of the Ca^{2+} binding sites are near the amino and two Ca^{2+} binding sites are near the carboxyl terminus.

The affinities of the four Ca^{2+} binding sites range over one order of magnitude. Consequently, it is difficult to deconvolve the simultaneous binding of four Ca^{2+} ions to the Ca^{2+} binding sites. To study the functional roles of the individual Ca^{2+} binding sites, some previous investigators have used tryptic fragments of calmodulin comprising either the N- or the C-terminal half (Linse et al., 1991) or point mutations that render some of the Ca^{2+} binding sites unable to bind Ca^{2+} (DeMaria et al., 2001).

Studies of calmodulin tryptic fragments have shown that each pair of binding sites cooperates in binding of Ca^{2+}, however, there is little cooperativity between pairs (Linse et al., 1991). Ca^{2+} binding to calmodulin is influenced by the presence of Mg^{2+} and by the ionic strength. Under physiological conditions, the two Ca^{2+} binding sites near the carboxyl terminus have higher affinity but slightly slower on rates than the sites near the amino terminus. For short (<1 ms) Ca^{2+} transients most of the Ca^{2+} ions bind to the sites near the amino terminus, while for longer (>100 ms) Ca^{2+} transients most of the Ca^{2+} ions bind to the sites near the carboxyl terminus of calmodulin. Physiological Ca^{2+} transients, which have time scales of 10 ms – 1 s, lead to a complex time dependence of calmodulin with Ca^{2+} bound to different sites

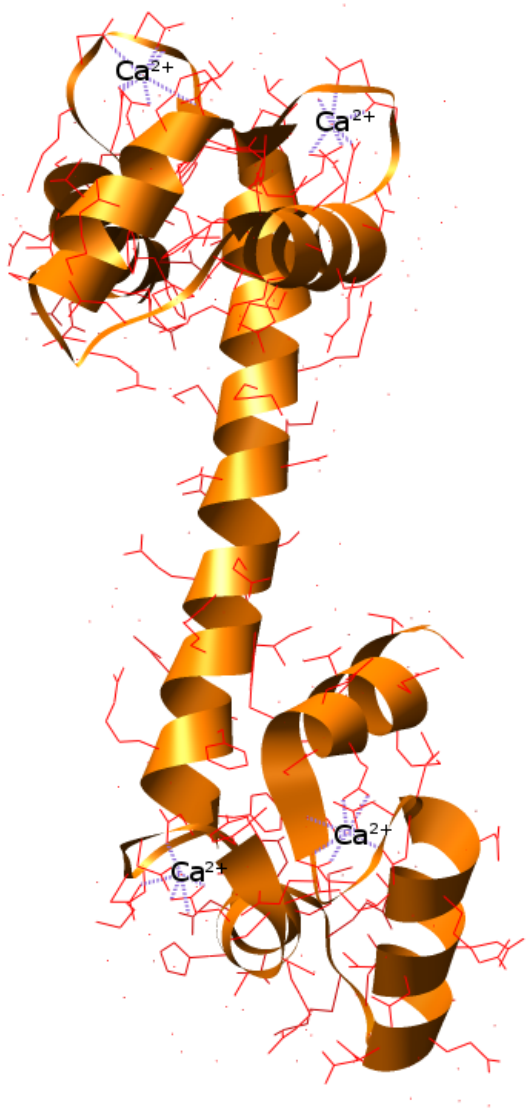

Figure 1.3. Calmodulin Structure: A 1.7$\mathring{A}$ crystal structure of calmodulin rendered from PDB 1CLL (Chattopadhyaya et al., 1992). Calmodulin's structure consists of two globular domains (lobe) connected by an α-helix. One lobe is near the amino terminus (upper) while the other lobe is near the carboxyl terminus. Each lobe has two Ca^{2+} binding sites on helix-loop-helix regions (EF hands).

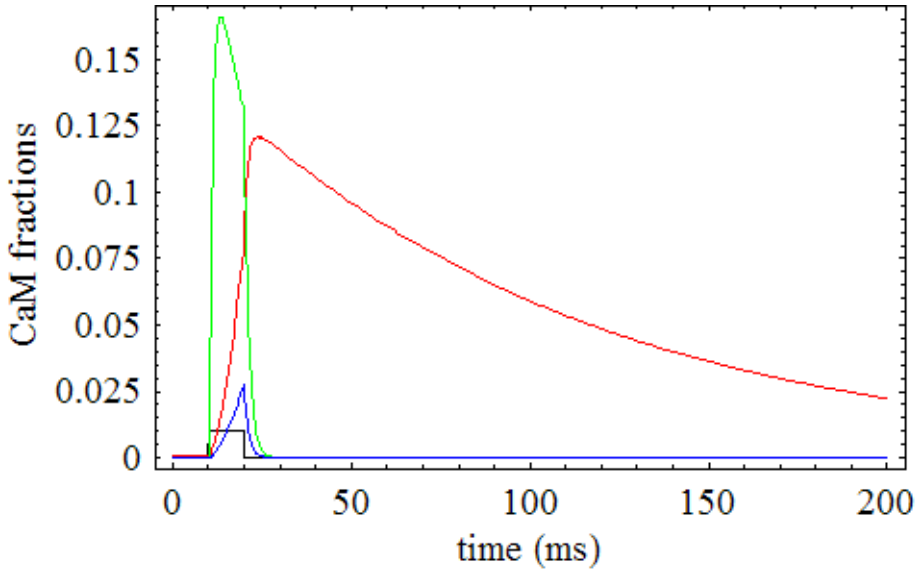

Figure 1.4. Time dependence of the fraction of calmodulin which has 2 Ca^{2+} ions bound to the N lobe (green), 2 Ca^{2+} ions bound to the C lobe (red) or 4 ions Ca^{2+} bound when Ca^{2+} concentration rapidly raises to 10 μM for 10ms (black).

(figure 1.4). Ca^{2+} binding to calmodulin leads to a change in its conformation which exposes hydrophobic residues that facilitate interactions with other proteins. When in Ca^{2+} bound form, calmodulin binds to other proteins with high affinities raging from 10^7 to $10^9 M^{-1}$.

1.6 CaMKII

In the central nervous system, one of the main targets for calcium-loaded calmodulin is Ca^{2+}/calmodulin-dependent protein kinase II (CaMKII). CaMKII is a broad specificity Ser/Thr protein kinase, which represents $1-2\%$ of the mass of the protein in a rat brain. It is enriched in the postsynaptic density (Kennedy et al., 1983). In mammalian cells CaMKII is expressed from four genes: α, β, γ and δ. In the forebrain, most of CaMKII consists of α and β isoforms, with an approximate abundance of 3:1 (Bennett et al., 1983). CaMKII holoenzymes are stochastic combinations of the two isoforms. CaMKII plays a crucial role in long term potentiation (LTP) of synapses. Mutant mice that do not express α-CaMKII have deficient LTP (Silva et al., 1992). Postsynaptic inhibition of CaMKII blocks induction of LTP (Otmakhov et al., 1997),

while injection of a constitutively active form of CaMKII mimics LTP effects and occludes subsequent induction of LTP (Lledo et al., 1995). CaMKII consists of a catalytic domain, a regulatory domain and an association domain. The regulatory domain contains an autoinhibitory region and a calmodulin binding region (figure 1.5). Via interactions of association domains, CaMKII assembles into dodecameric holoenzymes. The first evidence that CaMKII forms dodecameric holoenzymes came from biochemical studies (Bennett et al., 1983). This was later confirmed by cryo-electron-microscopy studies (Kolodziej et al., 2000), and X-ray structures (Rosenberg et al., 2006).

In the basal state the autoinhibitory domain is folded so that it blocks access to the catalytic domain. Binding of Ca^{2+}-loaded calmodulin to the calmodulin binding domain adjacent to the autoinhibitory region of CaMKII moves the autoinhibitory domain out of the catalytic site and relieves its inhibition. After activation, CaMKII can autophosphorylate at threonine 286, which renders its activity Ca^{2+} independent (Miller and Kennedy, 1986).

Autophosphorylation is a process that takes place between subunits of a holoenzyme. The most direct proof that autophosphorylation is an intraholoenzyme, intersubunit process comes from (Hanson et al., 1994). These authors expressed an inactivated CaMKII in which mutations in the catalytic domain destroyed its kinase activity. In a mixture of inactive CaMKII holoenzymes and active CaMKII holoenzymes under conditions that promote autophosphorylation only the active CaMKII were autophosphorylated. The failure of active CaMKII holoenzymes to phosphorylate inactive CaMKII holoenzymes shows that CaMKII autophosphorylation is an intraholoenzyme process. When the active and inactive CaMKII subunits are simultaneously expressed, leading to the formation of mixed holoenzymes, autophosphorylation leads to phosphate incorporation into both active and inactive CaMKII subunits. Therefore, the autophosphorylation happens between subunits.

Another line of evidence leading to the same conclusion comes from measuring the kinetics of autophosphorylation as a function of CaMKII concentration. When

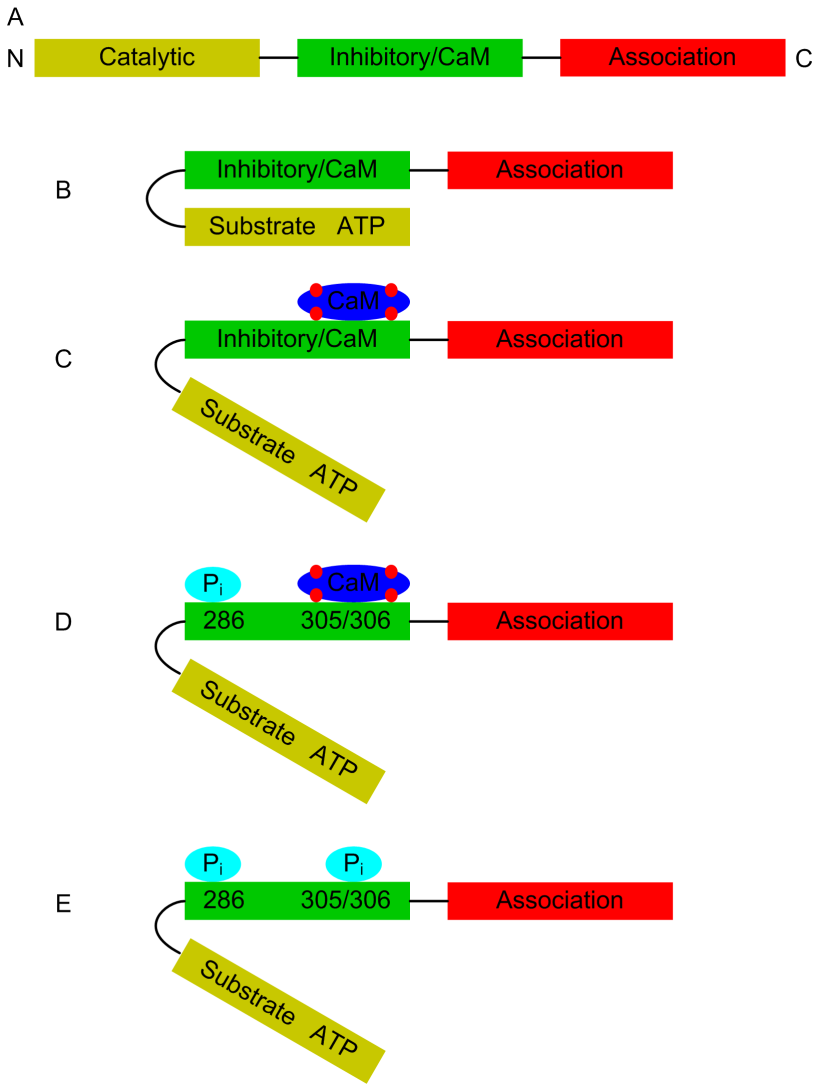

Figure 1.5. CaMKII Activation. **A** Domain map of CaMKII. The sequence of CaMKII contains a catalytic domain, a regulatory domain and an association domain. The catalytic domain contains a substrate binding region and an ATP binding region. The regulatory domain contains an inhibitory region and a calmodulin binding region. **B** In basal conditions, the regulatory domain is bound to the catalytic one, preventing its catalytic function. **C** Binding of Ca^{2+}-loaded calmodulin to a subunit leads to both the release of inhibition and the exposure of Thr286. The release of inhibition makes this CaMKII subunit catalytically active. The exposure of Thr286 makes this CaMKII subunit a potential substrate for a neighboring active CaMKII subunit. **D** A neighboring active CaMKII subunit can phosphorylate this CaMKII subunit at Thr286. **E** After unbinding of calmodulin, a CaMKII subunit which is phosphorylated at Thr286 maintains its catalytic activity. Subsequently, it autophosphorylates at Thr305 or 306, a process which prevents future calmodulin binding.

using CaMKII holoenzymes, the rate of autophosphorylation is independent of the concentration of CaMKII, pointing to a monomolecular reaction. A CaMKII mutant that has the association domain removed, and thus does not associate into holoenzymes, has an autophosphorylation rate that depends linearly on its concentration. This points to a bimolecular reaction for CaMKII subunits.

Hanson et al. (1994) also showed that autophosphorylation requires calmodulin binding to both the kinase and the substrate subunits. Thus, monomeric CaMKII subunits which were previously autophosphorylated can phosphorylate other substrates, but can not continue to autophosphorylate in the absence of Ca^{2+}.

As a result of autophosphorylation, CaMKII can, in theory, be activated by 100ms long Ca^{2+} transients and maintain its activity for minutes to hours. The importance of CaMKII autophosphorylation for synaptic plasticity and behavior was shown by (Giese et al., 1998). These authors mutated the Thr286 of α-CaMKII to Alanine (T286A-αCaMKII). This blocks the autophosphorylation of CaMKII, however it does not impair its Ca^{2+}-dependent activity. Mice with T286A-αCaMKII had no NMDA-dependent LTP and showed no spatial learning.

Besides having kinase activity even in the absence of Ca^{2+}, a CaMKII subunit that is phosphorylated at Thr286 has a vastly increased affinity for calmodulin (Meyer et al., 1992). Although calmodulin has a small probability of unbinding at this point, if it does the CaMKII subunit can autophosphorylate at either Thr305 or Thr306. Both Thr305 and Thr306 are situated in the calmodulin binding region and phosphorylation of one of them prevents future binding of calmodulin. This event is believed to function as an additional layer of regulation of CaMKII activity.

Active CaMKII can phosphorylate a large number of substrates. One of the substrates is the ionotropic receptor that contributes most to the EPSP, the AMPAR. Activation of CaMKII leads to a change in both the number of AMPARs, by regulating its trafficking, and the conductance of AMPAR, by direct phosphorylation (Hayashi et al., 2000). CaMKII can also phosphorylate the potassium channel Kv4.2. This modulation leads to an increase in surface expression of of A-type K^+ channels and consequently a change in neuronal excitability (Varga et al., 2004). Additionally,

CaMKII modulates the signaling cascades involved in reorganization of the actin cytoskeleton. For example, CaMKII phosphorylates SynGAP, increasing its GAP activity (Oh et al., 2004), which has a dramatic influence on spine morphology (Vazquez et al., 2004).

1.7 Previous Models

There have been several previous efforts to model CaMKII activation.

Okamoto and Ichikawa (2000) constructed a model for CaMKII activation that was focused on the bistability of a CaMKII/phosphatase system, in which the phosphatase was independent of Ca^{2+} concentration. In this study the authors did not keep track of which of the subunits in a holoenzyme is phosphorylated. They assumed that the autophosphorylation can happen between any two of the subunits in a holoenzyme.

Zhabotinsky (2000) also constructed a model for CaMKII activation that was focused on the bistability of a CaMKII/phosphatase system, in which both the kinase and the phosphatase activity are dependent on Ca^{2+} concentration. This model assumes a highly simplistic binding of Ca^{2+} to calmodulin, which is fit with a Hill dependence with a Hill coefficient of 4. In this model, the author considers the autophosphorylation as happening between neighboring CaMKII subunits in a ring. However, the author does not keep track of all the possible autophosphorylation states emerging from this autophosphorylation mechanism and pools the states which have the same number of phosphorylated subunits into one state.

Holmes (2000) constructed a very detailed model for CaMKII activation in dendritic spines using a compartmental model. In this model the author includes the possibility for calmodulin with less than four Ca^{2+} bound to bind to CaMKII. However, the binding of calmodulin to each CaMKII subunit is considered independent, and only calmodulin with four Ca^{2+} bound can promote autophosphorylation. Also, calmodulin states are characterized only by the number of Ca^{2+} ions bound and not by which of the Ca^{2+} binding sites are occupied. The details of the autophosphorylation mechanism are not included.

Kubota and Bower (2001) constructed a model for CaMKII activation aimed at reproducing the measurements of CaMKII autophosphorylation when the concentration of Ca^{2+}-loaded calmodulin varies in time (DeKoninck and Schulman, 1998). This model includes a detailed mechanism for CaMKII autophosphorylation by neighboring subunits in rings of four CaMKII subunits. However, this model includes little detail of Ca^{2+}/calmodulin/CaMKII interactions. Ca^{2+} binding to calmodulin is assumed to be at equilibrium, and calmodulin is required to have four Ca^{2+} ions bound to bind to CaMKII.

Miller et al. (2005) constructed a stochastic model for CaMKII activation aimed at estimating the lifetime of the two stable states in a bistable CaMKII/phosphatase system. The authors include a detailed model for for CaMKII autophosphorylation by neighboring subunits in rings of six CaMKII subunits. However, the authors fit the Ca^{2+}-dependent CaMKII activation with a Hill function and do not include calmodulin in the model.

Until recently there was little knowledge of the structure of CaMKII, making some of the assumptions used in previous models unrealistic. All these models are focused on fitting a specific output for the model and incorporate little detail of the biochemical steps in CaMKII activation. None of these models include the possibility of CaMKII subunits cooperating in binding of calmodulin. These models do not include the possibility that CaMKII is phosphorylated by calmodulin with less than four Ca^{2+} bound, nor do they include several CaMKII isoforms.

1.8 Summary

In this study I used modeling and experimental tools to help decipher the details of CaMKII activation under conditions approximating those in dendritic spines, that is, time varying Ca^{2+} concentrations in the low μM and nonsaturating levels of calmodulin. The models used are aimed at explaining experimental results, and include approximations appropriate for those particular experimental conditions. Modeling was, as well, used as a tool to design experiments which can better

distinguish between different CaMKII activation schemes.

Chapter 2 is focused on the measurements of several parameters critical to the model. One of these parameters, the autophosphorylation turnover number, was previously measured; however, the values obtained in previous studies differed by a factor of 20. In chapter 3, I constructed a new model for the interactions between calmodulin and CaMKII, which is motivated by the recently determined structure of CaMKII catalytic domain (Rosenberg et al., 2005). In chapter 4, I constructed and compared two models for the mechanism of CaMKII autophosphorylation. I used these models to design experiments that are capable of determining which mechanism is correct. I performed these experiments and compared the results with other data from the literature. In chapter 5, I constructed a model for simultaneous interactions between Ca^{2+}, calmodulin, and CaMKII. This model is a part of a continuing modeling effort to characterize the biochemical cascades leading to synaptic plasticity.

Bibliography

P. Ascher and L. Nowak. The role of divalent cations in the N-methyl-D-aspartate responses of mouse central neurones in culture. *J Physiol*, 399:247–266, May 1988.

M. K. Bennett, N. E. Erondu, and M. B. Kennedy. Purification and characterization of a calmodulin-dependent protein kinase that is highly concentrated in brain. *J Biol Chem*, 258(20):12735–12744, Oct 1983.

G. Q. Bi and M. M. Poo. Synaptic modifications in cultured hippocampal neurons: dependence on spike timing, synaptic strength, and postsynaptic cell type. *J Neurosci*, 18(24):10464–10472, Dec 1998.

T. V. Bliss and T. Lomo. Long-lasting potentiation of synaptic transmission in the dentate area of the anaesthetized rabbit following stimulation of the perforant path. *J Physiol*, 232(2):331–356, Jul 1973.

R. Chattopadhyaya, W. E. Meador, A. R. Means, and F. A. Quiocho. Calmodulin structure refined at 1.7 A resolution. *J Mol Biol*, 228(4):1177–1192, Dec 1992.

P. Cohen and C. B. Klee. *Calmodulin*. Elsevier, Amsterdam, 1988.

P. DeKoninck and H. Schulman. Sensitivity of CaM kinase II to the frequency of Ca2+ oscillations. *Science*, 279(5348):227–230, Jan 1998.

C. D. DeMaria, T. W. Soong, B. A. Alseikhan, R. S. Alvania, and D. T. Yue. Calmodulin bifurcates the local Ca2+ signal that modulates P/Q-type Ca2+ channels. *Nature*, 411(6836):484–489, May 2001. doi: 10.1038/35078091. URL `http://dx.doi.org/10.1038/35078091`.

K. P. Giese, N. B. Fedorov, R. K. Filipkowski, and A. J. Silva. Autophosphorylation at Thr286 of the alpha calcium-calmodulin kinase II in LTP and learning. *Science*, 279(5352):870–873, Feb 1998.

P. I. Hanson, T. Meyer, L. Stryer, and H. Schulman. Dual role of calmodulin in autophosphorylation of multifunctional CaM kinase may underlie decoding of calcium signals. *Neuron*, 12(5):943–956, May 1994.

K. M. Harris. Calcium from internal stores modifies dendritic spine shape. *Proc Natl Acad Sci U S A*, 96(22):12213–12215, Oct 1999.

Y. Hayashi, S. H. Shi, J. A. Esteban, A. Piccini, J. C. Poncer, and R. Malinow. Driving AMPA receptors into synapses by LTP and CaMKII: requirement for GluR1 and PDZ domain interaction. *Science*, 287(5461):2262–2267, Mar 2000.

D.O. Hebb. *The Organization of Behavior*. John Wiley & Sons, New York, 1949.

B Hille. *Ion Channels of Excitable Membranes*. Sinauer Associates, 2001.

W. R. Holmes. Models of calmodulin trapping and CaM kinase II activation in a dendritic spine. *J Comput Neurosci*, 8(1):65–85, 2000.

M. B. Kennedy. Signal-processing machines at the postsynaptic density. *Science*, 290 (5492):750–754, Oct 2000.

M. B. Kennedy, M. K. Bennett, and N. E. Erondu. Biochemical and immunochemical evidence that the "major postsynaptic density protein" is a subunit of a calmodulin-dependent protein kinase. *Proc Natl Acad Sci USA*, 80(23):7357–7361, Dec 1983.

J. Klingauf and E. Neher. Modeling buffered Ca2+ diffusion near the membrane: implications for secretion in neuroendocrine cells. *Biophys J*, 72(2 Pt 1):674–690, Feb 1997.

S. J. Kolodziej, A. Hudmon, M. N. Waxham, and J. K. Stoops. Three-dimensional reconstructions of calcium/calmodulin-dependent (CaM) kinase IIalpha and trun-

cated CaM kinase IIalpha reveal a unique organization for its structural core and functional domains. *J Biol Chem*, 275(19):14354–14359, May 2000.

Y. Kubota and J. M. Bower. Transient versus asymptotic dynamics of CaM kinase II: possible roles of phosphatase. *J Comput Neurosci*, 11(3):263–279, 2001.

R. A. Lester and C. E. Jahr. NMDA channel behavior depends on agonist affinity. *J Neurosci*, 12(2):635–643, Feb 1992.

X. G. Li, P. Somogyi, A. Ylinen, and G. Buzski. The hippocampal CA3 network: an in vivo intracellular labeling study. *J Comp Neurol*, 339(2):181–208, Jan 1994. doi: 10.1002/cne.903390204. URL `http://dx.doi.org/10.1002/cne.903390204`.

S. Linse, A. Helmersson, and S. Forsn. Calcium binding to calmodulin and its globular domains. *J Biol Chem*, 266(13):8050–8054, May 1991.

P. M. Lledo, G. O. Hjelmstad, S. Mukherji, T. R. Soderling, R. C. Malenka, and R. A. Nicoll. Calcium/calmodulin-dependent kinase II and long-term potentiation enhance synaptic transmission by the same mechanism. *Proc Natl Acad Sci U S A*, 92(24):11175–11179, Nov 1995.

H. Markram, J. Lbke, M. Frotscher, and B. Sakmann. Regulation of synaptic efficacy by coincidence of postsynaptic APs and EPSPs. *Science*, 275(5297):213–215, Jan 1997.

M. L. Mayer, G. L. Westbrook, and P. B. Guthrie. Voltage-dependent block by Mg2+ of NMDA responses in spinal cord neurones. *Nature*, 309(5965):261–263, 1984.

T. Meyer, P. I. Hanson, L. Stryer, and H. Schulman. Calmodulin trapping by calcium-calmodulin-dependent protein kinase. *Science*, 256(5060):1199–1202, May 1992.

P. Miller, A. M. Zhabotinsky, J. E. Lisman, and X. J. Wang. The stability of a stochastic CaMKII switch: dependence on the number of enzyme molecules and protein turnover. *PLoS Biol*, 3(4):e107, Apr 2005. doi: 10.1371/journal.pbio.0030107. URL `http://dx.doi.org/10.1371/journal.pbio.0030107`.

S. G. Miller and M. B. Kennedy. Regulation of brain type II Ca2+/calmodulin-dependent protein kinase by autophosphorylation: a Ca2+-triggered molecular switch. *Cell*, 44(6):861–870, Mar 1986.

L. Nowak, P. Bregestovski, P. Ascher, A. Herbet, and A. Prochiantz. Magnesium gates glutamate-activated channels in mouse central neurones. *Nature*, 307(5950): 462–465, 1984.

Z. Nusser, E. Mulvihill, P. Streit, and P. Somogyi. Subsynaptic segregation of metabotropic and ionotropic glutamate receptors as revealed by immunogold localization. *Neuroscience*, 61(3):421–427, Aug 1994.

J. S. Oh, P. Manzerra, and M. B. Kennedy. Regulation of the neuron-specific Ras GTPase-activating protein, synGAP, by Ca2+/calmodulin-dependent protein kinase II. *J Biol Chem*, 279(17):17980–17988, Apr 2004. doi: 074/jbc.M314109200. URL `http://dx.doi.org/074/jbc.M314109200`.

H. Okamoto and K. Ichikawa. Switching characteristics of a model for biochemical-reaction networks describing autophosphorylation versus dephosphorylation of Ca2+/calmodulin-dependent protein kinase II. *Biol Cybern*, 82(1):35–47, Jan 2000.

N. Otmakhov, L. C. Griffith, and J. E. Lisman. Postsynaptic inhibitors of calcium/calmodulin-dependent protein kinase type II block induction but not maintenance of pairing-induced long-term potentiation. *J Neurosci*, 17(14):5357–5365, Jul 1997.

O. S. Rosenberg, S. Deindl, R. J. Sung, A. C. Nairn, and J. Kuriyan. Structure of the autoinhibited kinase domain of CaMKII and SAXS analysis of the holoenzyme. *Cell*, 123(5):849–860, Dec 2005. doi: 10.029. URL `http://dx.doi.org/10.029`.

O. S. Rosenberg, S. Deindl, L. R. Comolli, A. Hoelz, K. H. Downing, A. C. Nairn, and J. Kuriyan. Oligomerization states of the association domain and the holoenyzme of Ca2+/CaM kinase II. *FEBS J*,

273(4):682–694, Feb 2006. doi: 10.1111/j.1742-4658.2005.05088.x. URL http://dx.doi.org/10.1111/j.1742-4658.2005.05088.x.

B. L. Sabatini, T. G. Oertner, and K. Svoboda. The life cycle of Ca(2+) ions in dendritic spines. *Neuron*, 33(3):439–452, Jan 2002.

G.M. Shepherd. *The Synaptic Organization of the Brain*. Oxford University Press, New York, 1998.

A. J. Silva, C. F. Stevens, S. Tonegawa, and Y. Wang. Deficient hippocampal long-term potentiation in alpha-calcium-calmodulin kinase II mutant mice. *Science*, 257 (5067):201–206, Jul 1992.

J. Spacek and K. M. Harris. Three-dimensional organization of smooth endoplasmic reticulum in hippocampal CA1 dendrites and dendritic spines of the immature and mature rat. *J Neurosci*, 17(1):190–203, Jan 1997.

R. W. Tsien, D. Lipscombe, D. V. Madison, K. R. Bley, and A. P. Fox. Multiple types of neuronal calcium channels and their selective modulation. *Trends Neurosci*, 11 (10):431–438, Oct 1988.

A. W. Varga, L. Yuan, A. E. Anderson, L. A. Schrader, G. Wu, J. R. Gatchel, D. Johnston, and J. D. Sweatt. Calcium-calmodulin-dependent kinase II modulates Kv4.2 channel expression and upregulates neuronal A-type potassium currents. *J Neurosci*, 24(14):3643–3654, Apr 2004. doi: 10.1523/JNEUROSCI.0154-04.2004. URL http://dx.doi.org/10.1523/JNEUROSCI.0154-04.2004.

L. E. Vazquez, H. J. Chen, I. Sokolova, I. Knuesel, and M. B. Kennedy. SynGAP regulates spine formation. *J Neurosci*, 24(40): 8862–8872, Oct 2004. doi: 10.1523/JNEUROSCI.3213-04.2004. URL http://dx.doi.org/10.1523/JNEUROSCI.3213-04.2004.

A. M. Zhabotinsky. Bistability in the Ca(2+)/calmodulin-dependent protein kinase-phosphatase system. *Biophys J*, 79(5):2211–2221, Nov 2000.

Chapter 2

Measurements of CaMKII Autophosphorylation Turnover Numbers

2.1 Introduction

Calcium/Calmodulin Protein Kinase II (CaMKII) is activated by binding of Ca^{2+}-loaded calmodulin. After binding of calmodulin, CaMKII can autophosphorylate at Thr286, which makes CaMKII active even in the absence of Ca^{2+}. The basal $[Ca^{2+}]$ (50−100 nM) is small compared to the concentrations of Ca^{2+} required for Ca^{2+}-dependent activation of CaMKII which is greater than 300 nM (Shifman et al., 2006). The rise in Ca^{2+} concentration in spines is transient (10−100 ms) which suggests that CaMKII activity mainly comes from the Ca^{2+}-independent, autophosphorylated subunits. Mice expressing T286A-αCaMKII, which has normal Ca^{2+}-dependent activity however no Ca^{2+}-independent activity, show no spatial learning (Giese et al., 1998). In order to characterize CaMKII autophosphorylation in physiological conditions, one needs to know the rate of CaMKII autophosphorylation. CaMKII autophosphorylation turnover number (k_P) is defined as the rate of autophosphorylation of CaMKII when each CaMKII subunit has Ca^{2+} loaded calmodulin bound. Estimates from Hanson et al. Hanson et al. (1994, Fig. 7) suggest a CaMKII autophosphorylation turnover number of 0.5 to 1 s^{-1}, however later measurements (Bradshaw et al., 2002) indicate a value of 20 s^{-1}.

After binding of Ca^{2+}, the conformation of calmodulin changes, exposing hydrophobic sites that contribute to protein-protein interactions. As a result, it was traditionally assumed that calmodulin requires 4 Ca^{2+} ions bound in order to bind to and activate calmodulin binding proteins. However, experiments on CaMKII activation in nonsaturating Ca^{2+} showed that the concentration of Ca^{2+} required for activation of CaMKII is more than one order of magnitude smaller than the concentration of Ca^{2+} required for formation of CaM with 4 Ca^{2+} bound (Shifman et al., 2006). One of the possible reasons for this fact is that calmodulin with less than 4 bound Ca^{2+} may be able to bind to and activate CaMKII. To test this hypothesis Shifman et al. expressed computationally-designed calmodulin mutants that have one of the lobes intact and the other lobe mutated. The mutated lobe has its two Ca^{2+} binding sites mutated in such a way that they do not bind Ca^{2+}; however, the structure remains similar to that in Ca^{2+} free conditions. The CaM mutant in which the Ca^{2+} binding sites near the carboxyl terminus are mutated is denoted as $CaM - N^{WT}$ while the one in which the amino terminus binding sites are mutated is $CaM - C^{WT}$.

In the course of our experiments, we made the novel finding that the time required to stop the autophosphorylation reaction when the conventional SDS stop buffer is added, is on the same scale as the inverse of the turnover number. This makes obtaining accurate measurements of CaMKII's autophosphorylation turnover number difficult. Hanson et al. (1994) measured calmodulin trapping as a function of time in low stoichiometric ratios of CaM to CaMKII. By extrapolating this measurement to saturating calmodulin one can estimate k_P as being in the range of 0.5 to 1 s^{-1}. On the other hand, Bradshaw et al. (2002) used rapid quench flow methods to measure k_P directly and stopped the autophosphorylation reaction by lowering the $[Ca^{2+}]$ by addition of the chelator EGTA. The reduction in $[Ca^{2+}]$ is very rapid; however, Ca^{2+} binding sites near the C terminus of calmodulin have a sufficiently slow off rate that contaminate these results.

In this study, I used quench flow methods for rapid mixing and an alternative method for rapidly stopping the autophosphorylation reaction to measure CaMKII

autophosphorylation turnover number. In order to be able to quantify the contribution of calmodulin with less than 4 Ca^{2+} bound to activation of CaMKII in physiological conditions, I used the same methods to measure the turnover number when CaMKII is activated by $CaM - N^{WT}$ and $CaM - C^{WT}$.

2.2 Methods

CaMKII was purified from rat forebrains as described in (Miller and Kennedy, 1985). $CaM - N^{WT}$ and $CaM - C^{WT}$ were obtained from M. Choi, of our laboratory (Shifman et al., 2006).

Rates of autophosphorylation were measured at 100 ms, 300 ms, 1 s, 3 s, 10 s, and 30 s after initiation of the reaction with the use of a Kintek Model RQF-3 Quench Flow apparatus (Kintek Corporation, Austin, Texas). Reactions were initiated by rapid mixing of two solutions. Solution 1 contained 50 mM Tris-HCl at p.H 7.2, 0.1 M NaCl, 1 mM MgCl2, 2 mM Ca^{2+}, 0.9 mg/ml BSA, 5 mM DTE, 1.4 μM CaMKII (catalytic sites), and either 12 μM CaM WT, 30 μM $CaM - C^{WT}$, or 60 μM $CaM - N^{WT}$. Solution 2 contained the same buffer, but CaMKII and CaM were replaced with 200 μM ATP. The two solutions were kept at 4 °C until they were transferred to the quench flow apparatus where they warmed for 1 min to 30 °C. Autophosphorylation was initiated by rapid mixing of 16 μL of the two solutions.

When we stopped the reaction with the denaturating agent SDS the autophosphorylation reaction was terminated by bringing the final concentrations to 3% SDS, 50 mM Tris-HCl (pH 7.2), 2% beta-mercaptoethaol, 5% glycerol, 40 μg/mL Bromphenol Blue and subjected to SDS-PAGE followed by immunoblotting with the phospho-CaMKII specific antibody 22B1.

Samples containing 0.23 μg of CaMKII were fractionated on an 8% SDS PAGE gel. Protein was transferred by electrophoresis onto a nitrocellulose membrane for 1 hour at a current of 350 mA in 25 mM Tris base, 0.2 M Glycine and 20% Methanol. The membranes were immunoblotted with 6.25 μg antibody 22B1 in 12.5 ml 50 mM Tris (pH 7.5), 0.5 M NaCl, 0.1% Tween 20 (TTBS), plus 2% normal goat serum

for 2 hrs at 21 °C. Monoclonal antibody 22B1 (anti-phospho-CaMKII; Affinity Bioreagents, CO) is specific for α and β subunits of CaMKII only when they are phosphorylated at Thr-286/287. Bound antibodies were visualized with fluorescent secondary antibody IRDye800-Anti-mouse (Rockland, Gilbertsville, PA; 1.5 μg in 30 mL TTBS). Fluorescence from the bound secondary antibody was visualized with an Odyssey Imaging System (Li-Cor Biosciences, Lincoln, NE).

When we stopped the reaction with a combination of reduced pH and SDS, solutions 1 and 2 were the same as the case for SDS stop, however, contained only 25 mM Tris-HCl. The autophosphorylation reaction was terminated by the rapid addition of a final concentration of 1% SDS, 3.3 mM Glycine-HCl, pH 2.9. The decrease in pH to 2.9 was necessary to stop reactions within ∼100 ms, whereas SDS denatured CaMKII over a period of ∼1 s. After quenching, all reactions were brought to a final concentration of 3% SDS, 2.64 mM Glycine, 66 mM Tris-HCl (pH 7.2), 2% beta-mercaptoethaol, 5% glycerol, 40 μg/mL Bromphenol Blue and subjected to SDS-PAGE followed by immunoblotting with 22B1 as described for the SDS stop.

The amount of autophosphorylated CaMKII was calculated by quantifying the integrated intensity of each band. The integrated intensity of a band is the integral of the intensity of each pixel in a band after subtracting the median value of the intensities of the pixels on the border of the band. The intensity of each band was then normalized to the intensity of a band corresponding to a standard of fully autophosphorylated CaMKII (CaMKII autophosphorylated for 30 s in the case of wild type calmodulin and for 100 s in the case of mutant calmodulins). For each set of experiments a standard curve was built by measuring the integrated intensity of known quantities of fully autophosphorylated CaMKII. The standard curve was fit with a power function:

$$Int(x) = \left(\frac{x}{x_0}\right)^n. \tag{2.1}$$

- n−free parameter which is fitted
- x−represents the amount of fully autophosphorylated CaMKII which was loaded

in the lanes used to construct the standard function

- $x_0 = 0.23\mu$g−represents the total amount of CaMKII which was loaded in each lane of the gels measuring the time dependence of CaMKII autophosphorylation

A power function was used since it has one free parameter, respects the constraints $Int(0) = 0$, $Int(x_0) = 1$ and fits well the observed nonlinearity.

The amount of autophosphorylated CaMKII in each lane was obtained using the inverse of the standard curve.

$$p286(t) = \left(\frac{Int(t)}{Int(tmax)}\right)^{\left(\frac{1}{n}\right)} \tag{2.2}$$

The time dependence of the fraction of CaMKII that is phosphorylated at Thr286 was fit with:

$$p286(t) = A\left(1 - e^{-k_P(t+t_0)}\right). \tag{2.3}$$

- A represents the maximal autophosphorylation fraction and is close to 1
- k_P represents the autophosphorylation turnover number
- t_0 represents the time it takes for the autophosphorylation reaction to be stopped

The autophosphorylation turnover numbers were obtained through nonlinear regression using the Levenberg Marquardt method implemented in Mathematica 5 (Wolfram Research).

2.3 Results

Autophosphorylation of CaMKII was measured with the use of quench flow techniques. An aliquot of CaMKII was mixed with Ca^{2+}, CaM and brought to

30 °C immediately preceding the experiment. The autophosphorylation reaction was started by addition of saturating ATP, and, in the first set of experiments, stopped by addition of a denaturing agent, the detergent SDS. The times between mixing of the solutions to start the reaction and mixing to stop it were 100 ms, 300 ms, 1 s, 3 s, 10 s, and 30 s. I repeated the experiment 4 times and the data were fit via nonlinear regression with $p286(t) = A\left(1 - e^{-k_P(t+t_0)}\right)$ with 3 free parameters: A, k_P, t_0. The regression was performed on the pooled data, not on the average of the experiments. The values for the free parameters that best fit the data are $A = 0.98 \pm 0.03$, $k_P = 0.47 \pm 0.08 s^{-1}$ and $t_0 = 0.68 \pm 0.18 s$ (figure 2.1 A). The values are written in the format mean ± standard error. As expected, the amplitude is close to 1, however, the best fit data intersects the time axis at $-0.68 s$. This nonzero intersect is a direct consequence of the observed high autophosphorylation fraction: 0.27 ± 0.02, at the shortest time point: 100 ms. I have repeated previous controls showing that at the start of experiments CaMKII is fully dephosphorylated.

There are two possible explanations for this nonzero intercept. One is that CaMKII autophosphorylation has two intrinsic time constants: a fast one with $k_{P1} = 3.2\ s^{-1}$ which leads to 27% phosphorylation in 100 ms and a slow one with $k_{P2} = 0.47\ s^{-1}$. A second possibility is that SDS takes an average of 0.68 s to denature CaMKII, thus stopping the autophosphorylation reaction. In order to distinguish between these two possibilities, I performed a measurement that included time points at 3 ms and 30 ms. The autophosphorylation obtained at both 3 ms and 30 ms was 32% (figure 2.1 B). This indicates that it takes on average 0.68 s to stop the autophosphorylation reaction using SDS. However, since the estimate for $1/k_P$ from these measurements is 2.1 s, the inability to stop the reaction faster than 0.68 s introduces errors in the measurement of k_P.

In order to more accurately measure k_P, a new stop method that stops the autophosphorylation reaction much faster was implemented. CaMKII loses its kinase activity at pHs lower than 6 (Kennedy et al., 1983, figure 3). Consequently, I decided to test if the autophosphorylation reaction would be stopped more quickly by a simultaneous drop in pH with the addition of SDS. The pH of the stop solution

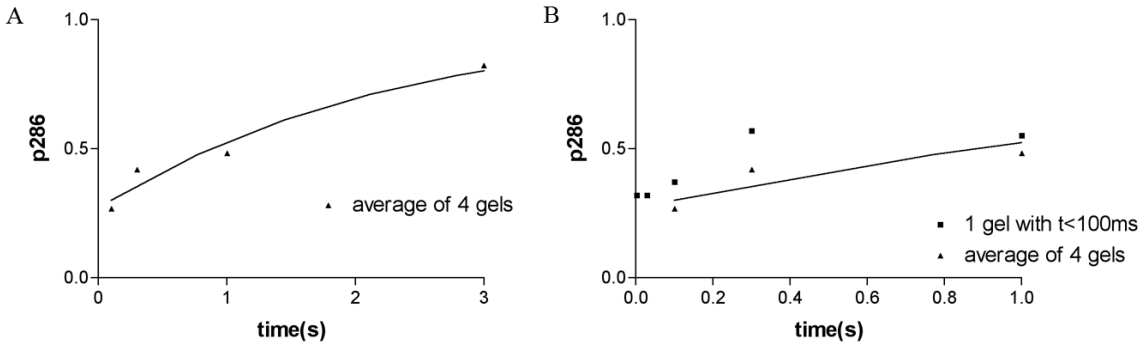

Figure 2.1. CaMKII autophosphorylation for short duration using SDS stop. **A**. Fraction of CaMKII which is autophosphorylated at Thr286 as a function of time. The measurements were performed in saturating Ca^{2+} and CaM and stopped using SDS. Data represent the average of 4 measurements. The solid line is the fit to the data using $p286(t) = A\left(1 - e^{-k_P(t+t_0)}\right)$ with 3 free parameters: A, k_P, t_0. **B**. The data and fit from **A** with the addition of an experiment in which CaMKII autophosphorylation fraction was measured at 3 ms and 30 ms.

used was 2.9. SDS has a lower solubility in acidic conditions. In the stop solution I used saturating SDS for a pH of 2.9 which is almost 3%. To more easily drop the pH of the reaction solution, the concentration of the pH buffer used in the reaction solution was reduced from 50mM Tris-HCl (pH 7.2) to 25 mM Tris-HCl (pH 7.2). After stopping, the solution was brought back to pH 7.5, which is the pH of the stacking gels in the immunoblotting procedure.

The data from 5 repeats of the k_P measurement with pH/SDS stop were simultaneously regressed. The best fit parameters are $A = 0.98 \pm 0.03$, $k_P = 0.96 \pm 0.14 s^{-1}$ and $t_0 = 0.099 \pm 0.061 s$ (figure 2.2). The 95% confidence intervals for the parameters are (0.93, 1.03) for A, (0.67, 1.26) for k_P and (-0.026, 0.223) for t_0. The best fit value for t_0 is an order of magnitude smaller than $1/k_P$. Consequently, the pH/SDS stop method stops the autophosphorylation reaction sufficiently rapidly to reliably measure k_P.

To quantify the importance of CaMKII autophosphorylation by calmodulin with less than 4 Ca^{2+} bound, I measured the CaMKII autophosphorylation turnover number when activated by $CaM - N^{WT}$ and $CaM - C^{WT}$ (figure 2.3). The measurements were performed in saturating Ca^{2+}. In saturating Ca^{2+} I assume

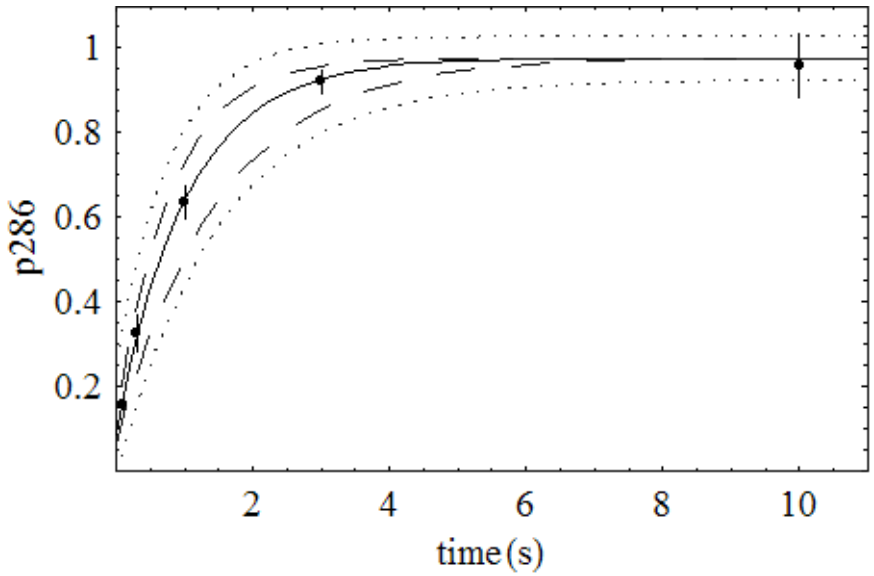

Figure 2.2. CaMKII autophosphorylation turnover number. Fraction of CaMKII which is autophosphorylated at Thr286 as a function of time. The measurements were performed in saturating Ca^{2+} and CaM, and stopped using pH/SDS. Data represent the average of 5 measurements and the vertical bar represents the standard error of the mean. The solid line is the fit to the data using: $p286(t) = A_e\left(1 - e^{-k_{Pe}(t+t_{0e})}\right)$. The dashed lines are $p286(t) = A_e\left(1 - e^{-k_{P1}(t+t_{0e})}\right)$ and $p286(t) = A_e\left(1 - e^{-k_{P2}(t+t_{0e})}\right)$. A_e is the best estimate for amplitude A, t_{0e} is the best estimate for time intersect t_0, k_{P1} and k_{P2} are the limits of the 95% confidence interval for the autophosphorylation turnover number kP. The dotted lines are $p286(t) = A_1\left(1 - e^{-k_{P1}(t+t_{01})}\right)$ and $p286(t) = A_2\left(1 - e^{-k_{P2}(t+t_{02})}\right)$. A_1, A_2, t_{01} and t_{02} are the limits of the 95% confidence interval for the amplitude and time intersect respectively.

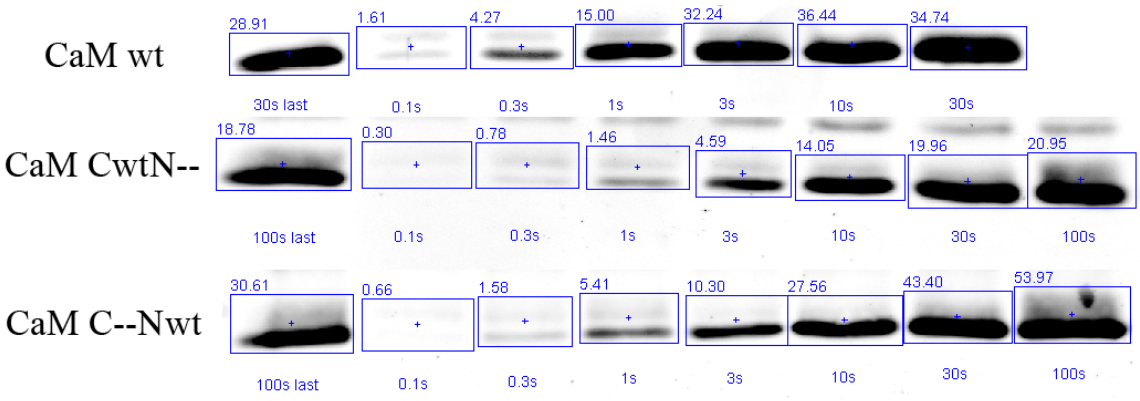

Figure 2.3. Aligned typical immunoblots of CaMKII activation by CaM mutants. Three sections from immunoblots using 22B1 antibody against CaMKII-Thr286P. Each band corresponds to αCaMKII, 50 kDa molecular weight. The order in which the measurements were done is from right to left. The left-most column has the same autophosphorylation time as the right-most column and it is used to control for the denaturation of CaMKII during an experiment. Each box has in its top left corner the integral intensity corresponding to the band. The integral intensity is calculated as the integral of the intensity of the points inside the box subtracting the median intensity of the edges. The boxes used to calculate the integral intensity were drawn by hand. Changes in the size of each box, as long as it fully contains the band, had minimal impact in the value of integral intensity obtained.

that $CaM - N^{WT}$ has a behavior identical to wild-type CaM with 2 Ca^{2+} bound to the amino lobe, while $CaM - C^{WT}$ has a behavior identical to wild-type CaM with 2 Ca^{2+} bound to the amino lobe. The dependence of CaMKII autophosphorylation on the concentration of mutant calmodulin was measured previously (Shifman et al., 2006). In these measurements the autophosphorylation time was 30 s. The half activation value for $CaM - N^{WT}$ is 20 μM while for $CaM - C^{WT}$ it is 5 μM. I used these values to estimate concentrations for mutant calmodulin which are close to saturation. For $CaM - N^{WT}$ I used 30 μM. I could not use a higher concentration since further increasing mutated calmodulin leads to a decrease in CaMKII autophosphorylation, possibly due to formation of aggregates (Choi, personal communication). For $CaM - C^{WT}$ I used 15 μM.

The best fit value for CaMKII autophosphorylation turnover number when CaMKII is activated by $CaM - N^{WT}$ (k_{PN}) is $0.117 \pm 0.018 s^{-1}$ (figure 2.4). The

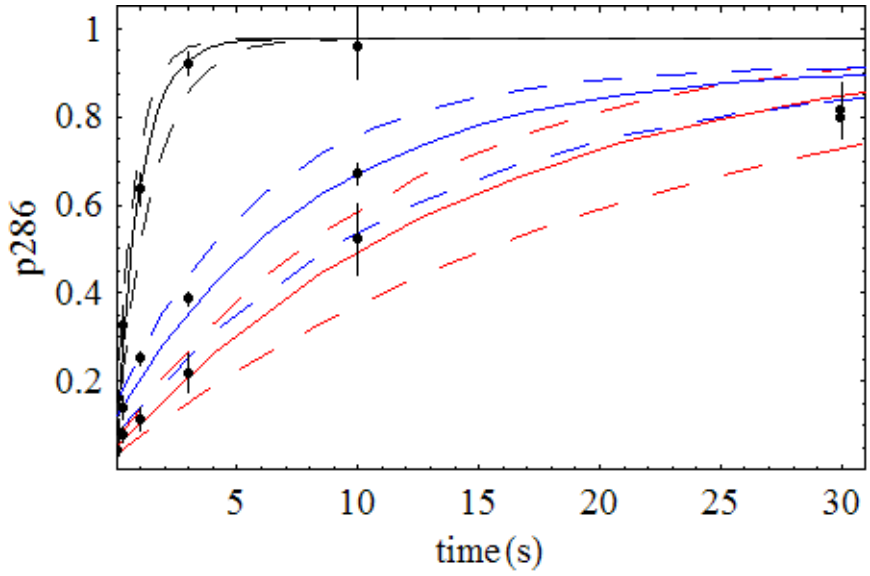

Figure 2.4. CaMKII autophosphorylation turnover number when activated by calmodulin mutants. Black lines represent CaMKII activated by CaMWT, blue and red lines CaMKII activated by $CaM - N^{WT}$ and $CaM - C^{WT}$ respectively. For CaMWT and $CaM - C^{WT}$ 5 experiments were performed. For $CaM - N^{WT}$ 3 experiments were performed.

95% confidence interval for k_{PN} is (0.079, 0.156). The best fit value for CaMKII autophosphorylation turnover number when CaMKII is activated by $CaM - C^{WT}$ (k_{PC}) is $0.064 \pm 0.010 s^{-1}$. The 95% confidence interval for k_{PC} is (0.044, 0.084).

When activated by each calmodulin mutant, the autophosphorylation turnover number is one order of magnitude smaller than the autophosphorylation turnover number when CaMKII is activated by wild type calmodulin. To test if the differences between k_{PN} and k_{PC} are significant I constructed the distribution of the differences between k_{PN} and k_{PC}. This distribution has 50 degrees of freedom, so I performed a Z test. CaMKII autophosphorylation turnover number when activated by calmodulin with intact N-terminus, k_{PN}, is significantly larger than CaMKII autophosphorylation turnover number when activated by calmodulin with intact C-terminus, k_{PC}, with a probability of error: 0.005. Even though the difference between k_{PN} and k_{PC} are small, they are statistically significant.

2.4 Discussions

The direction of the changes in synaptic strength that occur during storage of information in neural circuits is exquisitely sensitive to small changes in the concentration of postsynaptic Ca^{2+} that occur during a few milliseconds of repetitive electrical activity (Sjostrom and Nelson, 2002; Zucker et al., 1999). CaMKII is a key element in the Ca^{2+} messenger pathway leading to LTP. Most of the previous experimental efforts on characterizing CaMKII were performed using either saturating Ca^{2+} or long autophosphorylation times. This study was aimed at experimentally measuring some of the parameters that determine CaMKII behavior in physiologically relevant Ca^{2+} conditions.

In order to be able to measure the response to very short Ca^{2+} transients I used a quench flow technique that allows the mixture of small samples within 2 ms. We found it necessary to implement a new technique to stop the autophosphorylation reaction rapidly, by a rapid reduction in the pH of the reaction buffer. This stopping technique permitted us to measure CaMKII autophosphorylation turnover number (k_P) directly. k_P is a critical parameter for the modeling efforts aimed at predicting CaMKII autophosphorylation in spines under different stimulation conditions.

Previous models (Zhabotinsky, 2000; Holmes, 2000) have used values for k_P in the range of 0.5 - 1 s^{-1} estimating k_P from (Hanson et al., 1994, figure 7). Subsequent direct measurements of k_P (Bradshaw et al., 2002) put its value close to 12 s^{-1}. However, it is very likely that the latter measurements were overestimates because the authors neglected the time required to stop the autophosphorylation reaction. The value that I measured: $k_P = 0.96 \pm 0.14 s^{-1}$ is in good accordance with estimates from Hanson et al. (1994, figure 7).

In order to characterize CaMKII autophosphorylation in nonsaturating Ca^{2+} conditions I used calmodulin mutants that have either the amino or the carboxyl terminus binding sites mutated. These mutants mimic the intermediate stages of calmodulin in which there are either 2 Ca^{2+} bound to the C lobe (CaM2C) or 2 Ca^{2+} bound to the N lobe (CaM2N). The interaction between CaMKII and CaM with less

than 4 Ca^{2+} bound is of interest because competition for CaM2C or CaM2N within a synaptic spine may determine whether the synapse will be potentiated or depressed. This sensitivity to Ca^{2+} occurs at concentrations at which CaM2C and CaM2N will be present at higher concentrations than CaM with four bound Ca^{2+} (CaM4).

I have used the values reported in this study and data from Shifman et al. (2006) to estimate the relative concentrations of CaM2C bound to CaMKII (CaM2C-CaMKII), CaM2N bound to CaMKII (CaM2N-CaMKII), and CaM4 bound to CaMKII (CaM4-CaMKII) at 0.5 μM and 2 μM Ca^{2+} in the PSD. I assumed concentrations of 30 μM CaMKII subunits and 10 μM free CaM in the PSD; and a K_D of 50 nM for binding of CaM4 to CaMKII. Using a simple model for binding of CaM to CaMKII, at 0.5 μM Ca^{2+}, the concentration of CaM2C-CaMKII is $\sim$0.8 μM, which is $\sim$10 times higher than the concentration of CaM4-CaMKII. Because of the low affinity of CaM2N for CaMKII, its concentration is $\sim$80 times lower than the concentration of CaM2C-CaMKII. At 2 μM Ca^{2+}, the concentrations of CaM2C-CaMKII (2.3 μM) and CaM4-CaMKII (3.2 μM) are roughly equal; both still exceed CaM2N-CaMKII by a factor of 80. These numbers show that the enhanced affinity for the 3rd and 4th Ca^{2+}s bound to CaM when CaMKII is present results in formation of a significant amount of CaM4-CaMKII at 2 μM Ca^{2+}.

The activation of CaMKII by binding of CaM2C alone likely contributes to activation of CaMKII during small increases in Ca^{2+} in the PSD above the basal concentration of 80 nM, such as might occur during low-frequency stimulation. These findings demonstrate the importance of understanding the kinetics of interactions of CaM2C with its various targets in order to correctly simulate the biochemical responses to Ca^{2+} influx into the spine.

The affinity for CaMKII of $CaM - C^{WT}$ ($K_D = 5$ μM) is higher than that of $CaM - N^{WT}$ ($K_D = 20$ μM) (Shifman et al., 2006). The CaMKII autophosphorylation turnover number shows the converse relationship. When $CaM - N^{WT}$ binds to CaMKII, k_{PN} is $0.117 \pm 0.018 s^{-1}$; however, when $CaM - C^{WT}$ binds to CaMKII, k_{PC} is $0.064 \pm 0.010 s^{-1}$. While initially counterintuitive, both these effects can be explained by an analysis of the structure of CaMKII catalytic domain and holoenzyme.

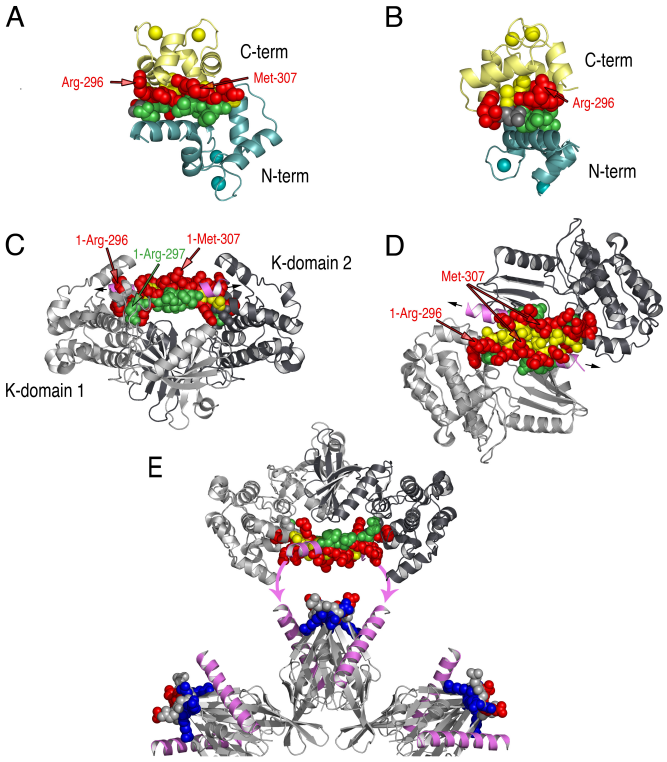

Figure 2.5. Binding sites for the amino- and carboxyl- halves of CaM in the α-subunit holoenzyme of CaMKII. **A** and **B**. X-ray structure of Ca^{2+}/CaM bound to a peptide with the sequence of the CaM binding domain in CaMKII (Meador et al., 1992). CaM is shown as a backbone ribbon and Ca^{2+} ions are shown as spheres. The N-terminus of CaM is blue and The C-terminus is yellow. The CaM binding peptide is shown in space-filling mode. Residues associating with the N-terminus of CaM are colored green; those associating with the C-terminus of CaM are colored red. PDB file: 1CDM. **C** and **D**. X-ray structure of the autoinhibited kinase domain of the α-subunit of CaMKII (Rosenberg et al., 2005). **C**. The CaM-binding domains are shown in space-filling mode. The residues of the CaM-binding domain are colored as in **A**. and **B**., except that residues whose side-chains participate in the coiled coil interaction are colored yellow. One kinase domain (K-domain 1) is colored silver and the other (K-domain 2) black. Arg-296 and Met-307 from K-domain 1 are labeled for comparison to **A**. and **B**. Arg-297, which is important for interaction with the N-terminus of CaM is also labeled in K-domain 1. PDB file: 2BDW **E**. Orientation of the kinase domains with respect to the association domains (Rosenberg et al., 2005, 2006). The structures of the kinase domain pairs and the oligomerized association domains were determined in separate crystals of peptides containing residues 1-318 and 340-468 of the α-subunit, respectively. No structure has been determined for the linking region containing residues 319-339. Three of the six arms formed by the twelve association domains in the CaMKII holoenzyme (Rosenberg et al., 2005) are depicted below the kinase domain pair. The alpha helix that links to the kinase domain is colored violet. The violet arrows indicate the approximate position that linking residues 319-339 would occupy in the proposed structure. Acidic residues at the tip of the arm of the association domains are colored red and basic residues are colored blue. The figure was obtained from Mary B. Kennedy.

The higher affinity for CaMKII displayed by $CaM - C^{WT}$ compared with $CaM - N^{WT}$ reflects, in part, the intrinsically higher affinity of $CaM - C^{WT}$ for the peptide sequence of the CaM binding domain in CaMKII (70 nM vs. 6 μM for $CaM - N^{WT}$) (Shifman et al., 2006). However, recently published structures of the catalytic and association domains of CaMKII (Rosenberg et al., 2006, 2005) suggest that $CaM - C^{WT}$ may also be less sterically hindered than $CaM - N^{WT}$ in its initial interaction with the appropriate site in the CaMKII holoenzyme (figure 2.5). The atomic structure of CaM bound to the alpha-helical calmodulin-binding segment of CaMKII (CaMKII-cbp) reveals that the carboxyl- and amino-termini of CaM interact with side chains on opposite faces of the helix (figure 2.5 **A** and **B**) (Meador et al., 1992). Residues Arg-296, Leu-299, Ile-303, Thr-306, Met-307 and Thr-310 (colored red in figure 2.5) make contact with the C-terminal lobe of CaM. Residues Arg-297, Lys-298, Gly-301, Leu-304, Thr-305, and Leu-308 (colored green in figure 2.5 **A** and **B**) contact the N-terminal lobe. The X-ray structure of the catalytic domain of CaMKII reveals that it forms a dimer held together by a coiled coil interaction between helices formed by residues 273 to 317, which includes the CaM binding domain (figure 2.5 **C** and **D**) (Rosenberg et al., 2005). The side chains that interact with the N-terminus of CaM (green) are buried in a pocket formed by the catalytic domains (figure 2.5 **C**). In contrast, many of the side chains that interact with the C-terminus of CaM (red) are exposed on one face of the dimer (figure 2.5 **D**). A structure of the entire dodecameric holoenzyme of CaMKII has been proposed based on the X-ray structures of the catalytic and association domains, and on small angle X-ray scattering (SAXS) data from the holoenzyme in solution. In this proposed structure, each dimerized pair of catalytic subunits is held in place by their association domains which interact with other association domains to form a rosette (Hoelz et al., 2003; Rosenberg et al., 2006, 2005). Their data suggest that the face of each dimer that contains the binding site for $CaM - C^{WT}$ is pointed toward the outward end of an arm of the rosette. Because the structure of about 20 of the residues that form the link between the kinase domain dimers and the arms of the rosette (figure 2.5 **E**) is unknown, the size of the gap into which the C-terminus of CaM must insert is not

well defined, and, in fact, may be flexible. For comparison, the violet alpha helices in the association domains depicted in figure 2.5 **E** are approximately 22 residues long.

In summary, each lobe of calmodulin has a different binding site on CaMKII. The C-terminus binding site is more exposed than the N-terminus binding site. This may account for the higher affinity of the C-terminus of calmodulin for CaMKII. It also follows that a greater conformational change is required for N-terminus binding. Consequently, in saturating conditions, CaM with intact N terminus provides a higher autophosphorylation turnover number for CaMKII.

In support of the notion that the linker region between the kinase and association domains influences affinity for the C-terminus of CaM, we note that affinity of CaM for the β-subunit of CaMKII is about 2-fold higher than for the α-subunit (Miller and Kennedy, 1985). The most prominent difference between these two subunits is the insertion into the β-subunit of 68 additional residues in the linker region between the catalytic and association domains (Bulleit et al., 1988). These additional residues may increase the size of the gap into which the C-terminus of CaM must insert, and thus increase the affinity of CaM for CaMKII.

This differential binding of the termini of CaM for different CaM-binding proteins has a precedent in the literature. The individual amino or carboxyl termini of CaM with bound Ca^{2+} can activate certain effector proteins, including phosphorylase kinase (Kuznicki et al., 1981), myosin light chain kinase, neuronal nitric oxide synthase (Persechini et al., 1994), and adenylate cyclase (Gao et al., 1993). These studies relied either on isolated N-terminal and C-terminal fragments of CaM generated by proteolysis (Kuznicki et al., 1981; Persechini et al., 1994), or on point mutants of CaM that have lost one or more Ca^{2+} binding sites (Gao et al., 1993). More recent studies have made use of CaM with single point mutations in each of the two N-terminal sites (CaM12) or the two C-terminal sites (CaM34) to show that the individual lobes of CaM have distinct functional effects on voltage-activated Ca^{2+} channels (DeMaria et al., 2001).

In this chapter I developed a new method to rapidly stop CaMKII autophosphorylation reaction. Using this method I more precisely measured the autophosphorylation

turnover number, a parameter which values in the literature differed by an order of magnitude. I used this method to measure the autophosphorylation turnover numbers for CaMKII when it is activated by calmodulin with 2 Ca^{2+} ions bound. This work is part of the first study to look at qualitative and quantitative aspects of CaMKII autophosphorylation by calmodulin with less than 4 Ca^{2+} ions bound (Shifman et al., 2006).

Bibliography

J. M. Bradshaw, A. Hudmon, and H. Schulman. Chemical quenched flow kinetic studies indicate an intraholoenzyme autophosphorylation mechanism for Ca2+/calmodulin-dependent protein kinase II. *J Biol Chem*, 277(23):20991–20998, Jun 2002. doi: 10.1074/jbc.M202154200. URL `http://dx.doi.org/10.1074/jbc.M202154200`.

R. F. Bulleit, M. K. Bennett, S. S. Molloy, J. B. Hurley, and M. B. Kennedy. Conserved and variable regions in the subunits of brain type II Ca2+/calmodulin-dependent protein kinase. *Neuron*, 1(1):63–72, Mar 1988.

C. D. DeMaria, T. W. Soong, B. A. Alseikhan, R. S. Alvania, and D. T. Yue. Calmodulin bifurcates the local Ca2+ signal that modulates P/Q-type Ca2+ channels. *Nature*, 411(6836):484–489, May 2001. doi: 10.1038/35078091. URL `http://dx.doi.org/10.1038/35078091`.

Z. H. Gao, J. Krebs, M. F. VanBerkum, W. J. Tang, J. F. Maune, A. R. Means, J. T. Stull, and K. Beckingham. Activation of four enzymes by two series of calmodulin mutants with point mutations in individual Ca2+ binding sites. *J Biol Chem*, 268 (27):20096–20104, Sep 1993.

K. P. Giese, N. B. Fedorov, R. K. Filipkowski, and A. J. Silva. Autophosphorylation at Thr286 of the alpha calcium-calmodulin kinase II in LTP and learning. *Science*, 279(5352):870–873, Feb 1998.

P. I. Hanson, T. Meyer, L. Stryer, and H. Schulman. Dual role of calmodulin

in autophosphorylation of multifunctional CaM kinase may underlie decoding of calcium signals. *Neuron*, 12(5):943–956, May 1994.

A. Hoelz, A. C. Nairn, and J. Kuriyan. Crystal structure of a tetradecameric assembly of the association domain of Ca2+/calmodulin-dependent kinase II. *Mol Cell*, 11 (5):1241–1251, May 2003.

W. R. Holmes. Models of calmodulin trapping and CaM kinase II activation in a dendritic spine. *J Comput Neurosci*, 8(1):65–85, 2000.

M. B. Kennedy, T. McGuinness, and P. Greengard. A calcium/calmodulin-dependent protein kinase from mammalian brain that phosphorylates Synapsin I: partial purification and characterization. *J Neurosci*, 3(4):818–831, Apr 1983.

J. Kuznicki, Z. Grabarek, H. Brzeska, W. Drabikowski, and P. Cohen. Stimulation of enzyme activities by fragments of calmodulin. *FEBS Lett*, 130(1):141–145, Jul 1981.

W. E. Meador, A. R. Means, and F. A. Quiocho. Target enzyme recognition by calmodulin: 2.4 A structure of a calmodulin-peptide complex. *Science*, 257(5074): 1251–1255, Aug 1992.

S. G. Miller and M. B. Kennedy. Distinct forebrain and cerebellar isozymes of type II Ca2+/calmodulin-dependent protein kinase associate differently with the postsynaptic density fraction. *J Biol Chem*, 260(15):9039–9046, Jul 1985.

A. Persechini, K. McMillan, and P. Leakey. Activation of myosin light chain kinase and nitric oxide synthase activities by calmodulin fragments. *J Biol Chem*, 269 (23):16148–16154, Jun 1994.

O. S. Rosenberg, S. Deindl, R. J. Sung, A. C. Nairn, and J. Kuriyan. Structure of the autoinhibited kinase domain of CaMKII and SAXS analysis of the holoenzyme. *Cell*, 123(5):849–860, Dec 2005. doi: 10.029. URL `http://dx.doi.org/10.029`.

O. S. Rosenberg, S. Deindl, L. R. Comolli, A. Hoelz, K. H. Downing, A. C. Nairn, and J. Kuriyan. Oligomerization states of the association domain and the holoenyzme of Ca2+/CaM kinase II. *FEBS J*, 273(4):682–694, Feb 2006. doi: 10.1111/j.1742-4658.2005.05088.x. URL `http://dx.doi.org/10.1111/j.1742-4658.2005.05088.x`.

J. M. Shifman, M. H. Choi, S. Mihalas, S. L. Mayo, and M. B. Kennedy. Activation of Ca2+ /calmodulin-dependent protein kinase II by computationally designed mutant calmodulins. *In press*, ., 2006.

P. J. Sjostrom and S. B. Nelson. Spike timing, calcium signals and synaptic plasticity. *Curr Opin Neurobiol*, 12(3):305–314, Jun 2002.

A. M. Zhabotinsky. Bistability in the Ca(2+)/calmodulin-dependent protein kinase-phosphatase system. *Biophys J*, 79(5):2211–2221, Nov 2000.

R. M. Zucker, E. S. Hunter, and J. M. Rogers. Apoptosis and morphology in mouse embryos by confocal laser scanning microscopy. *Methods*, 18(4):473–480, Aug 1999. doi: 10.1006/meth.1999.0815. URL `http://dx.doi.org/10.1006/meth.1999.0815`.

Chapter 3

Model of the Interactions between Calmodulin and CaMKII

3.1 Introduction

CaMKII is a broad specificity Ser/Thr protein kinase. It is an important element within the Ca^{2+} secondary messenger cascades leading to long term potentiation (LTP) of synaptic currents. Each CaMKII subunit consists of a catalytic domain, a regulatory domain which contains an autoinhibitory region and a calmodulin binding region, and an association domain. Via its association domain CaMKII assembles into dodecameric holoenzymes (Bennett et al., 1983; Rosenberg et al., 2006). In the basal state the autoinhibitory domain is bound to the catalytic one. Binding of Ca^{2+} loaded calmodulin to the autoinhibitory region of CaMKII relieves its inhibition thus making the kinase active. After activation, CaMKII can autophosphorylate and this renders its activity Ca^{2+} independent (Miller and Kennedy, 1986).

There are a large number of models of CaMKII activation that have focused on different aspects of the role of CaMKII in signaling: activation in varying $[Ca^{2+}]$ (Kubota and Bower, 2001), bistability (Zhabotinsky, 2000), coupled with a model of dendritic spines (Holmes, 2000) and coupled with other signaling cascades (Hayer and Bhalla, 2005). These models implement a rather simple model for calmodulin binding to CaMKII, in which each CaMKII subunit binds calmodulin independently. This simple binding model is supported by experiments examining phosphorylation of a peptide substrate by CaMKII in varying calmodulin concentrations that show a hill

coefficient of approximately 1 (Gaertner et al., 2004). However, the recent elucidation of the structure of the autoinhibited catalytic domain of CaMKII (Rosenberg et al., 2005) shows that it dimerizes and the calmodulin binding regions have a coiled-coil interaction. This interaction suggests that two CaMKII subunits will cooperate in binding calmodulin. Thus, the curve describing formation of CaM-CaMKII as a function of calmodulin concentration can be fitted with a Hill function with have a Hill coefficient higher than 1.

Several experiments aimed at characterizing the binding of calmodulin to CaMKII made use of fluorescently labeled calmodulins. When calmodulin is tagged with a single fluorophor, its fluorescence intensity is a measure of binding and depends on the energetics of the interaction between calmodulin and CaMKII. Fluorescence anisotropy is a direct measure of binding, and does not depend on the energetics of the interactions. Other experiments use calmodulin tagged with two fluorophors, a donor and an acceptor, which permit resonant energy transfer (FRET). FRET is a measure of conformational changes of calmodulin which modify the distance between the two fluorescent probes. FRET is an indirect measure of calmodulin binding to CaMKII, by measuring the conformational changes of calmodulin following binding. An increase in FRET can be experimentally measured as an increase in the emission of the acceptor or a decrease in the emission of the donor. The later was used by Torok et al. (2001). The distance between the fluorophors in different calmodulin conformations can be obtained by measuring the lifetime of the donor in the metastable state.

Experiments looking at binding of fluorescently labeled calmodulin to CaMKII were performed, however they looked at formation of CaM-CaMKII as a function of CaMKII concentration. The change in fluorescence of CaM-C75-IAEDANS when binding to CaMKII as a function of CaMKII concentration is best fit by a Hill function with a Hill coefficient of approximately 2 (Gaertner et al., 2004, figure 4); (Rosenberg et al., 2005, supplemental figure 3). The change in FRET of AEDANS,DDP-T34C/T110/C-calmodulin (DA-Cal) when binding to CaMKII has a Hill coefficient of approximately 1 (Torok et al., 2001).

The kinetics of binding and unbinding of a fluorescently labeled calmodulin

(dansyl-CaM) from CaMKII were measured using fluorescence anisotropy (Meyer et al., 1992).

Measuring the intensity of fluorescent light, the binding/unbinding of fluorescently labeled calmodulins (TA-Cal and DA-Cal) to CaMKII shows multiple exponential decays (Torok et al., 2001; Tzortzopoulos and Torok, 2004). This rich behavior suggests a more complex mechanism of binding of calmodulin to CaMKII than assumed in previous models. The double-labeled AEDANS,DDP-T34C/T110/C-calmodulin (DA-Cal) is a FRET sensor. Torok et al. (2001) measured both the change in FRET intensity and in fluorescence life-time upon binding of DA-Cal to CaMKII. DA-Cal has a change in FRET when the distance between the two probes changes. One of the probes is bound to the N-lobe, while the other is bound to the C-lobe. Upon initial binding, the FRET of DA-Cal changes little because it has not yet wrapped around its target. However, when DA-Cal wraps around its target, the distance between the fluorophors changes which results in a strong change of DA-Cal FRET. Another fluorescent calmodulin, 2-chloro-(epsilon-amino-Lys75)-[6-[4-(N,N-diethylamino)phenyl]-1,3,5-triazin-4-yl] calmodulin (TA-Cal) (Torok and Trentham, 1994), has the property of fluorescing more strongly when TA-Cal is unwrapped-bound to CaMKII than wrapped-bound to CaMKII. TA-Cal is a useful sensor in looking at the early stages of calmodulin binding to CaMKII while DA-Cal is useful for late stages. Fluorescence anisotropy captures a mixture of the two.

This chapter focuses on constructing a detailed model of binding of calmodulin to CaMKII. This model is consistent with the experimental data previously enumerated, and can explain the apparent contradictions in the measurements of calmodulin binding to CaMKII using different fluorescently labeled calmodulins.

3.2 Model

3.2.1 Relationship between Macroscopic and Microscopic Parameters Characterizing Cooperative Binding

A binding reaction in which one of the reactants (CaMKII) has multiple binding sites for the other reactant (calmodulin) and the binding of the first calmodulin influences the subsequent binding of other calmodulins is called cooperative binding. There are two traditional methods of describing cooperative binding. Both are aimed at describing the fraction of CaMKII subunits that have calmodulin bound, as a function of calmodulin concentration, when the CaMKII is present in small concentrations.The first method is presented in figure 3.1, C. It represents a reactant, CaMKII dimer, with two equivalent binding sites for the other reactant, calmodulin. The binding of the first calmodulin, with affinity $1/Kd_1$, changes the affinity of the second calmodulin binding site to $1/Kd_2$. This method is useful as Kd_1 and Kd_2 can be directly approximated from a more complex state model such as figure 3.1, A. A second way to describe cooperative binding is by fitting the fraction of CaMKII bound to calmodulin as a function of calmodulin concentration with a Hill function. This is a macroscopic description and most of the experimental data in the literature are fitted with a hill function. The fraction of CaMKII subunits bound to calmodulin in the two methods are

$$fr_1(CaM) = \frac{CaM(CaM + Kd_2)}{(CaM^2 + 2\ CaM\ Kd_2 + Kd_1\ Kd_2)} \tag{3.1}$$

$$fr_2(CaM) = \frac{CaM^h}{CaM^h + Kd^h}. \tag{3.2}$$

To determine the macroscopic parameters, Kd and h, from the microscopic ones, Kd_1 and Kd_2 I have imposed two constraints on the macroscopic description. First, the macroscopic description should give the same concentration of calmodulin for

half-maximal binding as the microscopic one.

$$fr_1^{-1}\left(\frac{1}{2}\right) = fr_2^{-1}\left(\frac{1}{2}\right)$$

This leads to

$$Kd = \sqrt{Kd_1\ Kd_2}.$$

Second, the slope of the curve describing the fraction of CaMKII with calmodulin bound when the fraction is 1/2 should be the same for both descriptions.

$$\left.\frac{d\ fr_1(CaM)}{d\ CaM}\right|_{CaM=Kd} = \left.\frac{d\ fr_2(CaM)}{d\ CaM}\right|_{CaM=Kd}$$

This leads to

$$h = \frac{2}{1+\sqrt{\frac{Kd_2}{Kd_1}}}.$$

If the binding of the first calmodulin does not influence the binding of the second one, $Kd_2 = Kd_1$, the Hill coefficient h is 1. In the limit that the second calmodulin binds with an affinity much greater than the first one, $Kd_2 << Kd_1$, the Hill coefficient is 2.

The reaction scheme presented in figure 3.1 C can be used to describe the binding of calmodulin to CaMKII when calmodulin is present at small concentrations ($< Kd$). The fraction of calmodulin subunits that are bound to CaMKII is given by

$$fr(CaMKII) = \frac{CaMKII}{CaMKII + Kd_1}. \tag{3.3}$$

This is a Hill function with half-maximal activation at the dissociation constant of calmodulin from a CaMKII with one calmodulin bound, and a Hill coefficient of 1. Consequently, cooperativity between CaMKII subunits in binding calmodulin is not sufficient to explain the observed Hill coefficient close to 2 in experiments looking at calmodulin fluorescence in varying CaMKII concentration (Gaertner et al., 2004; Rosenberg et al., 2005).

3.2.2 Microscopic Model of Calmodulin Binding to CaMKII

CaMKII is a dodecameric holoenzyme (Rosenberg et al., 2006) with the association domains forming two rings of six subunits each. The catalytic domains of a subunit from the upper and one from the lower ring form a dimer. Because, from the structure, there appears to be little interaction between dimers formed by the catalytic subunits, I have assumed that the binding of calmodulin to each of the six dimers occurs independently. In addition, I have assumed that, in the basal state, some of the dimers are closed (catalytic domains directly bound to each other) and some are open.

In a closed CaMKII dimer, calmodulin binding domains of the two subunits are in close proximity and binding of a second calmodulin is sterically hindered. The amount of steric hindrance is difficult to estimate. Therefore two limit models were used. In the first model, presented in figure 3.1, it is considered impossible for a second calmodulin to bind to a closed CaMKII dimer. In the second model, presented in figure 3.2, the binding of a second calmodulin to a closed CaMKII dimer is considered to be unaffected by the first binding. These two models represent bounds for the exact steric hindrance.

3.2.2.1 Model of Calmodulin Binding to CaMKII that Neglects the State with Two Calmodulins Bound to a Closed CaMKII Dimer

The binding of one calmodulin to a closed CaMKII dimer (Dc) is modeled as a three-stage process.

- Calmodulin and CaMKII diffusing in solution have to find each other and start interacting. When a dimer formed by CaMKII catalytic domains is closed, only one side of the calmodulin binding domain is available. This side contains the residues responsible for interactions to the C lobe of calmodulin. When in closed proximity, the C lobe of calmodulin binds to one of the subunits in the dimer. The calmodulin is now unwrapped-bound to CaMKII (Dc1CaMu).

- Binding of the C lobe of calmodulin induces a conformational change in CaMKII

during which the dissociation of the two catalytic subunits allows the dimer to be in an open conformation (Do1CaMu). This is a monomolecular process and represents an isomerization step for CaMKII. It results in increased exposure of several residues that correspond to the binding sites of the N lobe of calmodulin.

- Exposure of these residues permits a conformational change of calmodulin in which calmodulin wraps around the calmodulin binding domain on CaMKII (Do1CaMw). The N lobe of calmodulin binds to the corresponding residues leading to a wrapped-bound calmodulin. It is considered that a calmodulin can not be wrapped-bound to a closed CaMKII dimer.

The binding of one calmodulin to an open CaMKII dimer (Do) is modeled as a two stage process.

- Calmodulin binds to one of the two subunits of the open dimer leading to formation of Do1CaMu directly.

- A conformational change of calmodulin follows leading to DoCaM1w.

The binding of a second calmodulin to a dimer that already has a calmodulin bound follows a similar process. All these reactions are considered reversible, and both the forward and reverse reactions are presented in figure 3.1. All the reaction loops in the model automatically satisfy the thermodynamic constraint that the change in the free energy of a system when going around a loop is zero.

One simplifying approximation I used is to neglect the state in which a dimer in closed conformation has two unwrapped-bound calmodulins. This approximation is motivated by the fact that a closed dimer has the two calmodulin binding domains in close vicinity, thus making it difficult for two calmodulins to be bound simultaneously in this conformation. Additionally, if two calmodulins do bind to a closed dimer, it is very likely that dimer will be stabilized in its open conformation.

The sequence of approximations presented in figure 3.1 is used to relate the microscopic reaction events to the macroscopically observable ones.

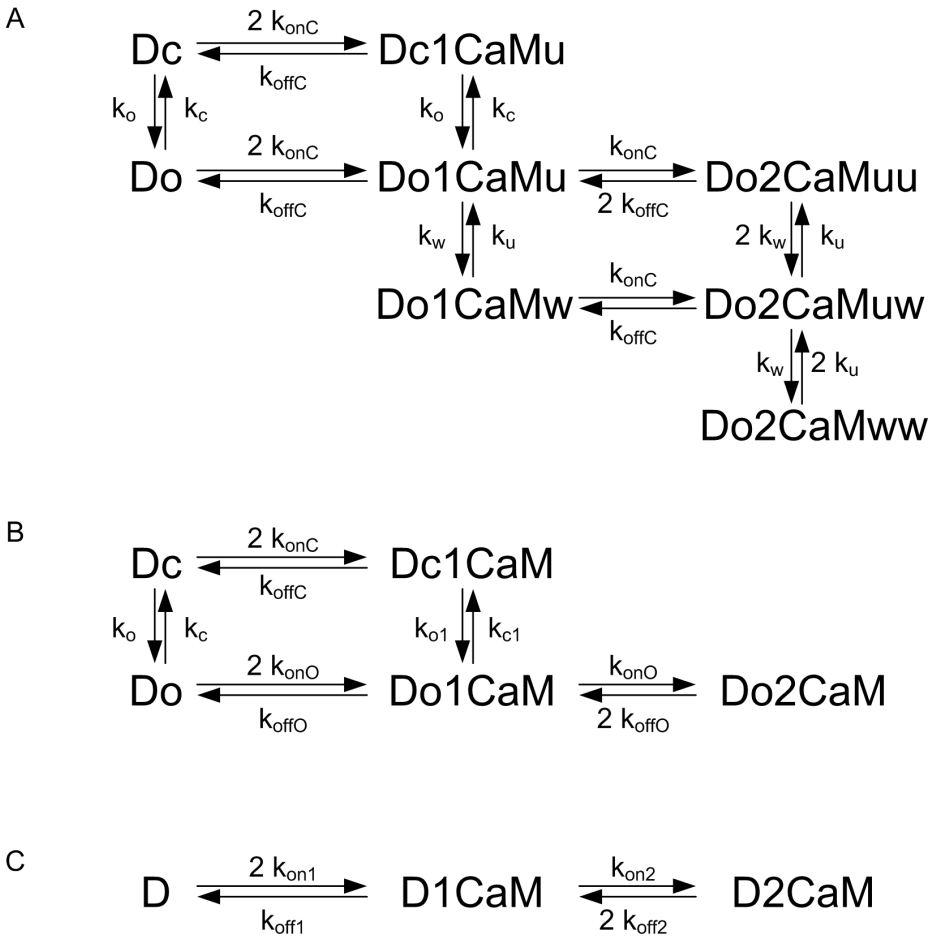

Figure 3.1. Models of calmodulin binding to CaMKII. **A**. Reaction scheme for calmodulin binding to CaMKII following the stages implied from structures. This reaction scheme keeps track of the conformational transitions of both CaMKII and calmodulin. I assume that the binding of a second calmodulin to a closed dimer is strongly sterically hindered. **B**. Reaction scheme for calmodulin binding pooling the wrapped and unwrapped states of calmodulin to an open dimer. This reaction scheme keeps track of the conformational transitions of CaMKII but not those of calmodulin. **C**. Reaction scheme for calmodulin binding, characterizing the state of a CaMKII dimer only by the number of calmodulins bound to it. See text for description of terms.

1. The first reaction scheme (figure 3.1 A) follows the microscopic transitions enumerated above. It keeps track of the conformational states of both calmodulin and CaMKII. The states and parameters described in figure 3.1 A are:

   - Dc - closed CaMKII dimer with no calmodulin bound
   - Dc1CaMu - closed CaMKII dimer with one unwrapped-bound calmodulin
   - Do - open CaMKII dimer with no calmodulin bound
   - Do1CaMu - open CaMKII dimer with one unwrapped-bound calmodulin
   - Do1CaMw - open CaMKII dimer with one wrapped-bound calmodulin
   - Do2CaMuu - open CaMKII dimer with two unwrapped-bound calmodulins
   - Do2CaMuw - open CaMKII dimer with two bound calmodulin, one unwrapped-bound, the other wrapped-bound
   - Do2CaMww - open CaMKII dimer with two wrapped-bound calmodulin
   - k_{onC} - on rate constant of calmodulin to a CaMKII subunit in a closed CaMKII dimer
   - k_{offC} - off rate constant of calmodulin from closed CaMKII dimers
   - k_o - rate of opening of CaMKII dimers
   - k_c - rate of closing of CaMKII dimers
   - k_w - rate of calmodulin transition from unwrapped-bound to wrapped-when calmodulin is bound to open CaMKII dimers
   - k_w - rate of calmodulin transition from wrapped-bound to unwrapped-when calmodulin is bound to open CaMKII dimers

   This reaction scheme is needed to describe the kinetic experiments of fluorescently labeled calmodulin binding to or unbinding from CaMKII. Fluorescently labeled calmodulins have different fluorescence in different calmodulin conformations, so keeping track of these conformations is necessary.

I have assumed that the rate constant of the initial binding of calmodulin is the same for open or closed dimers (k_{onC}). The initial stages of interaction between calmodulin and open or closed CaMKII dimers should be similar and are, at least in part, limited by diffusion.

2. The second reactions scheme (figure 3.1 B) pools the states in which a CaMKII dimer has the same conformation and the same number of calmodulin bound. It keeps track of the conformational changes of the CaMKII dimer but not of calmodulin.

   - $[Do1CaM] = [Do1CaMu] + [Do1CaMw]$ open CaMKII dimer with one calmodulin bound
   - $[Do2CaM] = [Do2CaMuu]+[Do2CaMuw]+[Do2CaMww]$ open CaMKII dimer with two calmodulins bound
   - k_{onO} - on rate constant of calmodulin to a CaMKII subunit in an open CaMKII dimer
   - k_{offO} - off rate constant of calmodulin from an open CaMKII dimers
   - k_{o1} - rate of opening of CaMKII dimers with one calmodulin bound
   - k_{c1} - rate of closing of CaMKII dimers with one calmodulin bound

   This reaction scheme is useful in describing CaMKII activation in which detail about CaMKII dimer conformation is needed while detail about calmodulin conformation is not. I used only this scheme to describe the simultaneous interactions of CaMKII dimers with calmodulin and with exogenous substrates. This reduced order model also provides a good description of the conformational changes of calmodulin if the conformational changes of calmodulin are faster than the conformational changes of CaMKII ($kw + ku >> ko + kc$), and if few of the two-calmodulin bound dimers have two unwrapped-bound calmodulins ($2kw >> ku$). Under these conditions, the relations between the parameters in

figure 3.1 A and B are

$$\begin{aligned} k_{onO} &\cong k_{onC}, \quad k_{offO} \cong k_{offC}\frac{k_u}{k_w + k_u} \\ k_{o1} &\cong k_o, \quad k_{c1} \cong k_c\frac{k_u}{k_w + k_u}. \end{aligned} \tag{3.4}$$

Note that in the results section I will describe how the parameters for scheme B were obtained from data fitted with scheme A. scheme A assumes the approximation that the initial binding of calmodulin is the same for open and closed CaMKII dimers. Thus, the parameters I use when implementing scheme B also assume this approximation, although scheme B does not require this approximation.

3. The third reaction scheme (figure 3.1 C) pools the states in which CaMKII dimers have the same number of calmodulins bound. It does not keep track of either the conformational changes of CaMKII or of calmodulin. The states of CaMKII are characterized by the number of calmodulins bound. This reaction scheme is useful in describing equilibrium binding of calmodulin and CaMKII. K_{D1} and K_{D2} are the macroscopic affinities for binding of the first and second calmodulin. Additionally,

$$K_{DC} = \frac{k_{offC}}{k_{onC}}, \quad K_{DO} = \frac{k_{offO}}{k_{onO}}, \quad K_{i1} = \frac{k_{o1}}{k_{c1}}. \tag{3.5}$$

The values for the macroscopic affinities are given by:

$$\begin{aligned} K_{D1} &= K_{DC}\frac{1}{K_{i1}+1} + K_{DO}\frac{K_{i1}}{K_{i1}+1} \\ K_{D2} &= K_{DO}\left(1 + \frac{1}{K_{i1}}\right). \end{aligned} \tag{3.6}$$

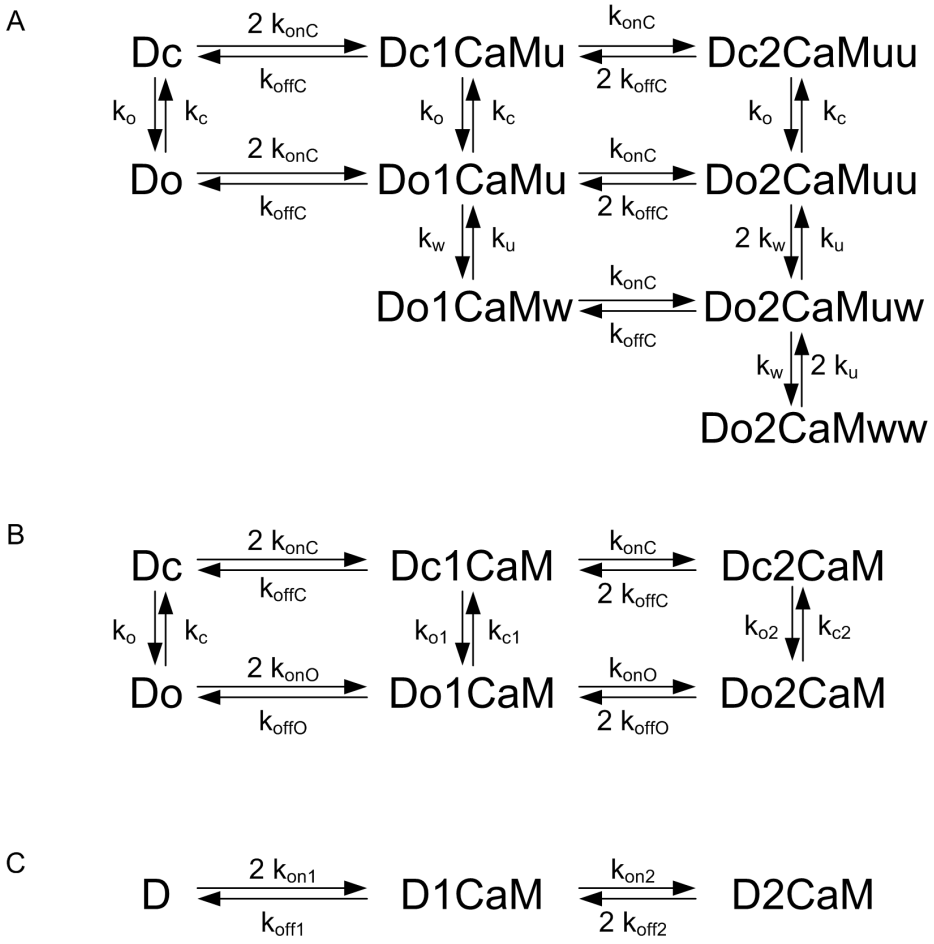

Figure 3.2. Model of calmodulin binding to CaMKII which includes a state with two calmodulin bound to a closed CaMKII dimer. The series of approximations for this model is the same as the one in 3.1. **A**. Reaction scheme for calmodulin binding to CaMKII following the stages implied from structures. This reaction scheme keeps track of the conformational transitions of both CaMKII and calmodulin. I assume that the binding of a second calmodulin to a closed dimer is strongly sterically hindered. **B**. Reaction scheme for calmodulin binding pooling the wrapped and unwrapped states of calmodulin to an open dimer. This reaction scheme keeps track of the conformational transitions of CaMKII but not those of calmodulin. **C**. Reaction scheme for calmodulin binding, characterizing the state of a CaMKII dimer only by the number of calmodulins bound to it.

3.2.2.2 Model of Calmodulin Binding to CaMKII that Neglects the Steric Hindrance for the Binding of a Second Calmodulin to a Closed CaMKII Dimer

The second model used neglects the steric hindrance for the binding of a second calmodulin to a closed CaMKII dimer and is presented in figure 3.2. The same series of approximations is used in the second model. The relation between reaction schemes A and B in figure 3.2 is given by:

$$\begin{aligned} k_{onO} &\cong k_{onC}, \quad k_{offO} \cong k_{offC}\frac{k_u}{k_w + k_u} \\ k_{o1} &\cong k_o, \quad k_{c1} \cong k_c\frac{k_u}{k_w + k_u} \\ k_{o2} &\cong k_o, \quad k_{c2} \cong k_c\left(\frac{k_u}{k_w + k_u}\right)^2. \end{aligned} \tag{3.7}$$

The parameters which are common in the models described inf figures 3.1 and 3.2 are given by the same equations as (3.5).

The relations between reactions schemes B and C in figure 3.2 are given by:

$$\begin{aligned} K_{D1} &= K_{DC}\frac{1}{K_{i1}+1} + K_{DO}\frac{K_{i1}}{K_{i1}+1} \\ K_{D2} &= K_{DC}\frac{1}{K_{i2}+1} + K_{DO}\frac{K_{i2}}{K_{i2}+1} \end{aligned} \tag{3.8}$$

$$\begin{aligned} where \quad K_{DC} &= \frac{k_{offC}}{k_{onC}} \\ K_{DO} &= \frac{k_{offO}}{k_{onO}} \\ K_{i1} &= \frac{k_{o1}}{k_{c1}} \\ K_{i2} &= \frac{k_{o2}}{k_{c2}} \end{aligned} \tag{3.9}$$

3.2.3 Effects of Substrates of CaMKII on Calmodulin Binding to CaMKII

In order to assess the effects of the presence of protein substrates that are phosphorylated by CaMKII on calmodulin binding I assumed that CaMKII substrates bind only to open CaMKII dimers, and that the binding of the substrate is independent of the binding of calmodulin. Since the conformation of CaMKII is important for substrate binding while the conformation of calmodulin is not, the reaction scheme B in figure 3.1 was expanded to include substrate binding (figure 3.3).

Scheme A in figure 3.3 can be simplified to scheme 3.3 B when used to describe the equilibrium binding of calmodulin and substrate to CaMKII. Scheme 3.3 B can be used to describe kinetics as well if the substrate binding kinetics are faster than those of calmodulin, and at every intermediate step in calmodulin binding, the binding of substrate reaches equilibrium. Scheme 3.3 B has the advantage of being identical to scheme 3.1 B, with the exception of the kinetics of closing of an open CaMKII dimer (k_{cs} and k_{cs1}). These two parameters relate to those describing the closing of an open CaMKII dimer in the absence of substrate by:

$$\begin{aligned} k_{cs} &= k_c \left(\frac{K_{Ds}}{K_{Ds} + [S]} \right)^2 \\ k_{c1s} &= k_{c1} \left(\frac{K_{Ds}}{K_{Ds} + [S]} \right)^2 . \end{aligned} \tag{3.10}$$

I also built a very similar model, which is presented in figure 3.4, starting from the model of calmodulin/CaMKII interactions presented in figure 3.2. It includes the state with two calmodulin bound to a closed CaMKII dimer. The additional parameter for that model is given by the same equation:

$$k_{c2s} = k_{c2} \left(\frac{K_{Ds}}{K_{Ds} + [S]} \right)^2 . \tag{3.11}$$

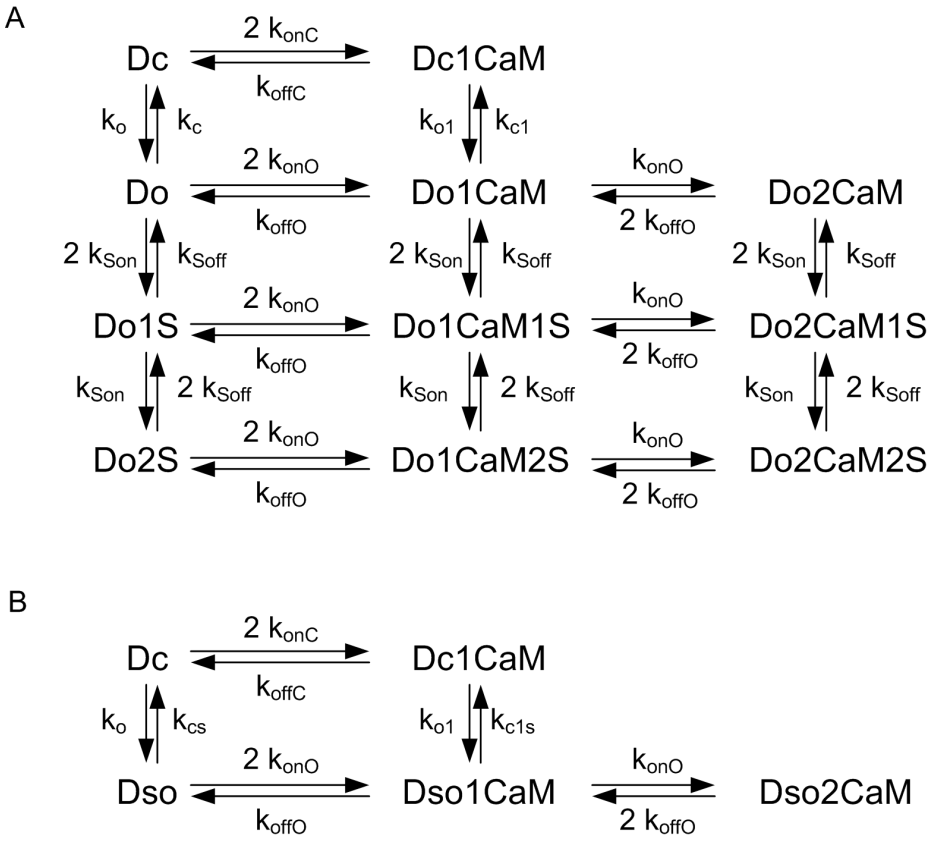

Figure 3.3. Model of simultaneous binding of substrate and calmodulin to CaMKII. **A**. It is assumed that CaMKII substrates bind only to open CaMKII dimers, and the binding of the substrate is independent on the binding of calmodulin. It is an extension of scheme B in figure 3.1. **B**. Simplified model for calmodulin binding to CaMKII in the presence of substrate. This model pools the open dimer states which have the same number of calmodulins bound: $[Dso] = [Do] + [Do1S] + [Do2S]$, $[Dso1CaM] = [Do1CaM] + [Do1CaM1S] + [Do1CaM2S]$, $[Dso2CaM] = [Do2CaM] + [Do2CaM1S] + [Do2CaM2S]$.

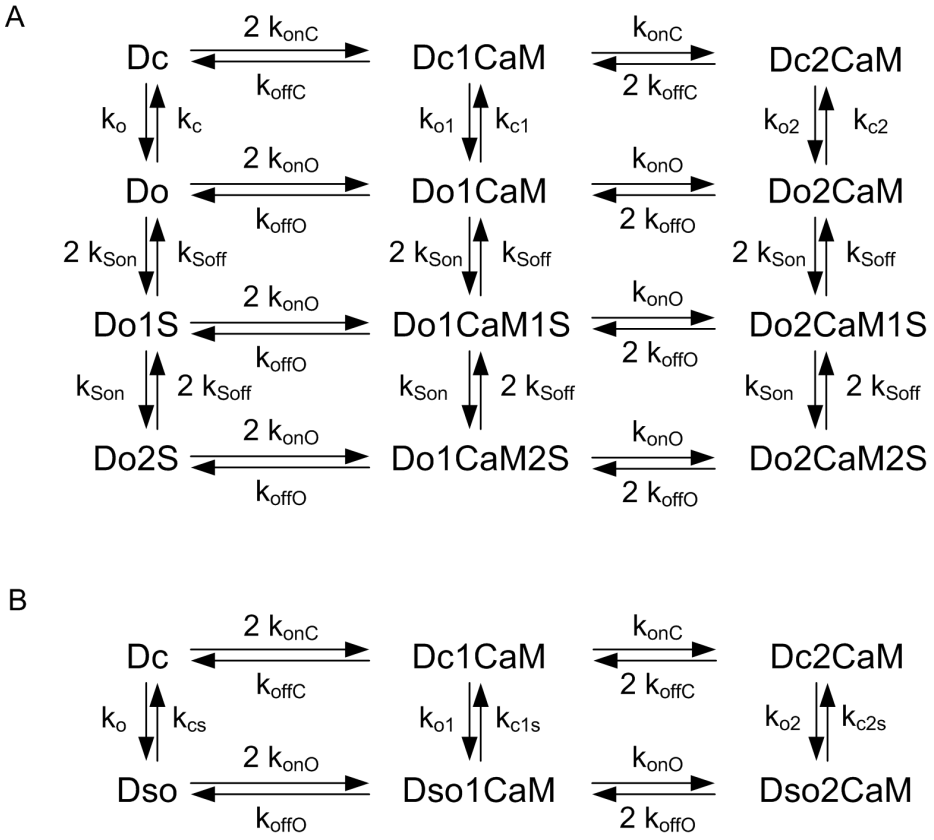

Figure 3.4. Model of simultaneous binding of substrate and calmodulin to CaMKII. **A**. It is assumed that CaMKII substrates bind only to open CaMKII dimers, and the binding of the substrate is independent on the binding of calmodulin. It is an extension of scheme B in figure 3.2. **B**. Simplified model for calmodulin binding to CaMKII in the presence of substrate.

These three equations represent the intuitive result that the only effect the substrate has on calmodulin binding is to increase the probability of a CaMKII dimer being in the open conformation.

3.3 Results

3.3.1 Determining the Parameters of the Model

Torok et al. used TA-Cal (single fluorophor) and DA-Cal (FRET fluorophors) to measure the kinetics of calmodulin binding to CaMKII (Torok et al., 2001; Tzortzopoulos and Torok, 2004). Both TA-Cal and DA-Cal have the property of fluorescing differently when calmodulin is unwrapped-bound or wrapped-bound. They can be used to indirectly assess the conformation of CaMKII as well, since when bound to a closed dimer calmodulin is unwrapped, and when bound to an open dimer some of the calmodulin is wrapped. The reaction scheme presented in figure 3.1 is an extension of Torok et al. (2001, scheme 1) which takes into account conformational changes of CaMKII in addition to those of calmodulin. The reaction scheme from Torok et al. (2001, scheme 1) is equivalent to one calmodulin binding to and unbinding from an open CaMKII dimer. I have reanalyzed their data to: put bounds on the kinetics of the conformational changes of calmodulin (section 3.3.1.1), calculate the fraction of calmodulin which is unwrapped when bound to open CaMKII dimers and the on and off rates of calmodulin from closed CaMKII dimers (section 3.3.1.2), and estimate the rates of opening and closing of CaMKII dimers (section 3.3.1.3).

3.3.1.1 Fluorescent Calmodulins Binding to Peptides

Experiments were performed at 21^{o}C using TA-Cal and DA-Cal (Torok et al., 2001; Torok and Trentham, 1994) were used to constrain how rapid the wrapping/unwrapping of these fluorescent calmodulins is. The change in FRET of DA-Cal when binding to peptides is the result of two serial reactions. DA-Cal first binds to

the peptide. This is followed by a conformational change in which DA-Cal wraps around its binding domain. The rate of change in FRET of DA-Cal as a function of peptide concentration should thus reach a plateau, and the maximal rate should be given by $k_w + k_u$. The rates of change in FRET of DA-Cal in different concentrations of several CaMKII-derived peptides were measured (Torok et al., 2001, figure 5). For the concentrations of peptide used, the rate does not reach a plateau. The highest value observed for this rate was $300s^{-1}$. Thus, the conformational changes of DA-Cal ($k_{w\ DA-Cal} + k_{u\ DA-Cal} > 300s^{-1}$) appear to be much faster than DA-Cal binding.

Figure 4 from Torok and Trentham (1994), which describes the interaction of TA-Cal with calmodulin binding peptides $k_{w\ TA-Cal} + k_{u\ TA-Cal} = 0.93\ s^{-1}$, reveals a relatively slow transition between unwrapped-bound to wrapped-bound state. Consequently, TA-Cal is useful for analyzing the initial binding of calmodulin binding to CaMKII before it makes the conformational transition to the wrapped state. For TA-Cal the reaction scheme in fig. 3.1 A has to be used.

3.3.1.2 Kinetics of Calmodulin Binding to CaMKII

When calmodulin is bound to an open dimer, the ratio of unwrapped-bound calmodulin to the wrapped-bound calmodulin can be calculated from the measurements of the lifetime of DA-Cal fluorescence after it has bound to CaMKII (Torok et al., 2001, figure 1, E). The estimate for the unwrapped-bound calmodulin to total calmodulin bound to open dimers is obtained from a simulation based on scheme A in figure 3.1 $k_u/(k_w + k_u) = 0.214$. This ratio is consistent with approximations used to obtain scheme B in figure 3.1.

The parameter values for the first stage of calmodulin binding to CaMKII were obtained from studies using TA-Cal. They are: $k_{onC} = 21\ 10^6\ M^{-1}\ s^{-1}$ (Torok et al., 2001, figure 3, B) $k_{offC} = 3.3s^{-1}$ (Torok et al., 2001, figure 3, C). When calmodulin binds to a closed CaMKII dimer, it can not wrap around its binding site before the CaMKII dimer opens. The dissociation constant of calmodulin from a closed CaMKII dimer is $K_{DC} = k_{offC}/k_{onC} = 157\ nM$. Since the conformational changes of calmodulin (DA-Cal) from unwrapped-bound to wrapped-bound are rapid, in terms

of scheme B in figure 3.1, k_{onO} is 21 10^6 M^{-1} s^{-1}.

There are several ways to calculate the off rate of calmodulin from an open CaMKII dimer. One uses the ratio between unwrapped-bound calmodulin and total bound calmodulin and equation 3.5. This leads to a $k_{offO} = 0.71$ s^{-1} and a corresponding $K_{DO} = 34$ nM.Bounds on k_{offO} can be obtained from experiments looking at the displacement of fluorescent calmodulin by WT calmodulin. The slow rate of unbinding of TA-Cal (Torok et al., 2001, fig. 3, C), which depends on both k_{offO} and on $k_{uTA-Cal}$ puts a lower limit on $k_{offO} > 0.36$ s^{-1}. The rate of unbinding of DA-Cal (Torok et al., 2001, fig. 2, D), which is a parallel unbinding from both closed and open dimers, puts an upper limit on $k_{offO} < 1.8$ s^{-1}. Thus, the calculated values for the kinetic parameters for calmodulin binding to CaMKII are consistent with several experiments which were not used to determine these values.

3.3.1.3 Conformational Changes of CaMKII

The FRET of DA-Cal changes mostly during the transition from unwrapped-bound calmodulin to wrapped-bound calmodulin. When DA-Cal is mixed with CaMKII, the observed change in FRET is the result of two parallel processes. The first process begins when DA-Cal binds to a closed dimer then the dimer opens up and allows DA-Cal to bind and wrap. This process is limited by either the DA-Cal binding to closed CaMKII dimers or the opening of the CaMKII dimer, depending on the CaMKII concentration. The dependence of the rate for this process on CaMKII concentration reaches a plateau, with a plateau value of approximately k_o. The second process consists of DA-Cal binding to already open CaMKII dimers, followed by a rapid DA-Cal isomerization to the wrapped from. The observed on rate for this process is linear with CaMKII concentration, with the rate $k_{obs2} \cong [CaMKII_{free}]k_{onC}k_o/(k_o+k_c)$. The total rate for the two processes is their sum: $k_{obs} \cong k_o+[CaMKII_{free}]k_{onC}k_o/(k_o+k_c)$.

The parameters characterizing the conformational changes of CaMKII (k_o and k_c) were fit from measurements of binding of DA-Cal to T286A CaMKII (Tzortzopoulos

and Torok, 2004, fig 3 C).

$$k_o \cong 1.67 s^{-1}, \quad \frac{k_o}{k_o + k_c} = 1.8/21 \tag{3.12}$$

This leads to $k_c = 19.5\ s^{-1}$. Using these constants it can be calculated from figure 3.1 A that for T286A CaMKII in the absence of calmodulin 8.5% of the dimers are in the open conformation. At equlibrium, the fraction of CaMKII dimers which have only one calmodulin bound that are open is 30%.

3.3.1.4 Macroscopic Dissociation Constants

The parameters I have discussed for the model of calmodulin binding to CaMKII are all microscopic constants. Using the series of approximations presented in figure 3.1, the estimated values for macroscopic binding of calmodulin to CaMKII dimers are: $K_D = 120$ nM and h = 1.01. Using the series of approximations presented in figure 3.2 the estimated values for macroscopic binding of calmodulin to CaMKII dimers are: $K_D = 97$ nM and h = 1.12. A surprising result is that even though the affinity of calmodulin for open CaMKII dimers is approximately 5 times larger than for closed CaMKII dimers, the Hill coefficient describing the macroscopic binding is relatively small.

3.3.1.5 Effects of Temperature on Kinetics

The measurements using both TA-Cal and DA-Cal were performed at 21 ^oC. To estimate the parameter values at 30 ^oC I have used the fluorescence anisotropy measurements performed by (Meyer et al., 1992). The values at 30^oC for dansylated calmodulin are $k_{onC\ dans} = 1.5\ 10^8\ M^{-1}\ s^{-1}$ and $k_{offO\ dans} = 2.2\ s^{-1}$. However, from competition assays it is known that dansylated calmodulin has a 3 times higher affinity for CaMKII than does WT calmodulin. The values I used for WT calmodulin are $k_{onC} = 1\ 10^8\ M^{-1}\ s^{-1}$ and $k_{offO} = 4.3\ s^{-1}$, which lead to a $K_D = 43\ nM$. This corresponds to a 5-fold increase in the on rate, a 6-fold increase in the off rate and a small, 20%, decrease in affinity at 30 ^oC compared to 21 ^oC.

3.3.2 Simulations of Calmodulin Binding to CaMKII

The binding of Calmodulin to CaMKII occurs on two time scales. The faster time scale corresponds to the rapid binding and unbinding of calmodulin to closed CaMKII dimers. The slower time scale corresponds to opening of the CaMKII dimers and subsequent wrapping of calmodulin around its binding site. The time dependence of the fraction of CaMKII subunits with calmodulin unwrapped-bound (green line in 3.5, C) is similar to the observed time dependence of the fluorescence of TA-Cal when it binds to CaMKII. The time dependence of the fraction of CaMKII subunits with calmodulin wrapped-bound (red line in 3.5, C) is similar with the observed time dependence of the FRET of DA-Cal as it binds to CaMKII.

3.3.3 Time Dependence of Ca^{2+}/Calmodulin-Dependent Activation of CaMKII

I assume that a calmodulin bound to an open CaMKII dimer is required for a subunit to be catalytically active, an assumption that is consistent with the structure of CaMKII catalytic domain (Rosenberg et al., 2005). The fraction of CaMKII dimers that are in the open conformation (8.5%) can be directly activated by calmodulin binding. The fraction of CaMKII dimers that are in the closed conformation (91.5%) require the additioanl step of CaMKII dimer opening after the binding of calmodulin. When high concentrations of Ca^{2+}-loaded calmodulin are present for short periods, for example in the vecinity of an NMDAR channel, the CaMKII dimer opening is the limiting step in Ca^{2+}/calmodulin-dependent CaMKII activation, as seen in figure 3.6.

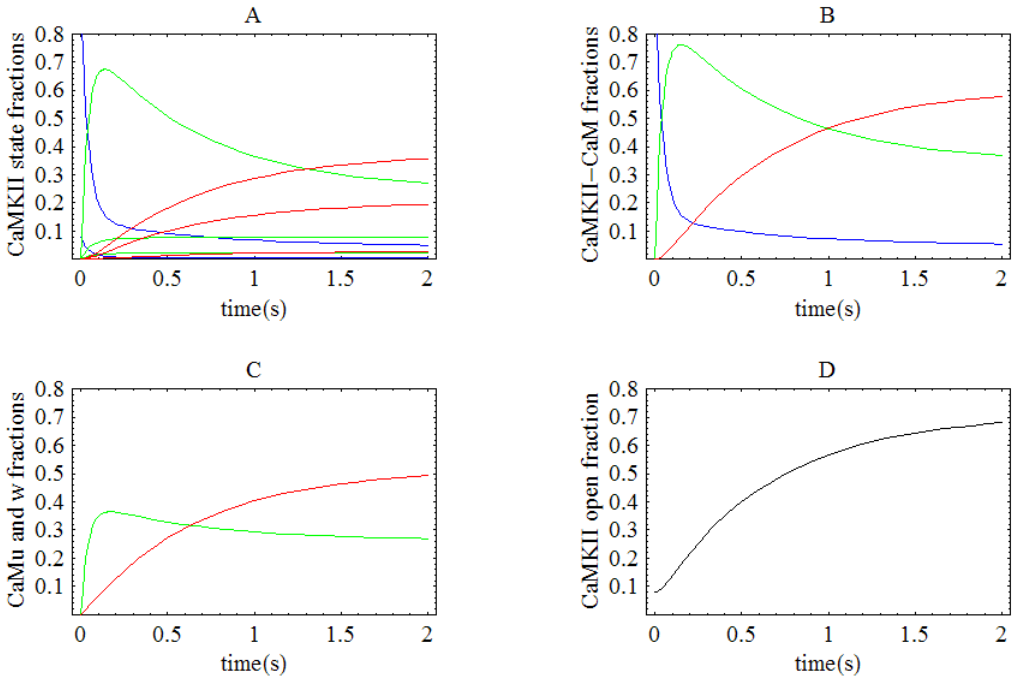

Figure 3.5. Simulation of the time dependence of binding of 500 μM calmodulin with 100 μM CaMKII in term of reaction scheme A in figure 3.1. **A.** Fraction of CaMKII in different sates corresponding to reaction scheme A. The blue graphs correspond to Dc top, Do bottom. The green graphs correspond to Dc1CaMu top, Do1CaMw middle, Do1CaMu bottom. The red graphs correspond to Do2CaMww top, Do2CaMuw middle, Do2CaMuu bottom. **B.** Fraction of CaMKII with different numbers of calmodulin bound. The blue line represents CaMKII dimers with no calmodulin bound, the green line represents CaMKII dimers with one calmodulin bound while the red line represents CaMKII dimers with two calmodulin bound. They are the sum of the blue, green and red graphs from panel A respectively. **C.** Green line represents the fraction of CaMKII subunits which have calmodulin unwrapped-bound. It is similar to the fluorescence of TA-Cal in rapid mixing experiments. Red line represents the fraction of CaMKII subunits which have calmodulin wrapped-bound. It is similar to the FRET of DA-Cal in rapid mixing experiments. **D.** The fraction of CaMKII dimers which are in the open conformation. The line starts at 0.08 which is the fraction of open dimers in the absence of Ca^{2+}/calmodulin.

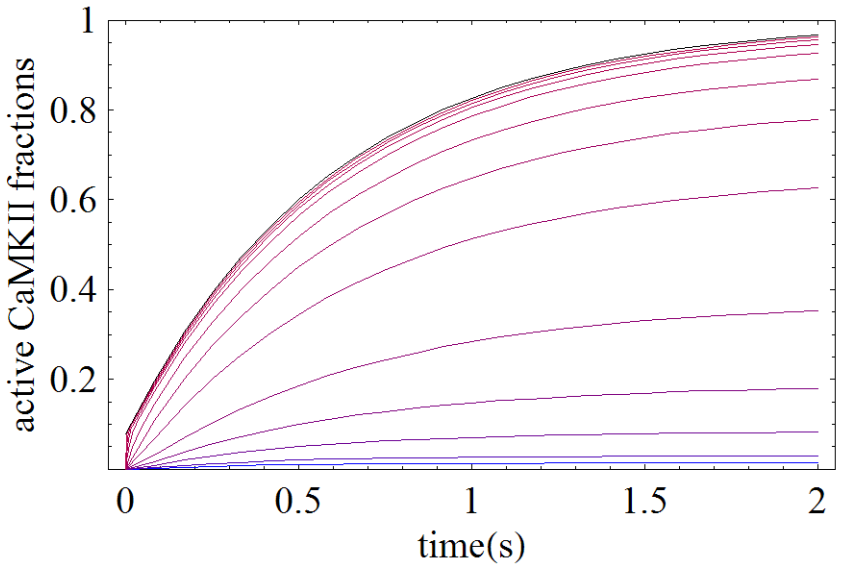

Figure 3.6. Activation of CaMKII as a function of time in: 0.01, 0.02, 0.05, 0.1, 0.2, 0.5, 1, 2, 5, 10, 20, 50 μM calmodulin, from blue to red graphs. The black line, which represents the asymptotic behavior in large calmodulin concentrations is $f + (1 - f)\left(1 - e^{k_o\ t}\right)$ where $f = k_o/(k_o + k_c)$ the fraction of CaMKII dimers open in the basal state.

3.4 Discussion

3.4.1 Nonhomogenous Basal State of CaMKII

Recently, there has been some controversy regarding the structure of CaMKII. Kolodziej et al. (2000), using cryo-EM studies, have reported a structure in which the individual catalytic domains of CaMKII are several nanometers above and below the symmetry plane in which the association domains reside. This structure was later observed again for homogeneous CaMKII holoenzymes formed by all CaMKII subunit types (Gaertner et al., 2004). However cryo-EM studies by a different group (Morris and Torok, 2001), and more recently small X-ray scattering experiments (Rosenberg et al., 2005), have revealed a structure in which the catalytic domains from dimers that are within the plane of symmetry of the holoenzyme. It has been suggested that the first structure might represent activated CaMKII; whereas, the second might represent inactive CaMKII.

Our estimates suggest that the basal state of CaMKII holoenzymes is heteroge-

neous. Over 90% of the catalytic domains are dimerized in the absence of Ca^{2+}, and as such lie in the plane of symmetry, while roughly 8% are in the open conformation. The fraction of CaMKII dimers in the open conformation is influenced by other factors such as the presence of CaMKII substrates. Thus, it is possible that different experimental conditions such as those in (Kolodziej et al., 2000) and (Rosenberg et al., 2005) alter the heterogeneous basal state towards either open or closed conformations.

3.4.2 Different Fluorescence of Unwrapped- and Wrapped-Bound Fluorescent Calmodulins

One of the most puzzling experimental results regarding calmodulin binding to CaMKII is the Hill coefficient close to 2 observed when plotting bound calmodulin as a function of CaMKII (Gaertner et al., 2004, fig 4). These experimental results were confirmed by (Rosenberg et al., 2005, supplemental figure 3). A possible explanation for these results is that the fluorescent calmodulin used in these studies (which is similar to TA-Cal, in having the fluorescent probe bound to the same residue, 75) fluoresces mainly when unwrapped-bound to CaMKII. When one calmodulin is bound to a CaMKII dimer, the calmodulin has a higher probability to be in the unwrapped-bound state then when two calmodulins are bound. Consequently, a calmodulin bound to CaMKII will have a higher fluorescence when it is bound alone to a dimer versus when two calmodulins are bound. This effect accounts for an apparent cooperativity between calmodulins when binding to CaMKII. However, even assuming that the fluorescence of double bound calmodulin to CaMKII is the same as that of free calmodulin, the effect would be smaller than that observed by (Gaertner et al., 2004). The only possibility I found to obtain an effect of a similar magnitude is to assume that the fluorescence of calmodulin when two calmodulins are bound to CaMKII is smaller than that of free calmodulin. This has as a side effect that when a high Hill coefficient is measured, the relative fluorescence in low CaMKII concentrations can be negative. This negative relative fluorescence is observed in (Gaertner et al., 2004, fig. 4 B), for β CaMKII, for which the highest Hill coefficient

Isoform	K_D	$h_{measured}$	h_0	h_{-1}
α CaMKII	62.4±25.1	1.9±0.7	1.24±0.02	1.8±0.03
β CaMKII	25.7±7.9	2.4±0.9	1.51±0.03	3.12±0.66
γ CaMKII	6.9±1.4	2.1±0.3	1.5±0.02	2.28±0.21
δ CaMKII	33.5±13.2	1.6±0.3	1.14±0.01	1.2±0.01

Table 3.1. Comparison of reported and simulated apparent Hill coefficients. The values for the dissociation constant and Hill coefficient are reported from (Gaertner et al., 2004). The values for the Hill coefficients h_0 and h_{-1} are fitted from simulations assuming the fluorescence of the double bound state, F_{D2CaM} is 0 or -1 respectively.

was measured.

To obtain a predicted Hill coefficient I performed a set of simulation of calmodulin binding to CaMKII according to scheme 3.4 B. The concentrations of CaMKII used in these simulations was the same as that used in the experiments from (Gaertner et al., 2004, fig. 4). For the half binding values I used their reported dissociation constants (summarized in table 3.1). This method predicts that the observed Hill coefficient when varying CaMKII concentration depends strongly on the ratio of the concentration of calmodulin used to its dissociation constant from CaMKII. It also depends on the actual cooperativity between CaMKII subunits in binding calmodulin. The authors of Gaertner et al. (2004) mention that they used either 25 nM or 100 nM calmodulin in their measurements, however they do not mention which value was used for which isoform. The assumption that the fluorescence of wrapped calmodulin is smaller than that of free calmodulin results in simulation results being consistent with their measurements if they used 100 nM calmodulin for α and β CaMKII and 25 nM calmodulin for γ and δ CaMKII isoforms.

This result is further supported by measurements of DA-Cal FRET as a function of CaMKII concentration. DA-Cal FRET is stronger when bound to open CaMKII dimers than to closed CaMKII dimers. The observed DA-Cal FRET as a function of CaMKII concentration is best fit with a Hill function with a Hill coefficient of 1 (Torok et al., 2001).

3.4.3 Lag in CaMKII Activation

A surprising effect of the dimeric structure of the CaMKII catalytic domain is that the time constant for the transformation from the closed to the open state (isomerization constant) imposes minimum time for Ca^{2+}/calmodulin-dependent activation of CaMKII. The time scale for Ca^{2+}/calmodulin-dependent activation of CaMKII in saturating Ca^{2+} and calmodulin is $\approx$ 500 ms. This value is of particular importance in subcellular compartments in which Ca^{2+} concentration fluctuates rapidly.

The measurements which I used to calculate the value of the isomerization constant were performed at 21^{o}C. I can not estimate its dependence on temperature as measurements at other temperatures are not available. The fold change over 10^{o}C for the on and off rates of calmodulin for CaMKII were roughly 6. If the isomerization constant has the same trend (Q_{10}), at 37^{o}C this process will be one order of magnitude faster than at 21^{o}C.

3.4.4 Effects of Substrate on Isomerization of CaMKII from the Closed to the Open States

The presence of CaMKII substrates has the effect of pushing the conformation of CaMKII dimers toward the open conformation. This has several consequences for the binding of calmodulin to CaMKII. The apparent affinity of calmodulin for CaMKII is increased, and the Hill coefficient gets closer to 1. In conditions of saturating substrate, both models 3.3 and 3.4 for calmodulin binding led to the same macroscopic dissociation constants for calmodulin binding to open CaMKII dimers: $Kd = 34\ nM$ and $h = 1$. The Hill coefficient of 1 obtained in saturating substrate is independent of the values of all the parameters in this model, and is dependent only on the assumption that substrate and calmodulin binding are independent. This can explain the low Hill coefficient of the measurements of Ca^{2+}/calmodulin-dependent CaMKII phosphorylation of exogenous substrate (Gaertner et al., 2004, fig. 5). Another effect of the presence of saturating CaMKII substrate is that the lag time observed in

Ca^{2+}/calmodulin-dependent activation of CaMKII decreases to zero.

Bibliography

M. K. Bennett, N. E. Erondu, and M. B. Kennedy. Purification and characterization of a calmodulin-dependent protein kinase that is highly concentrated in brain. *J Biol Chem*, 258(20):12735–12744, Oct 1983.

Tara R Gaertner, Steven J Kolodziej, Dan Wang, Ryuji Kobayashi, John M Koomen, James K Stoops, and M. Neal Waxham. Comparative analyses of the three-dimensional structures and enzymatic properties of alpha, beta, gamma and delta isoforms of Ca2+-calmodulin-dependent protein kinase II. *J Biol Chem*, 279(13):12484–12494, Mar 2004. doi: 10.1074/jbc.M313597200. URL `http://dx.doi.org/10.1074/jbc.M313597200`.

Arnold Hayer and Upinder S Bhalla. Molecular switches at the synapse emerge from receptor and kinase traffic. *PLoS Comput Biol*, 1 (2):137–154, Jul 2005. doi: 10.1371/journal.pcbi.0010020. URL `http://dx.doi.org/10.1371/journal.pcbi.0010020`.

W. R. Holmes. Models of calmodulin trapping and CaM kinase II activation in a dendritic spine. *J Comput Neurosci*, 8(1):65–85, 2000.

S. J. Kolodziej, A. Hudmon, M. N. Waxham, and J. K. Stoops. Three-dimensional reconstructions of calcium/calmodulin-dependent (CaM) kinase IIalpha and truncated CaM kinase IIalpha reveal a unique organization for its structural core and functional domains. *J Biol Chem*, 275(19):14354–14359, May 2000.

Y. Kubota and J. M. Bower. Transient versus asymptotic dynamics of CaM kinase II: possible roles of phosphatase. *J Comput Neurosci*, 11(3):263–279, 2001.

T. Meyer, P. I. Hanson, L. Stryer, and H. Schulman. Calmodulin trapping by calcium-calmodulin-dependent protein kinase. *Science*, 256(5060):1199–1202, May 1992.

S. G. Miller and M. B. Kennedy. Regulation of brain type II Ca2+/calmodulin-dependent protein kinase by autophosphorylation: a Ca2+-triggered molecular switch. *Cell*, 44(6):861–870, Mar 1986.

E. P. Morris and K. Torok. Oligomeric structure of alpha-calmodulin-dependent protein kinase II. *J Mol Biol*, 308(1):1–8, Apr 2001. doi: 10.1006/jmbi.2001.4584. URL `http://dx.doi.org/10.1006/jmbi.2001.4584`.

Oren S Rosenberg, Sebastian Deindl, Rou-Jia Sung, Angus C Nairn, and John Kuriyan. Structure of the autoinhibited kinase domain of CaMKII and SAXS analysis of the holoenzyme. *Cell*, 123(5):849–860, Dec 2005. doi: 10.029. URL `http://dx.doi.org/10.029`.

Oren S Rosenberg, Sebastian Deindl, Luis R Comolli, Andr Hoelz, Kenneth H Downing, Angus C Nairn, and John Kuriyan. Oligomerization states of the association domain and the holoenyzme of Ca2+/CaM kinase II. *FEBS J*, 273(4):682–694, Feb 2006. doi: 10.1111/j.1742-4658.2005.05088.x. URL `http://dx.doi.org/10.1111/j.1742-4658.2005.05088.x`.

K. Torok and D. R. Trentham. Mechanism of 2-chloro-(epsilon-amino-Lys75)-[6-[4-(N,N- diethylamino)phenyl]-1,3,5-triazin-4-yl]calmodulin interactions with smooth muscle myosin light chain kinase and derived peptides. *Biochemistry*, 33(43):12807–12820, Nov 1994.

K. Torok, A. Tzortzopoulos, Z. Grabarek, S. L. Best, and R. Thorogate. Dual effect of ATP in the activation mechanism of brain Ca(2+)/calmodulin-dependent protein kinase II by Ca(2+)/calmodulin. *Biochemistry*, 40(49):14878–14890, Dec 2001.

Athanasios Tzortzopoulos and Katalin Torok. Mechanism of the T286A-mutant alphaCaMKII interactions with Ca2+/calmodulin and ATP. *Bio-*

chemistry, 43(21):6404–6414, Jun 2004. doi: 10.1021/bi036224m. URL `http://dx.doi.org/10.1021/bi036224m`.

A. M. Zhabotinsky. Bistability in the Ca(2+)/calmodulin-dependent protein kinase-phosphatase system. *Biophys J*, 79(5):2211–2221, Nov 2000.

Chapter 4

Models of CaMKII Autophosphorylation

4.1 Introduction

After activation by Ca^{2+}-loaded calmodulin, CaMKII can autophosphorylate which renders its activity Ca^{2+} independent (Miller and Kennedy, 1986). As a result of autophosphorylation, CaMKII can be activated by 100ms long Ca^{2+} transients, and maintain its activity for minutes to hours.

Autophosphorylation is a process which takes place within a holoenzyme between subunits. Hanson et al. (1994) expressed inactivated CaMKII holoenzymes in which mutations in the catalytic domain eliminate its kinase activity. Mixture of inactive CaMKII holoenzymes and active CaMKII holoenzymes in conditions which promote autophosphorylation led to the phosphorylation of active CaMKII alone. Consequently, CaMKII autophosphorylation is an intraholoenzyme process. When active and inactive CaMKII subunits are simultaneously expressed, leading to the formation of mixed holoenzymes, autophosphorylation leads to phosphate incorporation in both active and inactive CaMKII subunits. Consequently, the autophosphorylation happens between subunits. Another line of evidence leading to the same conclusion comes from measuring the kinetics of autophosphorylation as a function of CaMKII concentration. When using CaMKII holoenzymes, the rate of autophosphorylation is independent of the concentration of CaMKII, pointing to a monomolecular reaction. A CaMKII mutant that has the association domain

removed, and thus remains monomeric, has an autophosphorylation rate which depends linearly on its concentration. This points to a bimolecular reaction for CaMKII subunits.

Autophosphorylation requires CaM binding to both CaMKII subunits involved in the reaction: the kinase and the substrate ones (Hanson et al., 1994). Monomeric CaMKII which was previously partially autophosphorylated can phosphorylate other substrates, but can not continue to autophosphorylate in the absence of Ca^{2+}.

CaMKII autophosphorylation has been generally modeled as a process occurring within the rings of the holoenzyme (Zhabotinsky, 2000; Kubota and Bower, 2001; Miller et al., 2005). In a ring-type model, the first step of autophosphorylation requires the binding of two CaM molecules to neighboring subunits, leading to autophosphorylation of one of these subunits. Subsequent autophosphorylations steps require one CaM molecule bound to a subunit adjacent an autophosphorylated subunit. Starting with a ring with one CaMKII subunit autophosphorylated, this can lead to the autophosphorylation of the entire ring with only one CaM bound at a time. In a ring model, CaMKII autophosphorylation kinetics is complex, and can be bistable when coupled with a protein phosphatase (Okamoto and Ichikawa, 2000; Zhabotinsky, 2000; Kubota and Bower, 2001). The mechanism of CaMKII autophosphorylation occurring in rings is intuitively supported by structures obtained via cryo electron microscopy (cryoEM) (Gaertner et al., 2004; Kolodziej et al., 2000). In these structures, CaMKII holoenzyme has a 622 symmetry, with the catalytic domains forming two rings approximately 20 nm apart. However, a recent structure of the catalytic and autoinhibitory domains of CaMKII (Rosenberg et al., 2005) shows a strong pair-wise interaction between subunits, leading to cooperative binding of CaM by CaMKII. Using small angle X-ray scattering (SAXS), Rosenberg et al. (2005) conclude that all 12 catalytic subunits in a holoenzyme are coplanar. This result is consistent with previous cryoEM structures (Morris and Torok, 2001). It is possible to reconcile the two observed structures by assuming that one (Rosenberg et al., 2005) is of inactive CaMKII, while the other (Kolodziej et al., 2000) is of active CaMKII. The strong pair-wise interaction between catalytic regions raises the question if CaMKII

autophosphorylation happens in pairs rather than rings.

In this chapter CaMKII autophosphorylation is modeled both in rings and in pairs, implementing the newly observed cooperative CaM binding by CaMKII. Autophosphorylation kinetics were also measured and compared to predictions from both models in order to distinguish between the two possible mechanisms.

4.2 Experimental Methods

CaMKII was purified from rat brains as described in Miller and Kennedy (1985). For these experiments CaMKII which elutes from the ion exchange column at 0.16 - 0.18 mM NaCl was used. This fraction represents mainly midbrain CaMKII and has a higher proportion of β CaMKII compared to the forebrain CaMKII. To calculate the fraction of α to β CaMKII subunits, 1 μg, 2 μg and 3 μg of midbrain CaMKII were separated using an SDS-PAGE gel. The gel was Coomassie stained and the integral intensity of the bands corresponding to α to β CaMKII were calculated using the border-median method for background subtraction in Odyssey Imaging System (Li-Cor Biosciences, Lincoln, NE).

High purity calmodulin was purchased from EMD Bioscience. Calmodulin concentration was determined by weighing and confirmed by bicinchoninic acid (BCA) assay.

The measurements of the rates of autophosphorylation for midbrain kinase were performed using methods very similar to those used in chapter 2. Rates of autophosphorylation were measured at 100 ms, 300 ms, 1 s, 3 s, 10 s, and 30 s after initiation of the reaction with the use of a Kintek Model RQF-3 Quench Flow apparatus (Kintek Corporation, Austin, Texas). Reactions were initiated by rapid mixing of 16 μL of two solutions. Solution 1 contained 25 mM Tris-HCl at p.H 7.2, 0.1 M NaCl, 1 mM MgCl2, 2 mM Ca^{2+}, 0.9 mg/mL BSA, 5 mM DTE, 2 μM CaMKII (catalytic sites), and either 6, 0.67 or 0.33 μM CaM. Solution 2 contained the same buffer, but CaMKII and CaM were replaced with 200 μM ATP. The two solutions were kept at 4 $^{\circ}C$ until they were transferred to the quench flow apparatus and

warmed for 1 min to 30 $^{\circ}C$.

The autophosphorylation reaction was terminated by the rapid addition of a final concentration of 1% SDS, 3.3 mM Glycine-HCl, pH 2.9. After quenching, all reactions were brought to a final concentration of 3% SDS, 2.64 mM Glycine, 66 mM Tris-HCl (pH 7.2), 2% beta-mercaptoethaol, 5% glycerol, 40 μg/mL Bromphenol Blue.

Samples containing 0.5 μg of CaMKII were fractionated on an 8% SDS PAGE gel. Protein was transferred by electrophoresis onto a nitrocellulose membrane for 1 hour at a current of 350 mA in 25 mM Tris base, 0.2 M Glycine and 20% Methanol. The membranes were immunoblotted with 6.25 μg antibody 22B1 in 12.5 ml 50 mM Tris (pH 7.5), 0.5 M NaCl, 0.1% Tween 20 (TTBS), plus 5% milk for 3 hrs at 21 $^{\circ}C$. Monoclonal antibody 22B1 (anti-phospho-CaMKII; Affinity Bioreagents, CO) is specific for α and β subunits of CaMKII only when they are phosphorylated at Thr-286/287. Bound antibodies were visualized with fluorescent secondary antibody IRDye800-Anti-mouse (Rockland, Gilbertsville, PA; 1.5 μg in 30 ml TTBS). Fluorescence from the bound secondary antibody was visualized with an Odyssey Imaging System (Li-Cor Biosciences, Lincoln, NE).

The differences from the experiments in chapter 2 are:

- using midbrain CaMKII rather than forebrain CaMKII,
- varying calmodulin concentrations,
- more CaMKII (0.5 μg) loaded on gels, and
- using milk rather than goat serum for blocking.

To test if the affinity of 22B1 antibody for α and β CaMKII isoforms is similar, its relative staining of α and β CaMKII isoforms from fully autophosphorylated midbrain CaMKII was measured.

The amount of autophosphorylated CaMKII was calculated quantifying the integrated intensity of each band. The integrated intensity of a band is the integral of the intensity of each pixel in a band minus the median value of the intensities of the pixels on the border of the band. The intensity of each band was then normalized

to the intensity of a band containing the same amounts of calmodulin and CaMKII autophosphorylated for 30 s. For all experiments one standard curve was built by measuring the integrated intensity of known quantities of fully autophosphorylated CaMKII. The standard curve was fit with a power function:

$$Int(x) = \left(\frac{x}{x_0}\right)^n. \tag{4.1}$$

- n - free parameter which is fitted
- x - represents the amount of CaMKII which was loaded in the lanes used to construct the standard function
- $x_0 = 0.5\mu g$ - represents the total amount of CaMKII which was loaded in each lane of the gels measuring the time dependence of CaMKII autophosphorylation

A power function was used since it has one free parameter, respects the constraints $Int(0) = 0$, $Int(x_0) = 1$ and fits well the observed nonlinearity. The advantage of a power function is that ratios of intensities do not depend on the value which was used in the normalization of the intensity.

$$\frac{Int(x_1)}{Int(x_2)} = \left(\frac{x_1}{x_0}\right)^n \left(\frac{x_0}{x_2}\right)^n = \left(\frac{x_1}{x_2}\right)^n \tag{4.2}$$

The amount of autophosphorylated CaMKII in each lane was obtained using the inverse of the standard curve.

$$p286(t) = \left(\frac{Int(t)}{Int(30s)}\right)^{\left(\frac{1}{n}\right)} \tag{4.3}$$

The time dependence of the fraction of CaMKII which is phosphorylated at Thr286 was fit with:

$$p286(t) = A\left(1 - e^{-k(t+t_0)}\right). \tag{4.4}$$

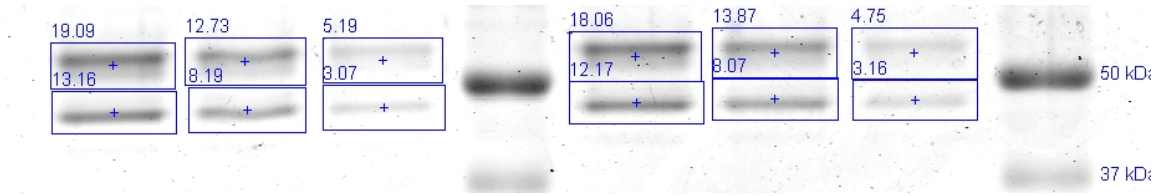

Figure 4.1. Coomassie stain of midbrain CaMKII. From left to right: 3 μg, 2 μg, 1 μg of midbrain CaMKII and protein weight markers were separated using an SDS-PAGE gel. The gel was Coomassie stained. The band which runs at slightly more than 50 kDa represents the β isoform of CaMKII and the bands which runs at slightly less than 50 kDa represents the α isoform of CaMKII. The integral intensity of the bands corresponding to α to β CaMKII were calculated using the border-median method for background subtraction in Odyssey Imaging System and is listed above the box.

- A represents the maximal autophosphorylation fraction and is close to 1
- k represents the rate of autophosphorylation
- t_0 represents the time it takes for the autophosphorylation reaction to be stopped

The rates of autophosphorylation were obtained through nonlinear regression using the Levenberg Marquardt method implemented in Mathematica 5 (Wolfram Research).

The methods for quantifying the experimental data are very similar to those in chapter 2. The amount of protein loaded in the lanes used to build the standard curve were changed to reflect a larger amount of protein loaded in the gels used to quantify the time dependence. The normalization was done to CaMKII autophosphorylated for 30s, while in chapter 2 it was either 30s for wild type calmodulin or 100s for mutant calmodulins.

4.3 Experimental Results

In order to determine the ratio of α to β CaMKII subunits in the midbrain kinase it was assumed that the integrated intensity of a band in Coomassie stain is proportional to the proportional to the mass of the protein in that band. The molar ratio of α to β

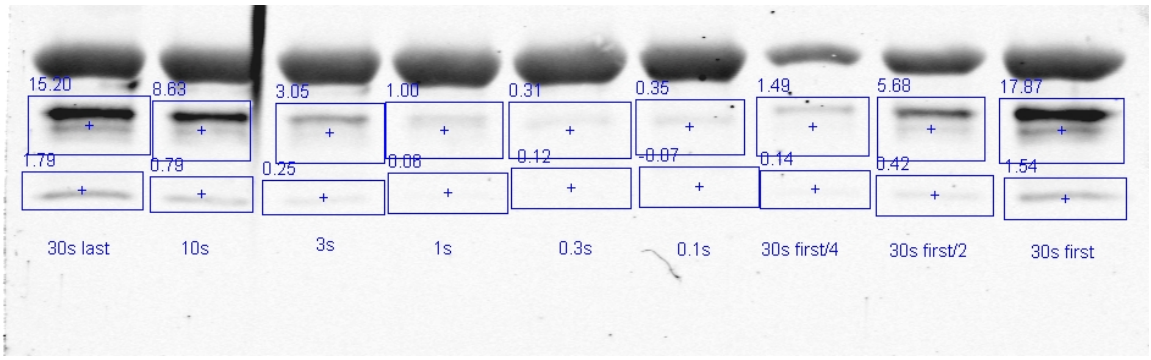

Figure 4.2. Typical immunoblot used to quantify the fraction of CaMKII autophosphorylated at Thr286. In this immunoblot, the concentration of CaMKII subunits used was 1 μM and the concentration of calmodulin 0.167 μM. In all the lanes, the top band represents a nonspecific staining of BSA, the middle band represents βCaMKII and the bottom band represents αCaMKII. The left-most lane, marked 30s last, has the same protein amount (0.5 μg) and the same autophosphorylation time (30 s) as the right-most lane, however was measured at the end of the experiment series. Lanes 2-6 contain 0.5 μg autophosphorylated for different times, and are marked by the autophosphorylation time. The right 3 lanes, marked 30s first, 30s first/2 and 30s first/4 are taken from the same sample and different amounts of protein were loaded: 0.5 μg, 0.25 μg and 0.125 μg respectively.

CaMKII subunits obtained from Coomassie stain (figure 4.1) is 0.434 ± 0.017. Molar ratio of α to β CaMKII subunits obtained from an immunoblot of fully phosphorylated CaMKII using the 22B1 antibody is 0.441 ± 0.051. These values are consistent with 22B1 antibody having identical affinities for phosphorylated α and β CaMKII subunits.

Each series of experiments takes an average of 20-30 minutes. In order to minimize CaMKII denaturation, the solution containing CaMKII has 1mg/ml BSA, is kept on ice prior to the experiment, and is the last solution loaded in the quench flow apparatus. To control for denaturation, all experimental series have a sample which is taken at the end and in which the autophosphorylation time is the same as the first sample. The observed denaturation during an experimental series is smaller than 20%. In order to prevent denaturation from introducing a bias in the measurements, all the experiments are preformed in duplicate, and the order in which the samples are taken are reversed.

Each immunoblot contains lanes loaded with different quantities of protein (lanes

7, 8 and 9 in figure 4.2). These lanes are used to construct a standard function (equation 4.1). The standard function used to calculate the autophosphorylation fractions is the average of the standard function obtained for all the gels.

The average intensity of CaMKII autophosphorylated for a given time (lanes 2-6 in figure 4.2) was normalized to the band corresponding to the same isoform from midbrain CaMKII autophosphorylated for 30s (lane 9 in figure 4.2). Since the standard function used preserves ratios (equation 4.2), this normalization represents the ratio between the fraction of CaMKII autophosphorylated at a given time to the fraction of CaMKII autophosphorylated at 30s. The time dependence was fit with an exponential function (equation 4.4). The experimental results and the corresponding fits are presented in figure 4.3. The best fit parameters are summarized in table 4.1. The rates of midbrain CaMKII autophosphorylation (α $0.472 \pm 0.148 s^{-1}$, β $0.560 \pm 0.197 s^{-1}$) in saturating calmodulin are smaller than the rate of forebrain CaMKII autophosphorylation ($k_P = 0.96 \pm 0.14 s^{-1}$). This result is consistent with previous measurements (Gaertner et al., 2004) which show a slower syntide phosphorylation by β CaMKII compared to α CaMKII. The final fraction represents the fraction of autophosphorylated α or β CaMKII after 30s to the total autophosphorylated CaMKII after 30s. The parameter relative rate * final fraction allows for a direct comparison of the absolute rates of autophosphorylation of α and β CaMKII. In saturating calmodulin the absolute rates of autophosphorylation of α and β CaMKII are similar while in limiting calmodulin the absolute rate of autophosphorylation of β CaMKII is 3-4 times higher than that of α CaMKII.

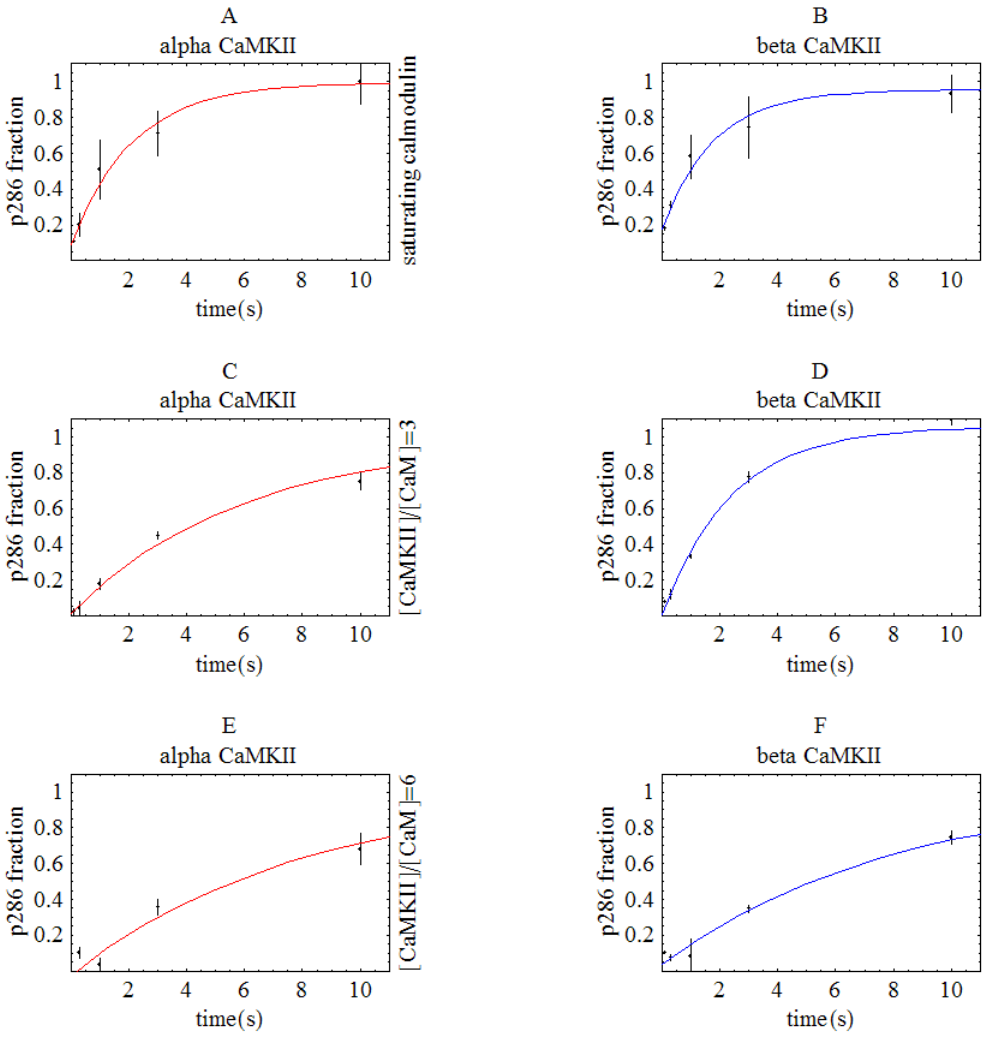

Figure 4.3. Measured autophosphorylation ratios. **A**, **C** and **E**. The ratio between the fraction of α-CaMKII autophosphorylated at a given time (lanes 2-6 in figure 4.2) to the fraction of α-CaMKII autophosphorylated at 30s (lane 9 in figure 4.2). **B**, **D** and **F**. The ratio between the fraction of β-CaMKII autophosphorylated at a given time to the fraction of β-CaMKII autophosphorylated at 30s. All the autophosphorylation reactions contained 1 μM midbrain CaMKII. The concentrations of calmodulin used in **A** and **B** is 3 μM, **C** and **D** is 1/3 μM, **E** and **F** is 1/6 μM. All data points are the average of two experiments. The vertical bars represent standard deviations. The time dependence was fit with an exponential function (equation 4.4). The parameters for the exponential fits are summarized in table 4.1

isoform	[CaM](μM)	rel. rate ($10^{-3}s^{-1}$)	fin. frac.	rate * fin. frac. ($10^{-3}s^{-1}$)
α	3	472 ± 148	0.471	222
β	3	560 ± 197	0.529	296
α	0.333	168 ± 21.7	0.445	75
β	0.333	419.5 ± 45	0.555	233
α	0.167	124 ± 26.2	0.225	28
β	0.167	119.8 ± 20.7	0.775	93

Table 4.1. Parameters characterizing the autophosphorylation of midbrain CaMKII in conditions of limiting calmodulin. The first column represents which isoform was measured. All experiments were performed in 1 μM CaMKII. The second column represents the concentration of calmodulin used in each of the experiments. A concentration of 3 μM for calmodulin is saturating, while 0.333 and 0.167 also represent the ratios of the number of calmodulins to the number of CaMKII subunits available in solution. The third column, relative rates, represent the rates of the exponential fits presented in figure 4.3. The fourth column, final fraction, represents the fraction of autophosphorylated CaMKII isoform after 30s to the total autophosphorylated CaMKII after 30s. The last column represents the product between the autophosphorylation rate for an isoform and the final autophosphorylation fraction for that isoform. This product allows for the direct comparison of the speeds of autophosphorylation between isoforms.

4.4 Model

4.4.1 Competition for Calmodulin Binding between Autophosphorylated CaMKII and Nonphosphorylated CaMKII

Autophosphorylation of CaMKII at Thr286 leads both to Ca^{2+}-independent activity (Miller and Kennedy, 1986) and in increased affinity for calmodulin (Meyer et al., 1992). The Ca^{2+}-independent activity which CaMKII gains as a result of autophosphorylation is a key element in CaMKII's function allowing it to have a prologued response to short Ca^{2+} transients. The importance of the increase in affinity for calmodulin depends on the conditions in which autophosphorylation takes place. In saturating Ca^{2+} and limiting calmodulin already autophosphorylated CaMKII subunits compete with the nonphosphorylated CaMKII subunits for the limiting calmodulin. Since autophosphorylated CaMKII has an affinity for

calmodulin three orders of magnitude larger than nonphosphorylated CaMKII, each autophosphorylated subunit practically traps one calmodulin molecule.

Given a known fraction of CaMKII autophosphorylation, the binding of calmodulin to partially phosphorylated CaMKII can be calculated from a system of ordinary differential equations (ODEs) corresponding to the reactions in figure 4.4. The parameters describing the binding of calmodulin to unphosphorylated CaMKII are described in chapter 3.2.1., corresponding to the kinetics at 30^oC. The parameters describing the binding of calmodulin to phosphorylated CaMKII are obtained from Meyer et al. (1992). It is assumed that the CaMKII pair which form a dimer in the basal state remains open if one of the CaMKII subunits is autophosphorylated. Consequently, there is no cooperativity between autophosphorylated CaMKII subunits in binding of calmodulin, and the measured on and off rates from autophosphorylated CaMKII are exactly the microscopic on and off rates. The values of the rate constants used for WT CaM are: $k_{onP} = 0.5\ 10^8\ M^{-1}\ s^{-1}$ and $k_{offP} = 3\ 10^{-3}\ s^{-1}$. These values are adjusted from those obtained (Meyer et al., 1992) using dansylated calmodulin, which has a 3-fold higher affinity for CaMKII.

The binding of calmodulin to an unphosphorylated CaMKII subunit pair (figure 4.4) was modeled using the simplified reaction scheme presented in figure 3.2 C. The binding of calmodulin to a CaMKII subunit pair which has one subunit phosphorylated at Thr286 is presented in figure 4.4 B. We assume that the autophosphorylation of one of the subunits is sufficient to keep the pair open. Consequently, the binding of a calmodulin to the subunit which is not phosphorylated is similar to the binding of a second calmodulin to an unphosphorylated CaMKII pair (k_{on2} and k_{off2}). The binding of a calmodulin to the subunit which is phosphorylated is characterized by k_{onP} and k_{offP}. The set of reactions presented in figure 4.4 B automatically satisfies the thermodynamic constraint for the affinities of a reaction loop. It is assumed that autophosphorylation forces a CaMKII dimer in the open conformation. Consequently, the binding of calmodulin to the two subunits of an autophosphorylated CaMKII dimer are considered independent.

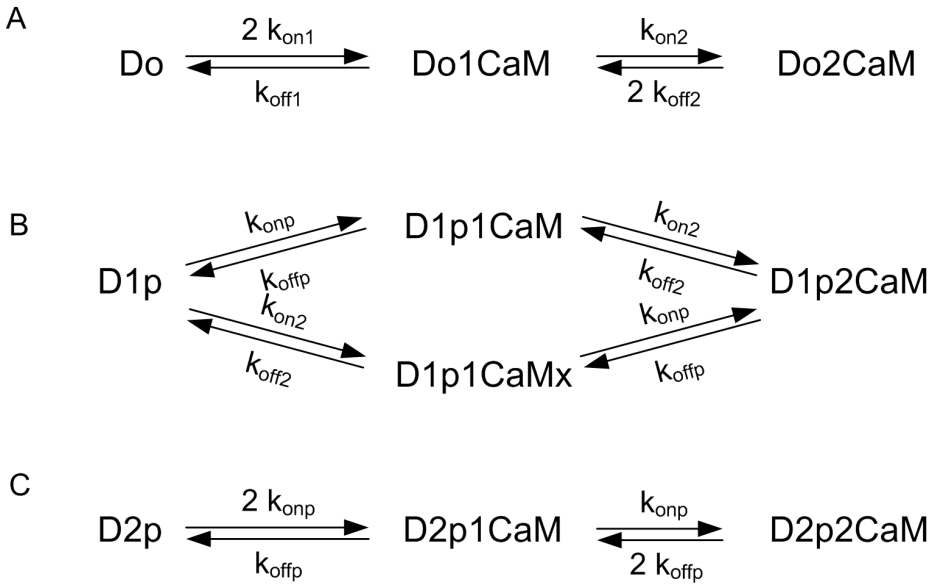

Figure 4.4. Simultaneous calmodulin binding to nonphosphorylated (A), partially phosphorylated (B) and autophosphorylated (C) CaMKII subunit pairs. The two subunits of CaMKII which dimerize in the absence of Ca^{2+}-calmodulin form a pair (Do). The parameters for calmodulin binding to and unbinding from unphosphorylated CaMKII (k_{on1}, k_{on2}, k_{off1}, k_{off2}) are described in chapter 3.2.1. When a CaMKII pair has one of the subunits phosphorylated (D1p), the binding of a calmodulin to the subunit which is phosphorylated leads to D1p1CaM, while the binding of a calmodulin to the subunit which is not phosphorylated leads to D1p1CaMx. Is is assumed that a phosphorylated CaMKII pair (D2p) is open regardless of the binding of calmodulin. This assumption makes the rates for the binding of the first calmodulin to a phosphorylated CaMKII pair identical to the rates for the binding of the second calmodulin. If the rates for the first and second calmodulin binding are equal, the macroscopic kinetic constants are equal to the microscopic ones. We used for the microscopic kinetic constants k_{onp} and k_{offp} the macroscopic values measured by Meyer et al. (1992) and included the observed three times higher affinity of dansylated calmodulin for α-CaMKII.

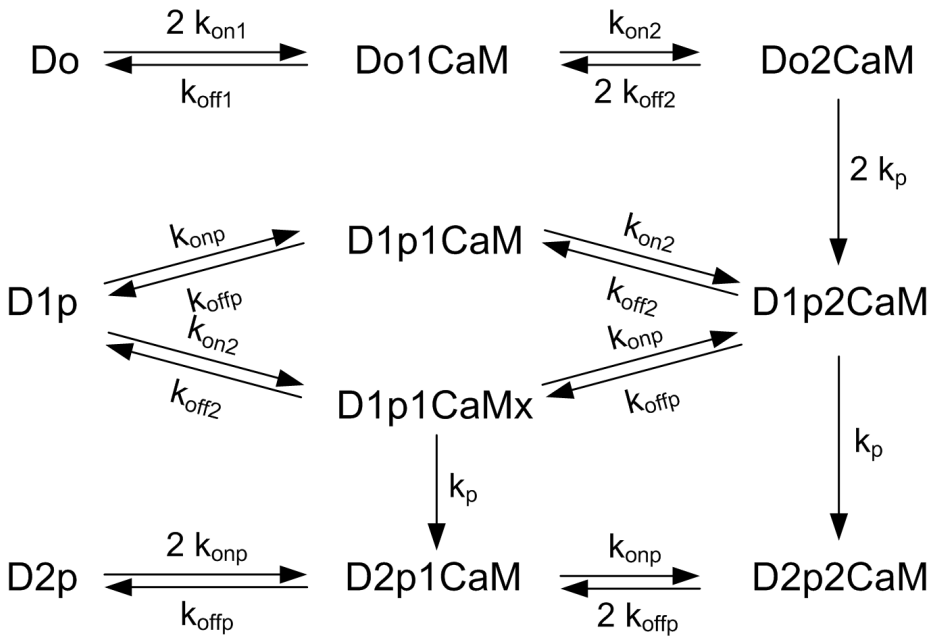

Figure 4.5. Model of autophosphorylation between the pair of CaMKII subunits which dimerize in basal conditions. The parameters for calmodulin binding are discussed in figure 4.4. We assumed that the rate of autophosphorylation when both subunits have calmodulin bound (Do2CaM) is the same as the rate of autophosphorylation when both subunits have calmodulin bound and one of the subunits is phosphorylated (D1p2CaM). This assumption allows the rate of CaMKII autophosphorylation in saturation calmodulin to be equivalent to the autophosphorylation turnover number. It is assumed that the rate of autophosphorylation of a CaMKII subunit which has calmodulin bound by a subunit which is phosphorylated but does not have calmodulin bound (D1p1CaMx) is the same as the autophosphorylation turnover number. This assumption does not largely affect our simulations since $k_{offP} = 3\ 10^{-3}\ s^{-1}$ is a very small number, and the state D1p1CaMx is present in very small concentrations.

4.4.2 Model for CaMKII Autophosphorylation in Pairs

If CaMKII autophosphorylation happens in pairs, figure 4.5, the reactions corresponding to autophosphorylation are easily added to the reactions corresponding to calmodulin binding of figure 4.4.

In accordance to the experimental results from (Hanson et al., 1994), a CaMKII subunit needs either to have CaM bound or be phosphorylated at Thr 286 to have catalytic activity. Additionally a CaMKII subunit needs to have calmodulin bound to become a substrate for phosphorylation at Thr 286. The autophosphorylation

turnover number k_P was directly measured as the rate of autophosphorylation in conditions of saturating Ca^{2+} and calmodulin.

4.4.3 Model for CaMKII Autophsophorylation in Rings

Modeling CaMKII autophosphorylation in rings requires solving simultaneously two coupled sets of ODEs. One set describes the simultaneous binding to nonphosphorylated and autophosphorylated CaMKII which is presented in figure 4.4 and denoted as binding ODEs. The other set of ordinary differential equations describe the autophosphorylation process in rings of 6 subunits (phosphorylation ODEs). It is possible to keep track of all the phosphorylation states of a CaMKII holoenzyme, however, for phosphorylation processes only, this system can be simplified without adding any approximation. The simplification takes into account that two clusters of unphosphorylated subunits will not influence each other in the future. Individual reactions for phosphorylation of clusters of unphosphorylated subunits and are presented in figure 4.6.

The binding ODEs have as an input the probability a CaMKII subunit to be phosphorylated, which is calculated in the phosphorylation ODEs. The phosphorylation ODEs have as an input the probability of a nonphosphorylated CaMKII subunit having calmodulin bound. This probability is calculated in the binding ODEs. These two sets of ODEs were solved simultaneously, without assuming the binding of calmodulin and CaMKII autophosphorylation are on different time scales.

4.5 Modeling Results

4.5.1 CaMKII Autophosphorylation under Conditions of Limiting Calmodulin

In conditions of saturating Ca^{2+} and limiting calmodulin, CaMKII autophosphorylation happens on two very different time scales. The first time scale is on

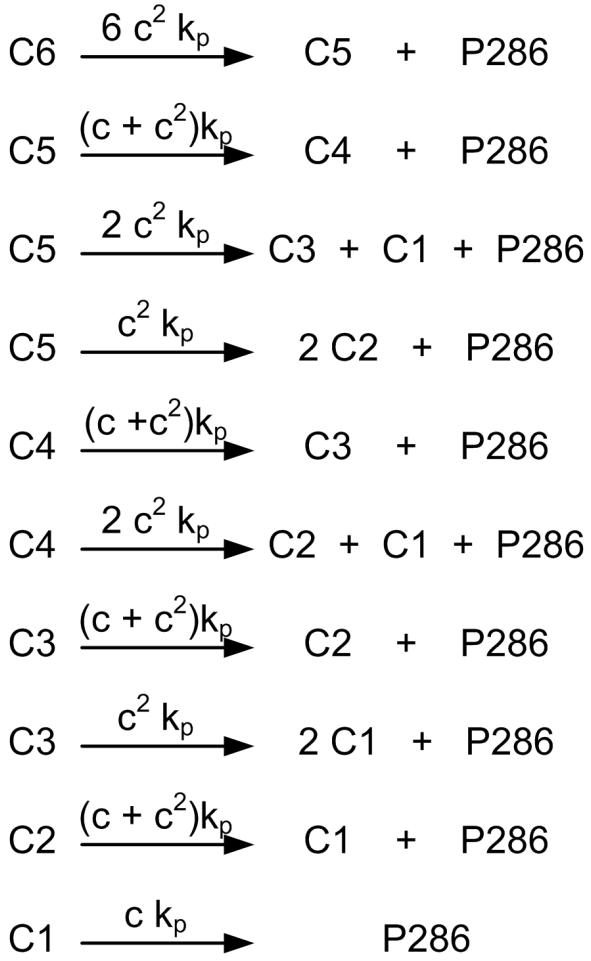

Figure 4.6. Reactions which describe CaMKII autophosphorylation in rings, using the cluster simplification. C6 represents a ring of six unphosphorylated CaMKII subunits. Cn, with $n = 1 - 5$ represents a cluster of n unphosphorylated subunits, and c represents the probability of an unphosphorylated subunit having calmodulin bound. The rate of the first reaction is composed of: 6 neighboring pairs of unphosphorylated CaMKII subunits in a ring; c^2 represents the probability of a neighboring pair of subunits both having calmodulins bound and k_P represents the rate of autophosphorylation if both neighboring subunits have calmodulin bound. In the second reaction, the phosphorylation of one of the terminal subunits in a cluster of 5 subunits (C5) leads to the formation of a cluster of 4 subunits (C4). This reaction can be realized through two processes: ck_p represents the rate of phosphorylation of the left-most subunit in the cluster, a phosphorylation event which is performed by an already phosphorylated subunit; c^2k_p represents the rate of phosphorylation of the right-most subunit in the cluster, phosphorylation which is performed by a nonphosphorylated subunit, which needs to bind a calmodulin to be have kinase activity. The rates for the following reactions are constructed in the same way as the first two.

the order of seconds, and corresponds to the concentration of phosphorylated CaMKII subunits reaching the total concentration of calmodulin. At this point, the phosphorylated CaMKII subunits trap almost all the calmodulin. The second time scale depends on the unbinding of calmodulin from this trapped states, which is on the order of tens of minutes−hours. How rapid the first time scale of autophosphorylation is depends on the model for CaMKII autophosphorylation considered. The rate of autophosphorylation depends on the probability of two neighboring subunits which can phosphorylate one another to have calmodulin bound. The probability that two subunits in a pair have calmodulin bound is higher than the probability that two neighboring subunits in a ring have calmodulin bound, since the subunits in a pair cooperate in binding of calmodulin. Consequently, the initial rate for autophosphorylation is higher if the autophosphorylation happens in pairs. Combining the sets of equations corresponding to the reaction in figures 4.4, 4.5 and 4.6 the predicted time dependence of CaMKII autophosphorylation in limiting calmodulin is presented in figure 4.7.

The most important parameter in the simulations presented in figure 4.7 is the cooperativity between the two CaMKII subunits in a pair in binding calmodulin. This cooperativity is characterized by the the ratio between the affinity of the second calmodulin binding to the affinity of the first calmodulin binding: $r = \frac{K_{D1}}{K_{D2}}$. The value of the cooperativity coefficient r has little impact on the rate of autophosphorylation in the ring autophosphorylation model. However, the value of the cooperativity coefficient r has changes the rate of autophosphorylation occurring in the pair autophosphorylation model.

In conditions of saturating calmodulin, both the ring and pair model predict the same rate for autophosphorylation, rate which is independent of the details of calmodulin binding to CaMKII. This property was used to test the simulations, and is presented in figure 4.8 A. Simulations of one experiment capable to distinguish between the ring and pair autophosphorylation models, the time dependence of CaMKII autophosphorylation in calmodulin and CaMKII concentrations lower that their dissociation constant, is presented in figure 4.8 B. This experiment uses CaMKII

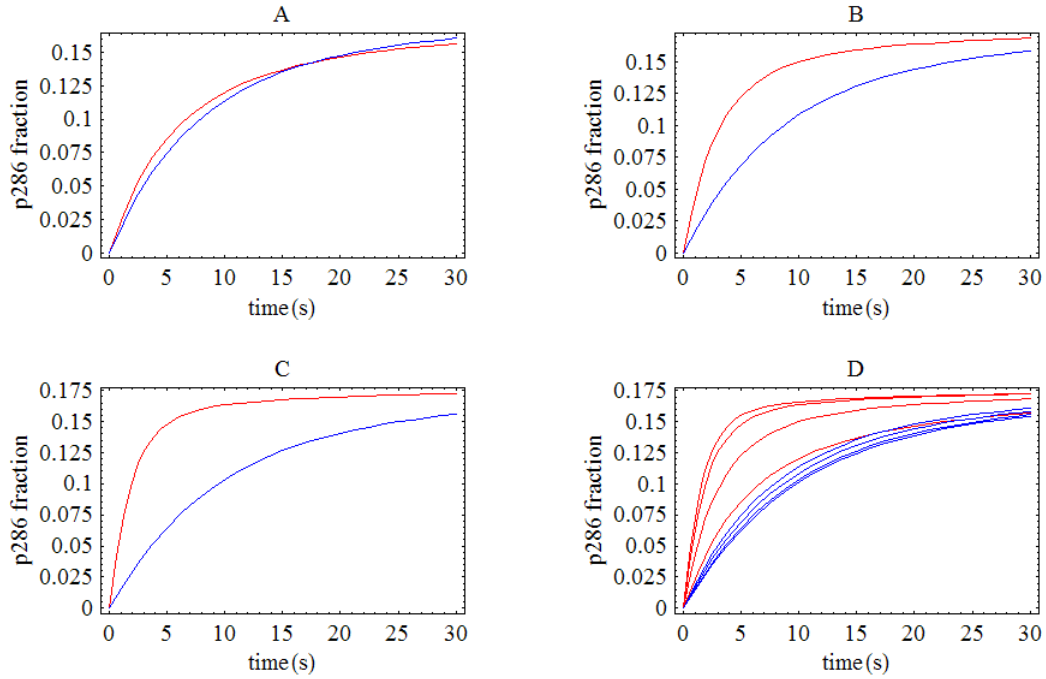

Figure 4.7. Simulations of the time dependence of α-CaMKII autophosphorylation in conditions of limiting calmodulin: [CaM]=0.167μM, [CaMKII]=1μM. The parameter on the vertical axis, p286 fraction, represents the fraction of CaMKII subunits phosphorylated at a given time. The red lines correspond to pair autophosphorylation model while the four blue lines correspond to ring autophosphorylation model for various cooperativity coefficients. The values for the cooperativity coefficient $r = K_{D1}/K_{D2}$ are: **A** r=1.6, **B** r=6.4, **C** r=40, **D** previous 3 panels and r=160. Panel **D** is reproduced in figure 4.8 with a focus on smaller time scales.

concentrations for which the autophosphorylation fraction can not be assessed by immunoblots. Simulations of relatively similar experiments, that use large CaMKII concentrations (1 μM) and limiting calmodulin concentrations, are presented in figure 4.8 C and D. These simulations are for homogeneous αCaMKII and are not directly comparable to the experimental results from section 4.4. which used heterogeneous α and β CaMKII.

4.5.2 Hill Coefficient of CaMKII Autophosphorylation Dependence on Calmodulin Concentration

In accordance with experimental data, both kinase and substrate CaMKII subunits must have calmodulin bound in order for autophosphorylation reaction to occur. If the cooperativity coefficient is small (1.6), the simulated Hill coefficient for both autophosphorylation models is close to 2 (figures 4.9 A and 4.10 A). If the the cooperativity coefficient is large (160), the simulated Hill coefficient for the pair autophosphorylation model is close to 2, while the simulated Hill coefficient for the ring autophosphorylation model is close to 4 (figures 4.9 D and 4.10 D). The simulated Hill coefficient for the pair autophosphorylation model depends little on the cooperativity coefficient r, and remains close to 2. The simulated Hill coefficient for the ring autophosphorylation model depends on the cooperativity coefficient r, and varies between 2 and 4 when r varies between 1 and ∞.

Using the experimental conditions from (DeKoninck and Schulman, 1998), the simulations using four values for the cooperativity coefficient r (1.6, 6.4, 40, 160) are presented in figures 4.9 and 4.10. The Hill coefficients were obtained by a resampling of the model outputs using a set of calmodulin concentrations similar to those used in the measurements from (DeKoninck and Schulman, 1998), and then fitting the output with a Hill function. The values for the Hill coefficients measured (α 1.6$\pm$0.1 and β 1.8$\pm$0.1, (DeKoninck and Schulman, 1998)) are best fitted by the model of CaMKII autophosphorylation in pairs, with a low cooperativity between CaMKII subunits in binding calmodulin.

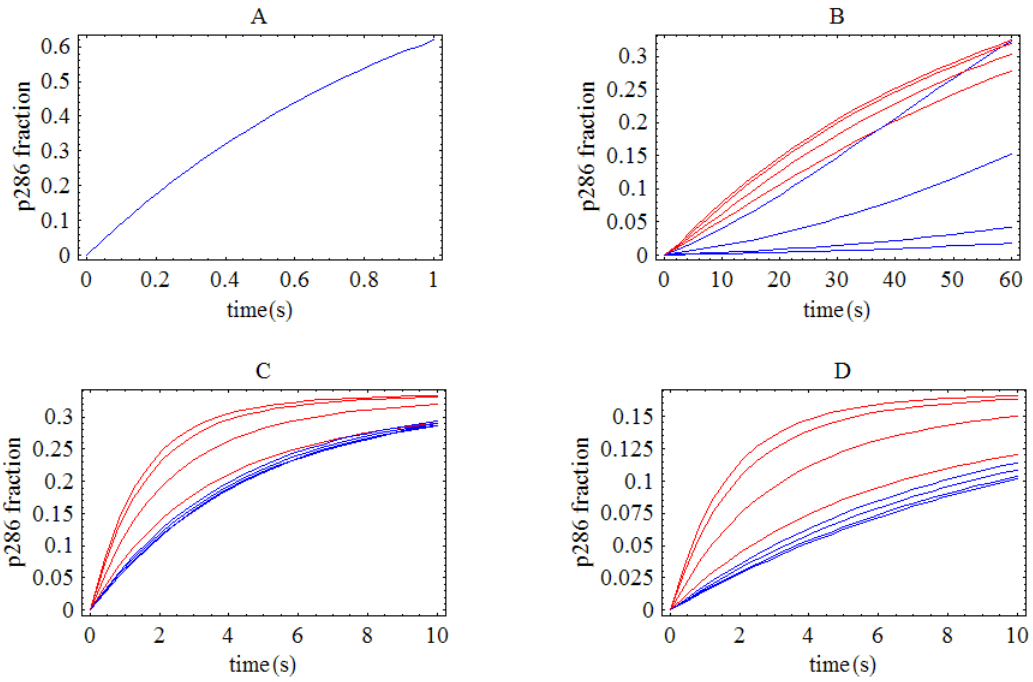

Figure 4.8. Simulations of the time dependence of α-CaMKII holoenzymes autophosphorylation different values for the cooperativity coefficient r. **A.** The fraction of CaMKII autophosphorylation as a function of time in saturating calmodulin concentration is plotted for both pair and ring autophosphorylation models at varying r (1.6, 6.4, 40, 160). All the eight curves superimpose. The predicted time dependence of CaMKII autophosphorylation in conditions of saturating calmodulin is the same for ring and pair model and it is independent on the cooperativity between CaMKII subunits in binding calmodulin. **B.** Time dependence of α-CaMKII autophosphorylation at small calmodulin and CaMKII concentrations: [CaM]=10nM, [CaMKII]=10nM. The four red lines correspond to pair autophosphorylation model, with r=1.6, r=6.4, r=40, r=160 from bottom to top. The four blue lines correspond to ring autophosphorylation model, with r=1.6, r=6.4, r=40, r=160 from top to bottom. **C.** Time dependence of α-CaMKII autophosphorylation in limiting calmodulin: [CaM]=0.33μM, [CaMKII]=1μM. The four red lines correspond to pair autophosphorylation model, with r=1.6, r=6.4, r=40, r=160 from bottom to top. The four blue lines correspond to ring autophosphorylation model, with r=1.6, r=6.4, r=40, r=160 from top to bottom. **D.** Time dependence of α-CaMKII autophosphorylation in limiting calmodulin: [CaM]=0.167μM, [CaMKII]=1μM. The four red lines correspond to pair autophosphorylation model, with r=1.6, r=6.4, r=40, r=160 from bottom to top. The four blue lines correspond to ring autophosphorylation model, with r=1.6, r=6.4, r=40, r=160 from top to bottom.

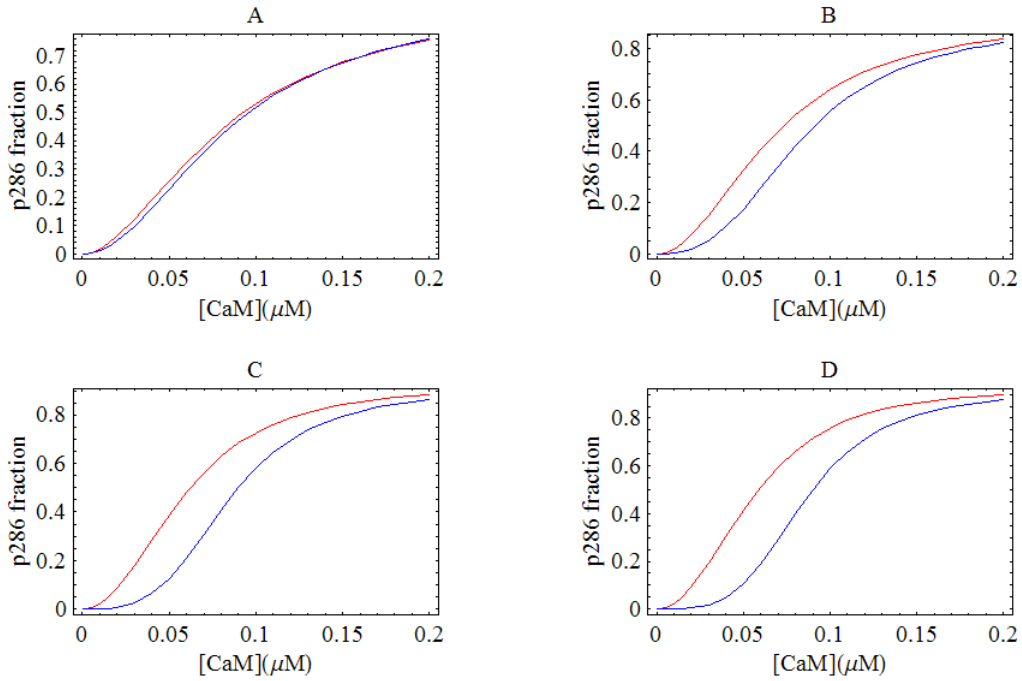

Figure 4.9. Simulations of the dependence of α-CaMKII autophosphorylation on calmodulin concentration. The simulations are done in the experimental conditions used by (DeKoninck and Schulman, 1998). For **A**, the parameters used for α-CaMKII are those obtained in chapter 3. For **B, C, D** all the parameters for α-CaMKII are those obtained in chapter 3, except the cooperativity coefficient. **A** With the cooperativity coefficient r=1.6, the Hill coefficient for autophosphorylation in pairs is 1.83 and the Hill coefficient for autophosphorylation in rings is 2.01. **B** With the cooperativity coefficient r=6.4, the Hill coefficient for autophosphorylation in pairs is 2.03 and the Hill coefficient for autophosphorylation in rings is 2.73. **C** With the cooperativity coefficient r=40, the Hill coefficient for autophosphorylation in pairs is 2.20 and the Hill coefficient for autophosphorylation in rings is 3.45. **D** With the cooperativity coefficient r=160, the Hill coefficient for autophosphorylation in pairs is 2.25 and the Hill coefficient for autophosphorylation in rings is 3.77.

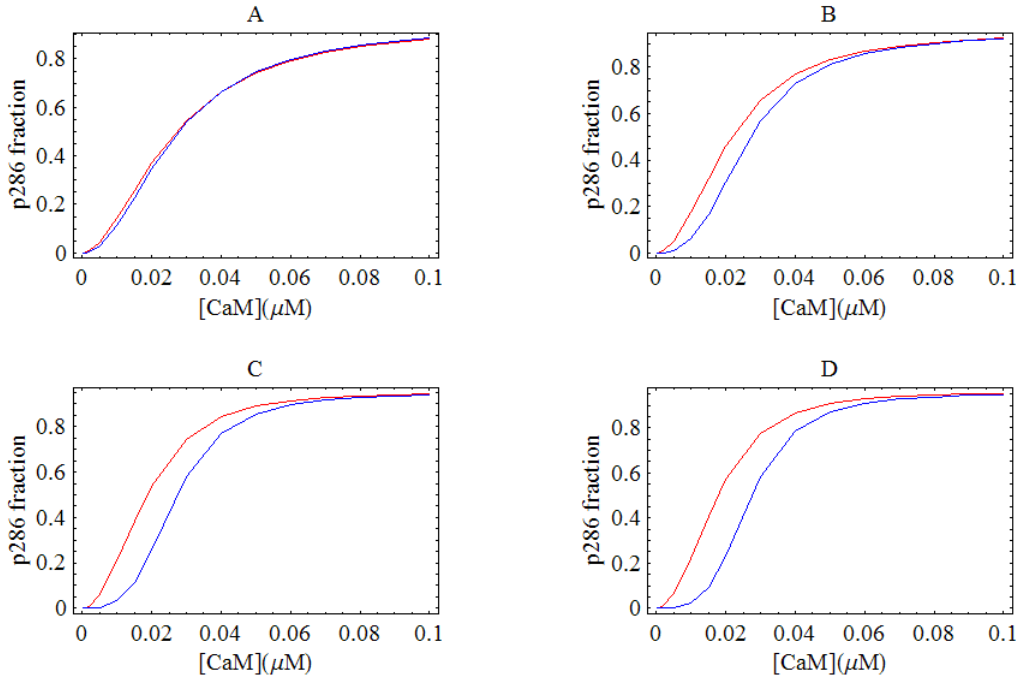

Figure 4.10. Simulations of the dependence of β-CaMKII autophosphorylation on calmodulin concentration. The affinity of calmodulin for β-CaMKII is assumed to be three times larger than the affinity of calmodulin for α-CaMKII. **A** With the cooperativity coefficient r=1.6, the Hill coefficient for autophosphorylation in pairs is 1.88 and the Hill coefficient for autophosphorylation in rings is 2.07. **B** With the cooperativity coefficient r=6.4, the Hill coefficient for autophosphorylation in pairs is 2.11 and the Hill coefficient for autophosphorylation in rings is 2.81. **C** With the cooperativity coefficient r=40, the Hill coefficient for autophosphorylation in pairs is 2.29 and the Hill coefficient for autophosphorylation in rings is 3.56. **D** With the cooperativity coefficient r=160, the Hill coefficient for autophosphorylation in pairs is 2.36 and the Hill coefficient for autophosphorylation in rings is 3.89.

4.5.3 Initial Rates of Heterogeneous CaMKII Autophosphorylation

CaMKII purified from rat brains forms heterogeneous holoenzymes with a mixture of α and β. Therefore, in order to compare with the experimental results from section 4.3, a model was developed to calculate the initial rates of autophosphorylation of heterogeneous CaMKII holoenzymes.

In both the ring and pair autophosphorylation models, the initial rate of autophosphorylation has two components: the intrinsic autophosphorylation turnover number (k_P) which gives the rate of autophosphorylation of a subunit when the neighboring subunit has calmodulin bound, and the probability of a neighboring subunit to have calmodulin bound. In the case of the ring autophosphorylation model the probability of a neighboring subunit in a ring having calmodulin bound matters. In the case of a pair autophosphorylation model, the probability of the other subunit in a pair having calmodulin bound matters. To calculate these probabilities we built a model for competition between α and β CaMKII for calmodulin (figure 4.11). This model has a similar structure to the model for competition between phosphorylated and nonphosphorylated α CaMKII. The model used for calmodulin binding to homomeric αCaMKII pairs is obtained from figure 3.2 C. The same model is used for calmodulin binding to homomeric βCaMKII pairs with the assumption that the off rates of calmodulin from βCaMKII are 3 times slower than from αCaMKII.

In the case of a ring autophosphorylation model, the probability of a CaMKII subunit with CaM bound to have an α-CaMKII subunit with CaM bound on its right is:

$$pring_{\alpha} = \frac{1}{Dtot}\left(D\alpha\alpha 2CaM + \frac{1}{2}\left(D\alpha\alpha 1CaM + D\alpha 1CaM\beta + D\alpha\beta 2CaM\right)\right), \tag{4.5}$$

where $Dtot$ represents the total number of CaMKII pairs.

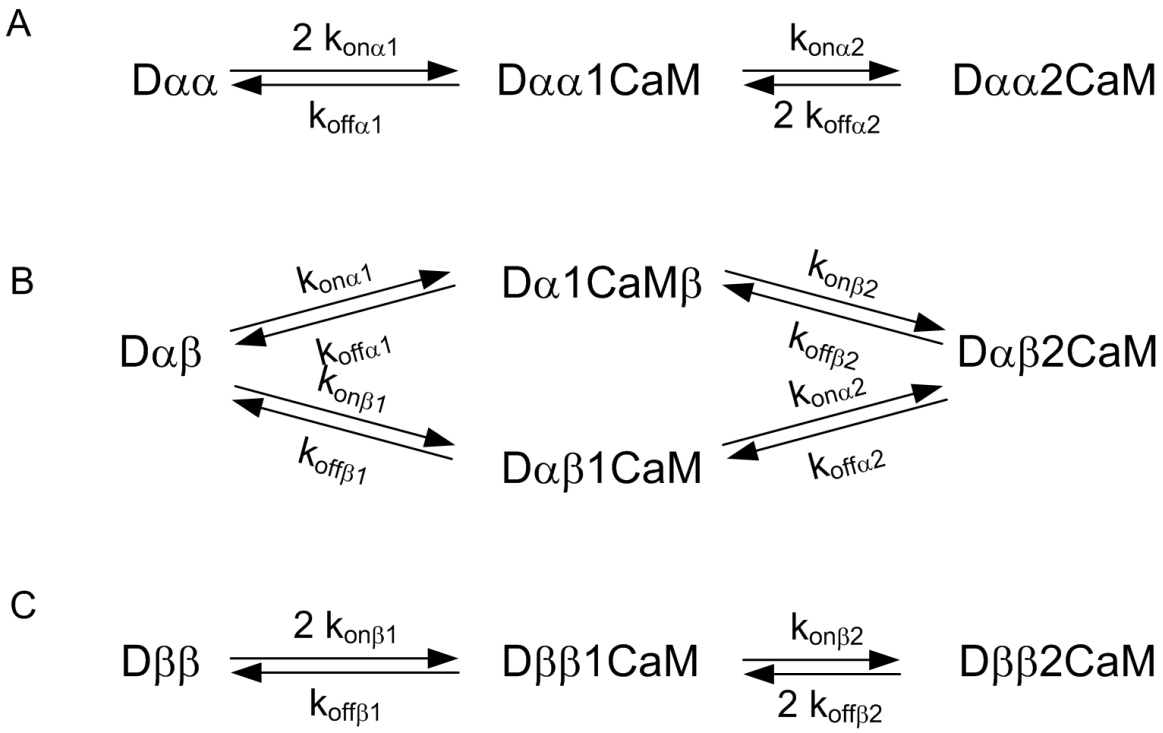

Figure 4.11. Cooperative binding of calmodulin to α, β and mixed CaMKII subunit pairs.

The probability for the β isoform is:

$$pring_{\beta} = \frac{1}{Dtot}\left(D\beta\beta 2CaM + \frac{1}{2}\left(D\beta\beta 1CaM + D\alpha\beta 1CaM + D\alpha\beta 2CaM\right)\right). \tag{4.6}$$

In the case of a pair autophosphorylation model, the probability of a CaMKII subunit with CaM bound to have an α-CaMKII subunit with CaM bound in the same pair is:

$$ppair_{\alpha} = \frac{D\alpha\alpha 2CaM + \frac{1}{2}D\alpha\beta 2CaM}{CaM_{bound}/2} \tag{4.7}$$

$$\begin{aligned} CaM_{bound} &= 2\left(D\alpha\alpha 2CaM + D\alpha\beta 2CaM + D\beta\beta 2CaM\right) + \\ &\quad + D\alpha\alpha 1CaM + D\alpha\beta 1CaM + D\alpha 1CaM\beta + D\beta\beta 1CaM, \end{aligned} \tag{4.8}$$

while for a β isoform it is:

relative rate($10^{-3}s^{-1}$)	ring r=1.6	ring r=6.4	ring r=160	pair r=1.6	pair r=6.4	pair r=160
rate for α at [CaM]=0.333μM	85.2	84.6	84.5	104.7	133.2	249
rate for β at [CaM]=0.333μM	231.4	229.9	224.6	283.4	359.2	659
rate for α at [CaM]=0.167μM	75.2	74.3	71.8	102.7	149.3	402
rate for β at [CaM]=0.167μM	87.2	86.2	82.6	118.9	172.6	460

Table 4.2. Predicted rates of autophosphorylation in conditions of limiting calmodulin. These rates are calculated so that they are directly comparable to the rates in column 3 of table 4.1.

$$ppair_{\beta} = \frac{D\beta\beta 2CaM + \frac{1}{2}D\alpha\beta 2CaM}{CaM_{bound}/2}. \tag{4.9}$$

The relation between these probabilities and the rates of autophosphorylation measured in chapter 4.3 are:

$$rate = probability \frac{k_p}{final fraction}, \tag{4.10}$$

where k_p is the autophosphorylation turnover number, the probability is either pring_{α}, pring_{β}, ppair_{α} or ppair_{β} and the corresponding measured final fractions are summarized in table 4.1

The initial rates of autophosphorylation, relative to autophosphorylation in saturating calmodulin, can be calculated directly from the reactions presented in fig 4.11. We used the parameters calculated in section 3.3.1.4 corresponding to figure 3.2 C and assumed the ratio between the affinity of β CaMKII and α CaMKII for calmodulin to be 3. The results of the simulations are summarized in table 4.2.

The measured rates for autophosphorylation of midbrain CaMKII are more consistent with CaMKII autophosphorylation occurring in pairs, and a relatively low cooperativity between CaMKII subunits in binding calmodulin.

4.6 Discussions

4.6.1 Comparison between Experimental and Simulated Values for the Hill Coefficient of CaMKII Autophsophorylation Dependence on Calmodulin Concentration

The dependence on calmodulin concentration of CaMKII autophosphorylation fraction after a fixed time has been measured in several studies (DeKoninck and Schulman, 1998; Gaertner et al., 2004). This dependence is particularly relevant if the time for autophosphorylation is on the same order of magnitude as the inverse of the autophosphorylation turnover number or if the concentration of CaMKII used is small compared to the K_d of CaMKII for calmodulin, in order to minimize the effects of calmodulin trapping. In the experimental setup used by DeKoninck and Schulman (1998, figure 3, A), CaMKII was immobilized and bound to a tube, and the calmodulin solution was refreshed, such that the concentration of free calmodulin remained constant. The time for autophosphorylation was 6s at 30^oC. In the experimental setup used by Gaertner et al. (2004, figure 6), the autophosphorylation reaction was performed for 15s at 0^oC.

The dependence on calmodulin concentration of CaMKII autophosphorylation fraction after a fixed time is generally fit with a Hill function. The measured Hill coefficients are close to 2. DeKoninck and Schulman (1998) have obtained for α- and β-CaMKII Hill coefficients of 1.6 ± 0.1 and 1.8 ± 0.1 respectively. Gaertner et al. (2004) have obtained for α-, β-, γ- and δ-CaMKII Hill coefficients of 1.9 ± 0.1, 2.4 ± 0.3, 1.7 ± 0.3 and 1.8 ± 0.3 respectively.

The values we obtained from simulations in the experimental conditions from DeKoninck and Schulman (1998) are consistent with CaMKII autophosphorylation in pairs, with a cooperativity coefficient similar to that obtained in section section 3.3.1.4 corresponding to figure 3.2 C. For the ring autophosphorylation model, all values of the cooperativity coefficient used in simulations result in Hill coefficients that are significantly different from the measured Hill coefficients.

4.6.2 Comparison between Experimental and Simulated Values for the Time Dependence of CaMKII Autophosphorylation in Conditions of Limiting Calmodulin

The two proposed models for autophosphorylation are difficult to distinguish if the cooperativity coefficient between CaMKII subunits in binding calmodulin is small. The value of 1.6 for the cooperativity coefficients which was predicted in chapter 3, makes it rather difficult but not impossible to make the distinction using purely autophosphorylation assays. One way to make the distinction is to perform phosphorylation assays in very low concentration of calmodulin (figure 4.8 B). However, performing experiments in such a low calmodulin concentration is rather difficult. In this work a slightly different experimental strategy was implemented. Compared to the dissociation constant, rather large calmodulin concentrations and even larger CaMKII concentrations were used. After partial autophosphorylation, the CaMKII which are autophosphorylated trap calmodulin, thus dropping the free calmodulin concentrations to the levels which make the two models distinguishable.

The experimental values for the autophosphorylation rates in limiting calmodulin are consistent with the simulated values if autophosphorylation occurs within pairs, and the cooperativity between a pair of CaMKII subunits in binding calmodulin is relatively small.

The measurements for autophosphorylation rates when the ratio [CaMKII]/[CaM] is 3 are significantly different than the simulated rate of autophosphorylation in rings for any cooperativity coefficient. When the ratio [CaMKII]/[CaM] is 6, the differences between the measured rates and the simulated rates of autophosphorylation in rings are not always significant, however the measured rates are still better predicted by simulated rates of autophosphorylation in pairs.

4.6.3 Does the Mechanism for Autophosphorylation Influence the Function of CaMKII?

All of the modeling efforts to date which include details of the mechanism for autophosphorylation have assumed that autophosphorylation is happening in rings. One area which was thoroughly explored is the possibility for CaMKII to have two autophosphorylation stable states when coupled to a phosphatase (Okamoto and Ichikawa, 2000; Zhabotinsky, 2000; Miller et al., 2005). One fundamental characteristic of the system that allows for this bistability to appear in models is the difference in the probability of the first autophosphorylation to happen, which requires two calmodulin bound, and the probabilities of subsequent autophosphorylations within a ring, which require only one bound calmodulin. After an initial autophosphorylation, the ability of autophosphorylation to continue easily to another 1 (pairs) or another 5 (rings) subunits significantly impacts the conditions under which CaMKII/phosphatase systems are bistable. Measuring the bistability experimentally is rather difficult since the rate of denaturation of CaMKII is higher when CaMKII is autophosphorylated, which can introduce a bias into measurements of autophosphorylation over long periods of time. One experimental setup designed to minimize this problem (Bradshaw et al., 2003) consisted of looking at CaMKII autophosphorylation at 0^oC. Bradshaw et al. (2003) did not observe bistability in their measurements; however, it is difficult to directly simulate their experiments since the dependence on temperature of all the parameters used in the model is not known. The influence of the exact mechanism of CaMKII autophosphorylation on its function has yet to be addressed.

An additional possible mechanism for autophosphorylation is that autophosphorylation happens both in rings and in pairs. This model is equivalent to a very high mobility for the catalytic domains of CaMKII subunits once the coiled-coil interaction of a dimer has been disrupted. In such a model, it is possible that the initial autophosphorylation events, while calmodulin is binding, to occur mainly in pairs, and the subsequent autophosphorylation events, happening after dephosphorylation,

to occur both in rings and pairs. This model, also, is consistent with our experimental results, since it would have very similar time dependence of autophosphorylation to the pair-only model.

Bibliography

J. M. Bradshaw, Y. Kubota, T. Meyer, and H. Schulman. An ultrasensitive Ca2+/calmodulin-dependent protein kinase II-protein phosphatase 1 switch facilitates specificity in postsynaptic calcium signaling. *Proc Natl Acad Sci U S A*, 100(18):10512–10517, Sep 2003. doi: 10.1073/pnas.1932759100. URL `http://dx.doi.org/10.1073/pnas.1932759100`.

P. DeKoninck and H. Schulman. Sensitivity of CaM kinase II to the frequency of Ca2+ oscillations. *Science*, 279(5348):227–230, Jan 1998.

T. R. Gaertner, S. J. Kolodziej, D. Wang, R. Kobayashi, J. M. Koomen, J. K. Stoops, and M. N. Waxham. Comparative analyses of the three-dimensional structures and enzymatic properties of alpha, beta, gamma and delta isoforms of Ca2+-calmodulin-dependent protein kinase II. *J Biol Chem*, 279(13):12484–12494, Mar 2004. doi: 10.1074/jbc.M313597200. URL `http://dx.doi.org/10.1074/jbc.M313597200`.

P. I. Hanson, T. Meyer, L. Stryer, and H. Schulman. Dual role of calmodulin in autophosphorylation of multifunctional CaM kinase may underlie decoding of calcium signals. *Neuron*, 12(5):943–956, May 1994.

S. J. Kolodziej, A. Hudmon, M. N. Waxham, and J. K. Stoops. Three-dimensional reconstructions of calcium/calmodulin-dependent (CaM) kinase IIalpha and truncated CaM kinase IIalpha reveal a unique organization for its structural core and functional domains. *J Biol Chem*, 275(19):14354–14359, May 2000.

Y. Kubota and J. M. Bower. Transient versus asymptotic dynamics of CaM kinase II: possible roles of phosphatase. *J Comput Neurosci*, 11(3):263–279, 2001.

T. Meyer, P. I. Hanson, L. Stryer, and H. Schulman. Calmodulin trapping by calcium-calmodulin-dependent protein kinase. *Science*, 256(5060):1199–1202, May 1992.

P. Miller, A. M. Zhabotinsky, J. E. Lisman, and X. J. Wang. The stability of a stochastic CaMKII switch: dependence on the number of enzyme molecules and protein turnover. *PLoS Biol*, 3(4):e107, Apr 2005. doi: 10.1371/journal.pbio.0030107. URL `http://dx.doi.org/10.1371/journal.pbio.0030107`.

S. G. Miller and M. B. Kennedy. Distinct forebrain and cerebellar isozymes of type II Ca2+/calmodulin-dependent protein kinase associate differently with the postsynaptic density fraction. *J Biol Chem*, 260(15):9039–9046, Jul 1985.

S. G. Miller and M. B. Kennedy. Regulation of brain type II Ca2+/calmodulin-dependent protein kinase by autophosphorylation: a Ca2+-triggered molecular switch. *Cell*, 44(6):861–870, Mar 1986.

E. P. Morris and K. Torok. Oligomeric structure of alpha-calmodulin-dependent protein kinase II. *J Mol Biol*, 308(1):1–8, Apr 2001. doi: 10.1006/jmbi.2001.4584. URL `http://dx.doi.org/10.1006/jmbi.2001.4584`.

H. Okamoto and K. Ichikawa. Switching characteristics of a model for biochemical-reaction networks describing autophosphorylation versus dephosphorylation of Ca2+/calmodulin-dependent protein kinase II. *Biol Cybern*, 82(1):35–47, Jan 2000.

O. S. Rosenberg, S. Deindl, R. J. Sung, A. C. Nairn, and J. Kuriyan. Structure of the autoinhibited kinase domain of CaMKII and SAXS analysis of the holoenzyme. *Cell*, 123(5):849–860, Dec 2005. doi: 10.029. URL `http://dx.doi.org/10.029`.

A. M. Zhabotinsky. Bistability in the Ca(2+)/calmodulin-dependent protein kinase-phosphatase system. *Biophys J*, 79(5):2211–2221, Nov 2000.

Chapter 5

Quantitative Model of Ca^{2+}/Calmodulin/CaMKII Interactions

5.1 Introduction

Calmodulin (CaM) is a ubiquitous and very abundant protein which meditates many second messenger actions of Ca^{2+}, and it is highly conserved among species. The crystal structure of Ca^{2+} loaded calmodulin shows two globular structures corresponding to amino (N) and carboxyl (C) terminus connected by an alpha helix (Babu et al., 1985), with a similar structure in solution (Heidorn and Trewhella, 1988).

Calmodulin has 4 Ca^{2+} binding sites on EF hands, two at the amino and two at the carboxyl terminus. Ca^{2+} binding had been shown to be cooperative between the two sites at each terminus, however not cooperative between the termini (Linse et al., 1991). Carboxyl terminus sites have a higher affinity for Ca^{2+} than the amino terminus ones however the carboxyl terminus sites have a slower on rate for binding Ca^{2+} table 5.1. Consequently, a fast, milliseconds long transient rise in Ca^{2+} concentration leads to binding of Ca^{2+} to the N lobe first, while a slow rise in Ca^{2+} concentration leads to binding of Ca^{2+} to the C lobe first.

A large number of proteins bind calmodulin in a Ca^{2+} dependent manner. The interaction is via a set of hydrophobic sites which are exposed by conformational

changes in calmodulin upon binding Ca^{2+}.

Ca^{2+} second messenger signaling results in many different behaviors. There is a great variety in the concentration, time course and degree of localization of Ca^{2+} signaling. It is possible that the downstream effectors are capable of deciphering not only the presence of Ca^{2+}, but changes in its time dependence and localization. One extreme example is Ca^{2+} signaling in dendritic spines of cortical pyramidal neurons where Ca^{2+} concentration raises by as much as 10μM for less than 100ms the signal being localized to a spine (Sabatini et al., 2002) with typical volumes of $0.3\mu m^3$.

When comparing measured peak Ca^{2+} concentrations during physiological stimulations (low μM) to the measured dissociation constants of Ca^{2+} from calmodulin, table 5.1, one would predict that calmodulin would very rarely have 4 Ca^{2+} bound. However, downstream effects of calmodulin mediated pathways are observed even at low Ca^{2+} concentrations, counter to the common assumption that calmodulin must have 4 bound Ca^{2+} to function.

Some of the possible ways to explain this apparent contradiction are:

1. the presence of calmodulin binding proteins which bind calmodulin in a Ca^{2+} dependent manner increase the apparent affinity of calmodulin for Ca^{2+},

2. calmodulin with less than 4 Ca^{2+} bound can bind to and activate the target proteins,

3. while the measured Ca^{2+} concentration is quite low, it represents an average Ca^{2+} concentration. Very close to Ca^{2+} sources there are nanodomains of considerable Ca^{2+} concentration which are too small to be measured. A strong colocalization of Ca^{2+} sources and with second messenger machinery can have an influence on average signaling output.

In this chapter I examine Ca^{2+}-dependent CaMKII activation in nonsaturating Ca^{2+} concentration by constructing a quantitative model of the interactions between Ca^{2+}, calmodulin and CaMKII. The goals of this work are:

1. to build a general model for Ca^{2+}/Calmodulin interaction with calmodulin binding proteins,

2. to calculate the model parameters for the case of Ca^{2+}/Calmodulin/CaMKII interaction and

3. to analyze the dependence of Ca^{2+} dependent activation of CaMKII on the parameters characterizing the Ca^{2+} transient.

5.2 Model

5.2.1 Sequential Binding Model of Calmodulin

A traditional way to model calmodulin is to characterize a state by the number of Ca^{2+} bound and to disregarding the exact binding sites of Ca^{2+} is bound to 5.1. This model is motivated by experiments measuring the average number of Ca^{2+} ions bound to a molecule of calmodulin as a function of Ca^{2+} concentration (Linse et al., 1991). This sequential binding model has 5 states and 4 equilibrium parameters: macroscopic binding constants. This model is not suitable to describe calmodulin behavior in time varying Ca^{2+} concentration since the higher affinity Ca^{2+} binding sites have a smaller on rate.

5.2.2 Approximations for Two Termini Model

Figure 5.1 B represents the two termini model of Ca^{2+} binding to calmodulin. In this model the states of calmodulin are characterized by the number of Ca^{2+} bound to each of the termini rather than the total number of Ca^{2+} bound.

- Approximation 1. If the conformational changes of calmodulin caused by Ca^{2+} binding/unbinding are much faster than Ca^{2+} binding/unbinding itself than each state in calmodulin model can be characterized by which of the Ca^{2+} binding sites have Ca^{2+} bound. NMR studies are the most suitable for kinetic measurements on the ms time scale. By comparing studies of 43Ca NMR which measure Ca^{2+} unbinding from calmodulin (Andersson et al., 1982) and 1H NMR which measure the conformational changes of calmodulin following by Ca^{2+}

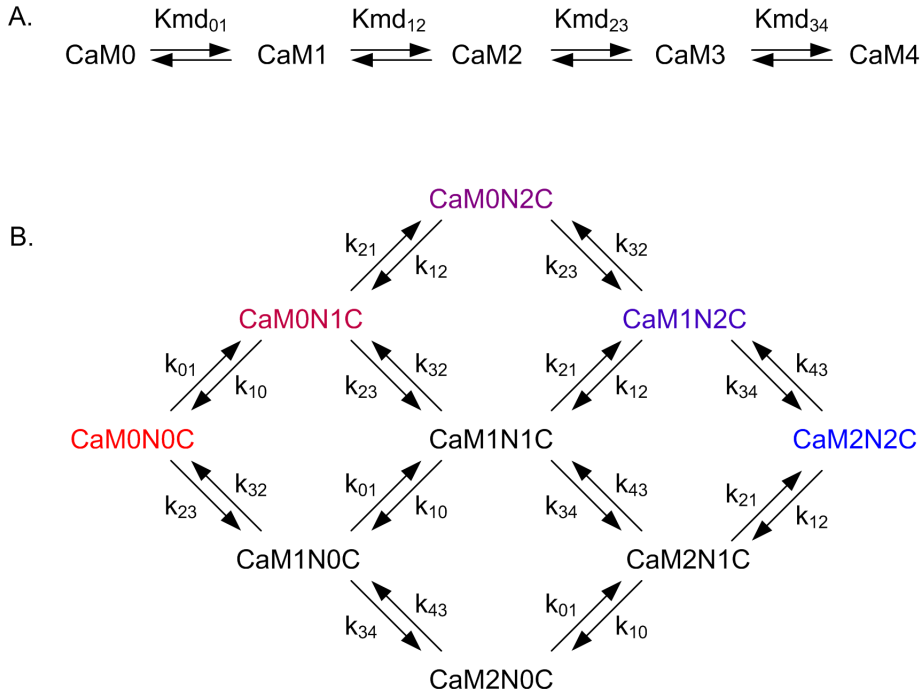

Figure 5.1. Models of Ca^{2+} binding to calmodulin. **A.** Sequential binding model. In this model a state of calmodulin is characterized by the number of Ca^{2+} ions bound. The dissociations constants Kmd_{01}, ..., Kmd_{34} are called macroscopic dissociation constants. The values for the macroscopic dissociation constants are obtained from Shifman et al. (2006). **B.** Two termini binding model. In this model a state of calmodulin is characterized by the number of Ca^{2+} ions bound to each of the calmodulin termini. The parameters of the model are called microscopic dissociation constants. Under the assumptions described in chapter 5.2.2, for the description of equilibrium binding, the two termini binding model has the same number of parameters as the sequential binding model. Consequently, the microscopic dissociation constants can be calculated from the macroscopic ones via the equations presented in chapter 5.2.3. The additional parameters for describing the microscopic on and off rates are obtained from (Persechini et al., 1996; Peersen et al., 1997; Brown et al., 1997). The obtained values are summarized in table 5.1

unbinding (Ikura et al., 1983) it can be estimated that the timescale of the conformational changes alone is smaller than 0.75ms. Since the downstream effects of calmodulin are on a much longer timescale than its conformational changes, the calmodulin states can be characterized by which of the Ca^{2+} binding sites have Ca^{2+} bound. Unbinding of Ca^{2+} from the amino terminus sites is on the same time scale so some of the calmodulin with 1 Ca^{2+} bound at the N lobe will still have the conformation of apocalmodulin. Additionally, some of the calmodulin with 0 Ca^{2+} bound, from which 1 Ca^{2+} recently unbound from the N lobe will still be in the conformation of CaM1N0C. These two states are presents in very low quantities, they do compensate each other and thus, they are not included in the model.

Using only approximation 1, a calmodulin model has 16 states and 32 equilibrium/64 dynamical parameters. A simple notation which can be used to denote these states is: CaM_{ijkl} with i, j, k, l $\in$0,1.

- Approximation 2. Binding of Ca^{2+} to amino terminus sites is not influenced by the occupancy of the carboxyl terminus Ca^{2+} binding sites and the reciprocal. This approximation is motivated by analysis of 3D structure which shows the two termini as distant globular structures linked by an alpha helix.

  Using approximation 1 and 2 the number of parameters in calmodulin model is reduced to 8 equilibrium or 16 dynamical parameters.

- Approximation 3.

  - The model does not distinguish between the two sites at the carboxyl terminus. The cooperativity between these two sites in binding Ca^{2+} comes from a change in the off rate only. This approximation will average the behavior of calmodulin with 1 Ca^{2+} bound to one of the two sites of the carboxyl terminus.
  - Additionally, the model does not distinguish between the two sites at the amino terminus. The cooperativity between these two sites in binding

Ca^{2+} is also assumed to come from a change in the off rate only.

This approximation is in part motivated by the high cooperativity between the two sites within each terminus which increase the affinity for Ca^{2+} of the second site making the 1 Ca^{2+} bound forms short lived.

Using approximations 1, 2 and 3 the two termini calmodulin model has 9 states and 4 equilibrium or 8 dynamical parameters 5.1 B.

The number of parameters used in two termini model (microscopic dissociation constants) is the same as the number of parameters used in the sequential binding model (macroscopic dissociation constants). However, two termini model keeps track how many of Ca^{2+} ions bound to calmodulin are bound at the amino and/or carboxyl termini.

5.2.3 Determination of the Microscopic Dissociation Constants

The microscopic dissociation constants are obtained from the characterized macroscopic dissociation constants by solving the following system of algebraic equations:

$$\left.\begin{array}{c} [CaM0] * [Ca^{2+}] = Kmd_{01} * [CaM1] \\ \vdots \end{array}\right\}$$

4 equations describing the macroscopic dissociation constant of Ca^{2+} from CaM corresponding to reactions in Fig 1.A

$$\left.\begin{array}{c} [CaM0] * [Ca^{2+}] = Kd_{01} * [CaM0N1C] \\ [CaM0] * [Ca^{2+}] = Kd_{23} * [CaM1N0C] \\ \vdots \end{array}\right\}$$

8 equations describing the microscopic dissociation constant of Ca^{2+} from CaM corresponding to reactions in Fig 1.B

	C, 1^{st} Ca^{2+}	C, 2^{nd} Ca^{2+}	N, 1^{st} Ca^{2+}	N, 2^{nd} Ca^{2+}
K_d (10^{-6} M)	9.94	1.47	38.5	7.43
k_{off} (s^{-1})	68	10	4150	800
k_{on} (10^6 $M^{-1}s^{-1}$)	6.8	6.8	108	108

Table 5.1. Parameters for Ca^{2+} binding/unbinding from calmodulin

$$\left.\begin{aligned}[CaM1N0C] + [CaM0N1C] = [CaM1] \\ \vdots\end{aligned}\right\} \quad \text{3 equations relating microscopic binding state to macroscopic binding states}$$

$$\left.\sum [CaMn] = [CaMtot]\right\} \quad \text{conservation of mass equation}$$

5.2.4 Values for Two Termini Calmodulin Model Parameters

The value for the macroscopic dissociation constants of Ca^{2+} from calmodulin are obtained from Shifman et al. (2006). The values for the microscopic dissociation constants are calculated from the macroscopic ones and summarized in table 5.1. Values for the dynamical parameters were obtained from Persechini et al. (1996); Peersen et al. (1997); Brown et al. (1997).

5.2.5 Model of Ca^{2+}/Calmodulin Interaction with a Calmodulin Binding Protein

Most of the calmodulin binding proteins bind calmodulin in a Ca^{2+} dependent manner. Calmodulin with less than 4 Ca^{2+} bound can bind to its target proteins. This has been concluded from experiments of calmodulin unbinding from its target proteins in the presence or absence of Ca^{2+} (Brown et al., 1997). It has been directly observed in the case of CaMKII (Shifman et al., 2006). This work focuses on the binding to CaMKII, however the same model can be used for calmodulin interaction with other binding partners. The model presented in figure 5.2 incorporates the two termini binding of Ca^{2+} to calmodulin from figure 5.1 B, into a Ca^{2+}/calmodulin/CaMKII

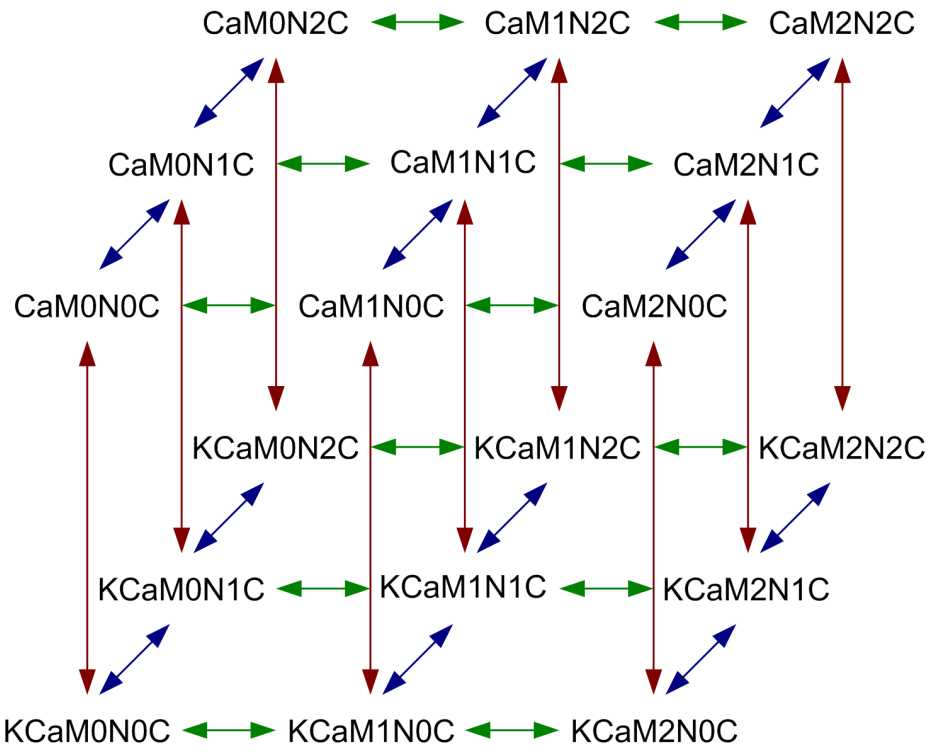

Figure 5.2. Model for simultaneous binding of Ca^{2+}, calmodulin and CaMKII. The top layer represents the binding of Ca^{2+} to calmodulin and is identical to figure 5.1 B. The blue arrows correspond to Ca^{2+} binding to the C-terminus of calmodulin while the green arrows correspond to Ca^{2+} to the N-terminus of calmodulin. The bottom layer represents Ca^{2+} binding to or unbinding from calmodulin when calmodulin is bound to CaMKII. KCaMnNmC with $n, m \in 0, 1, 2$ represent CaMnNmC bound to CaMKII. The red arrows represent the binding/unbinding

binding model in which every calmodulin state can bind to CaMKII.

5.2.6 Thermodynamic Constraint on Affinities

The change in free energy on a chemical reactions loop is 0. Thus every reaction loop imposes a constrain for the affinities of the reactants involved. One such constraint is exemplified for the loop: CaM2N2C - KCaM2N2C - KCaM1N2C - CaM1N2C -

CaM2N2C. The dissociation constants for these reactions are respectively:

$$\begin{aligned} Kd_{CaM2C2N} &= x_0 e^{\frac{G^0_{KCaM2C2N} - G^0_{CaM2C2N} - G^0_{CaMKII}}{RT}} \\ Kd_{34}/s4 &= x_0 e^{\frac{G^0_{KCaM2C2N} - G^0_{KCaM2C1N} - G^0_{Ca}}{RT}} \\ Kd_{CaM2C1N} &= x_0 e^{\frac{G^0_{KCaM2C1N} - G^0_{CaM2C1N} - G^0_{CaMKII}}{RT}} \\ Kd_{34} &= x_0 e^{\frac{G^0_{CaM2C2N} - G^0_{CaM2C1N} - G^0_{Ca}}{RT}}. \end{aligned} \tag{5.1}$$

The ratio between the affinity of Ca^{2+} for CaM2C1N to the affinity of Ca^{2+} for KCaM2C1N (CaM2C1N bound to CaMKII) is defined as cooperativity coefficient S4. These equations lead to:

$$Kd_{CaM2C1N} = \frac{Kd_{CaM2C2N} Kd34}{Kd34/s4} = s4 Kd_{CaM2C2N}. \tag{5.2}$$

Binding to CaMKII increases the affinity of CaM2C1N for Ca^{2+} by s4. Consequently the affinity for CaMKII of CaM2C1N compared to the affinity of CaM2C2N is decreased by the same factor s4. The equilibrium binding of Ca^{2+}/calmodulin/CaMKII can be characterized by the parameters for Ca^{2+} binding to calmodulin, the affinity of CaM2N2C for CaMKII and 4 cooperativity coefficients. Two of these coefficients characterize the increase in affinity of the N lobe of calmodulin for Ca^{2+} upon calmodulin binding to CaMKII. They also characterize the decrease in affinity of CaMKII for CaMnN2C (n$\in$0,1). The other two cooperativity coefficients characterize the increase in affinity of the C lobe for Ca^{2+}, and the decrease in affinity for CaM2NnC. The two cooperativity coefficients for a lobe are assumed to be equal.

5.3 Results

5.3.1 Obtaining Equilibrium Parameter Values for Ca^{2+}/Calmodulin/CaMKII Binding model

This model requires two sets of parameters: the affinities of Ca^{2+} for calmodulin (which are discussed in section 5.2.4) and the affinities of different states of calmodulin for CaMKII. The affinities of Ca^{2+} for calmodulin when calmodulin is bound to CaMKII can be obtained from the previous two sets of parameters via the method discussed in 5.2.6.

Shifman et al. (2006) measured the half activation of CaMKII by mutant calmodulins which mimic CaM2C0N and CaM0C2N. The half activation can not be directly extrapolated to an affinity since there are irreversible steps in CaMKII activation. Consequently, I used the model for autophosphorylation which was developed in chapter 4 to fit the raw data from the experiments looking at the CaMKII autophosphorylation after a fixed time in varying concentrations of calmodulin.

The fitting was done using an automatic parameter search algorithm. The automatic parameter search algorithm makes use of an error function which is the sum of the squared differences between experimental results and model prediction. The simplex method for gradient descent was preferred since it does not need calculations of derivatives and does not get stuck in local minima to often.

Using a simplified model for calmodulin binding, in which calmodulin binding to the two subunits in a pair are considered independent, and considering CaMKII autophosphorylation as happening in rings, the value for the affinity of CaM2C0N for CaMKII is 8.44 μM. The affinity of CaM0C2N is 16.67 μM.

Using the model for calmodulin binding and CaMKII autophosphorylation occurring in pairs the values for the affinities of the first and second mutant calmodulin binding to CaMKII were calculated. For CaM2C0N the dissociation constant for the first dissociation is 6.867 μM while for the second dissociation is 10.92 μM. This leads to an average dissociation of 8.66 μM. For CaM0C2N the dissociation constant for

the first dissociation is 13.67 μM while for the second dissociation is 21.74 μM. This leads to an average dissociation of 17.24 μM.

The difference between the two autophsophorylation models used in fitting the parameters for interactions between Ca^{2+}, calmodulin and CaMKII is relatively small. For the rest of the models the values for the cooperativity coefficients derived from the pair model of autophosphorylation were used.

5.3.2 Obtaining Dynamical Parameter Values for Ca^{2+}/Calmodulin/CaMKII Binding Model

To determine how much of the cooperativity comes from a change in on or off rates I used a simplified model for binding of calmodulin to CaMKII, in which the binding is solely characterized by the average affinity. The model was simultaneously fit to three sets of experiments from the literature using the simplex method for gradient descent for the automatic parameter search. During the parameter search all equilibrium constants and the on and off rates of Ca^{2+} for calmodulin were not varied, the search being done for the on and off components of the cooperativity coefficients alone. The measurements to which the model was fit are:

1. Ca^{2+} unbinding from Ca^{2+}/calmodulin/CaMKII (Gaertner et al., 2004b)
2. calmodulin unbinding from Ca^{2+}/calmodulin/CaMKII in saturating Ca^{2+} (Meyer et al., 1992; Singla et al., 2001)
3. calmodulin unbinding from Ca^{2+}/calmodulin/CaMKII in low Ca^{2+} (Meyer et al., 1992; Singla et al., 2001)

The error function used is sum over the 3 experiments of the integral to 1s of the squared difference between the model prediction and the experimental values.

$$Error(model) = \sum_{i=1}^{3} \left(\int_0^{1s} \left(experiment_i(t) - model_i(t) \right)^2 dt \right) \tag{5.3}$$

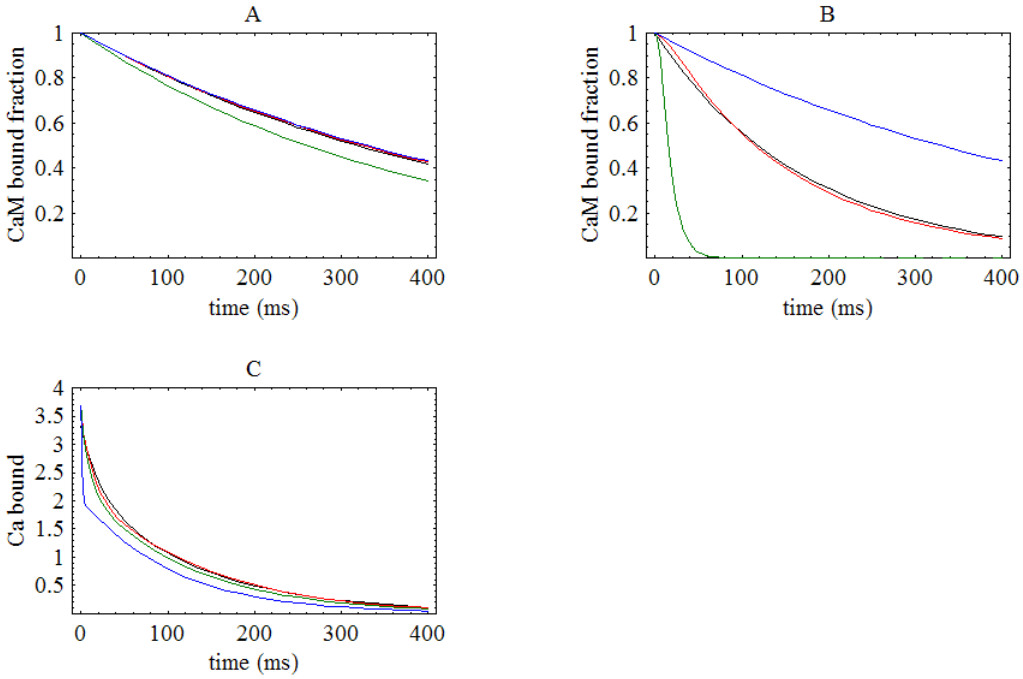

Figure 5.3. Comparing model predictions (red) with experimental results (black) in experiments of: **A.** calmodulin unbinding from Ca^{2+}/calmodulin/CaMKII in high Ca^{2+} (Meyer et al., 1992), **B.** calmodulin unbinding from Ca^{2+}/calmodulin/CaMKII in low Ca^{2+} (Meyer et al., 1992; Singla et al., 2001) and **C.** Ca^{2+} unbinding from Ca^{2+}/calmodulin/CaMKII (Gaertner et al., 2004b). The blue lines represent model predictions when all the cooperativity is assumed to come from a change in on rates, while the green lines represent model predictions when all the cooperativity is assumed to come from a change in off rates.

	C, 1^{st} Ca^{2+}	C, 2^{nd} Ca^{2+}	N, 1^{st} Ca^{2+}	N, 2^{nd} Ca^{2+}
K_d (μM)	0.746	0.110	4.07	0.79
k_off (s^{-1})	33	4.87	310	60
k_on ($\mu M^{-1}s^{-1}$)	44	44	76	76

Table 5.2. Parameters for Ca^{2+} binding/unbinding from calmodulin when calmodulin is bound to CaMKII

The automatic parameter search algorithm led to the unexpected result that the global minimum of the error function does not correspond to a change in the off rates only. Additionally there are no local minima close to the point corresponding to a change in off rates only. Both on and off rates changed, as shown in table 5.2.

It is interesting to remark that the increase in affinity for Ca^{2+} of calmodulin upon binding to CaMKII is done differently for the two lobes. The C terminus has a slow on and slow off rate; the increase in its affinity for Ca^{2+} is obtained via an increase in the on rate. The N terminus has a fast on and fast off rate and the increase in affinity is obtained by a decrease in the off rate. Consequently the two lobes will have more similar dynamics when calmodulin is bound to CaMKII compared to free calmodulin. The kinetic parameters for Ca^{2+} binding/unbinding from calmodulin when calmodulin is bound to CaMKII are summarized in table 5.2.

5.4 Discussions

5.4.1 Choice of Parameter Values

We used the values for the macroscopic dissociation constants of Ca^{2+} from calmodulin reported in (Shifman et al., 2006) since the measurements were done in solutions mostly resembling mammalian intracellular media. The dependence of calmodulin affinity for Ca^{2+} as a function of ionic strength has been precisely measured by (Linse et al., 1991), however the measurement was in the absence of Mg^{2+}. These data give similar values for the affinity of the first Ca^{2+} binding to each of the termini, however in the presence of Mg^{2+} the affinity for binding of the second Ca^{2+} is decreased. The same trend was observed by (Cohen and Klee, 1988, table 1,

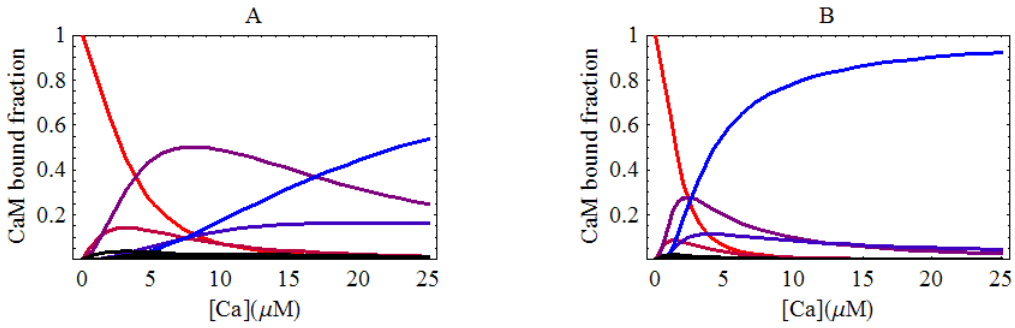

Figure 5.4. Equilibrium binding of Ca^{2+} to calmodulin in absence (**A**) or presence **B** of CaMKII. **A.** Equilibrium binding of Ca^{2+} to calmodulin using the two termini model. The color coding is the same as in figure 5.1 B; red represents calmodulin with 0 Ca^{2+} bound, blue represents calmodulin with 4 Ca^{2+} bound and violet represents calmodulin with 2 Ca^{2+} bound to the C lobe and 0 Ca^{2+} bound to the N lobe. **B.** Equilibrium binding of Ca^{2+} to 30 μM calmodulin in the presence of 30 μM CaMKII, conditions which are similar to those in the postsynaptic density. Each of the lines represent the sum between the fraction of a free calmodulin state and the corresponding calmodulin state bound to CaMKII. For example, the red line represents calmodulin with 0 Ca^{2+} bound, both free and bound to CaMKII.

page 37).

5.4.2 Calmodulin in Time-Invariant Ca^{2+}

The results for the two termini model for calmodulin in constant Ca^{2+} concentration are similar to those obtained from sequential binding model. The additional states in the two termini model reach their maximum value at 6 μM Ca^{2+} concentration and represent less than 8% of the total calmodulin (figure 5.4). Between 3.8 and 17 μM Ca^{2+} concentrations CaM0N2C is the prevalent state figure 5.4, panel A.

5.4.3 Influence on Ca^{2+} Binding to Calmodulin of the Presence of CaMKII

Since CaMKII binds to calmodulin in a Ca^{2+} dependent manner, the macroscopic binding of calmodulin to Ca^{2+} is influenced by the presence of CaMKII. The net result is an increase in the affinity of calmodulin for Ca^{2+}. As shown in figure 5.4, the concentration of Ca^{2+} at which half of calmodulin is in the 4 Ca^{2+} bound form

(CaM2N2C + KCaM2N2C) is 22.8 μM in the absence of CaMKII and 4.29 μM if 30 μM calmodulin are in the presence of 30 μM CaMKII.

5.4.4 Ca^{2+}/Calmodulin/CaMKII in Time-Varying Ca^{2+}

The observed time scale for Ca^{2+} transients in a spine is 10ms (from equation 1.1). That is one order of magnitude faster than the unbinding of Ca^{2+} from C terminus and one order of magnitude slower than the unbinding of Ca^{2+} from N terminus. Consequently the two termini will have very different behaviors under physiologically relevant Ca^{2+} transients. Since the subsequent biochemical steps generally have longer time scales than Ca^{2+} activation of calmodulin one of the most physiologically relevant outputs is the time integral of various calmodulin states during Ca^{2+} transients.

Because Ca^{2+} dissociation from the C terminus is slower than the Ca^{2+} transients, its activation is largely governed by the integral of Ca^{2+} concentration. Using square Ca^{2+} pulses of length varying between 8 and 16 ms and different Ca^{2+} concentrations between 5 and 25 μM both the maximum value and the time integral of CaM2C fraction varied linearly with the integral of the Ca^{2+} concentration in the pulse (r^2 value of 0.994) (figure 5.5 panel A).

The N terminus is faster than the Ca^{2+} transient, and thus its activation at a given time depends mainly on the Ca^{2+} concentration at that particular time. Using the same square Ca^{2+} pulses the maximal N terminus activation depends linearly on the maximal Ca^{2+} concentration in the pulse. The time integral of CaM2N fraction varied linearly with the integral of the Ca^{2+} concentration in the pulse as well (r^2 being 0.988) (figure 5.5 panel B). The approximately linear dependence depends on the values of maximal Ca^{2+} concentration and is a result of partial compensation of cooperativity Ca^{2+} binding with saturation of calmodulin. It holds only for Ca^{2+} pulses with peak values in the 5-15 μM range and durations much longer than 1ms and much shorter than 100ms. It is a very limited range however it encompasses some of the physiologically relevant stimuli.

An interesting aspect is that both termini respond linearly with the integral of

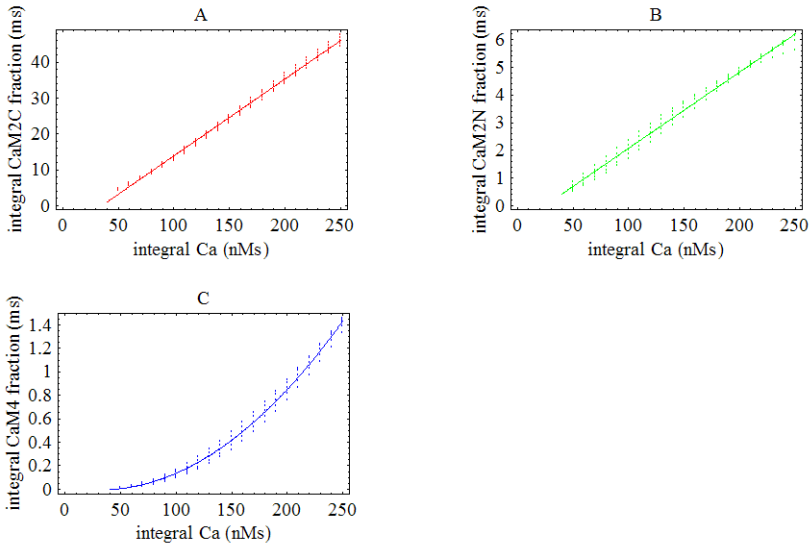

Figure 5.5. Formation of different calmodulin states as a result of one Ca^{2+} pulse with different maximum Ca^{2+} concentrations and different pulse durations. On the vertical axis is the integral of the fraction of a calmodulin state. On the horizontal axis is the integral of the Ca^{2+} concentration during a stimulation. **A** CaM2C, **B** CaM2N and **C** CaM4 fractions.

Ca^{2+} concentration during a pulse, making the integral of CaM4 have a quadratic dependence on integral of Ca^{2+} concentration during a pulse (r^2 being 0.987) (figure 5.5 panel C).

The dependence of Ca^{2+} activation of CaMKII under the same time dependence of Ca^{2+} concentration is presented if figure 5.6. When the frequency of the stimulation is maintained constant, Ca^{2+}-dependent activation of CaMKII depends mainly on the integral of the Ca^{2+} concentration during the stimulation.

Next, the dependence of Ca^{2+}-dependent activation of CaMKII on the frequency of Ca^{2+} stimulation was analyzed.

The formation of calmodulin with two Ca^{2+} bound at either the C or the N lobe depends little on the frequency of Ca^{2+} transients. Calmodulin with two Ca^{2+} bound to the N lobe forms rapidly after a Ca^{2+} transient onset, and decays rapidly after a Ca^{2+} transient offset. Calmodulin with two Ca^{2+} bound to the C lobe forms slowly during a Ca^{2+} transient onset, and outlasts the Ca^{2+} transient offset by approximately 100ms. Consequently, the formation of four Ca^{2+} bound calmodulin depends on Ca^{2+}

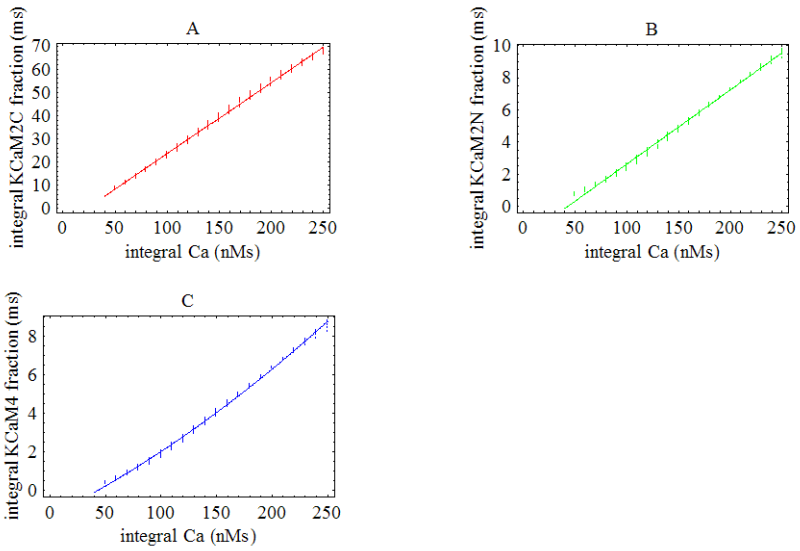

Figure 5.6. Formation of different calmodulin states bound to CaMKII as a result of one Ca^{2+} pulse with different maximum Ca^{2+} concentrations and different pulse durations. On the vertical axis is the integral of the fraction of a calmodulin state bound to CaMKII. On the horizontal axis is the integral of the Ca^{2+} concentration during a stimulation. **A** KCaM2C, **B** KCaM2N and **C** KCaM4 fractions.

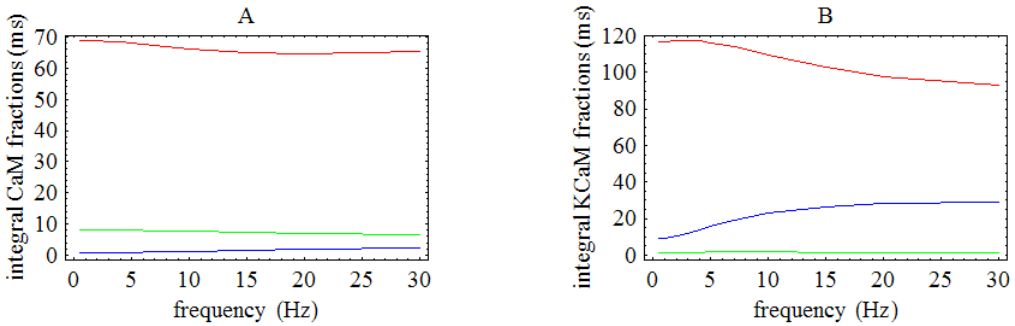

Figure 5.7. **A** Integral of CaM2N0C (green), CaM0N2C (red), CaM2N2C (blue) resulting from a stimulation with 5 Ca^{2+} pulses of 10ms duration and 10μM amplitude. **B** Integral of KCaM2N0C (green), KCaM0N2C (red), KCaM2N2C (blue) resulting from a stimulation with 5 Ca^{2+} pulses of 10ms duration and 10μM amplitude when 30μM calmodulin and 30μM CaMKII are present.

transients frequency. If the period is considerably longer than 100ms there is little overlap between the formation of CaM2N from one Ca^{2+} pulse with the formation of CaM2C from the previous Ca^{2+} pulse. If the period is considerably shorter than 100ms, formation of CaM2N from one Ca^{2+} pulse strongly overlaps with the formation of CaM2C from the previous Ca^{2+} pulse. Thus, changes in frequency around 10Hz have the most impact in formation of CaM2N2C. This behavior is enhanced and slightly shifted to lower frequencies by the presence of CaMKII. In figure 5.7 B, the integral of KCaM2N2C changes little below 2Hz or above 20Hz, and changes by a factor of 3 between 2Hz and 20Hz.

In summary, using quantitative models for interactions between Ca^{2+}, calmodulin and CaMKII I find that the Ca^{2+}-dependent activation of CaMKII is largely determined by the integral of Ca^{2+} concentration and the frequency of Ca^{2+} stimulation.

5.4.5 Conclusions

This work has largely focused on developing physiologically realistic models to aid in our understanding of CaMKII activation in dendritic spines.

One parameter that is critical for CaMKII activation is the turnover number of CaMKII autophosphorylation. Its reported values in the literature differ by a factor of 20. In chapter 2, by developing a new experimental method to rapidly stop the autophosphorylation reaction, I measured this parameter directly. Additionally, this is the first study to measure the autophosphorylation turnover number of CaMKII when it is activated by calmodulin with less than 4 Ca^{2+} ions bound.

Previous models of CaMKII activation assumed that binding of calmodulins to individual CaMKII subunits is independent. Independent binding is supported by experiments measuring phosphorylation of an exogenous substrate as a function of calmodulin concentration (Gaertner et al., 2004a). However, a recent structure of CaMKII (Rosenberg et al., 2005) suggests that its subunits cooperate in binding calmodulin. In chapter 3, I constructed a model for calmodulin binding to CaMKII in which CaMKII subunits cooperate in binding calmodulin. I used data from

the literature to fit the parameters for this model. The model reconciled previous experimental results from the literature that appeared contradictory.

Previous detailed models of CaMKII activation assumed that autophosphorylation occurs within a ring of 6 subunits. The recently determined structure of the CaMKII catalytic region (Rosenberg et al., 2005) raises the possibility that the autophosphorylation instead occurs within pairs of subunits. I constructed two models for CaMKII autophosphorylation, in which autophosphorylation can occur either in rings or pairs. I used these models and experimental data from the literature to predict which of the two autophosphorylation mechanisms occurs in a CaMKII holoenzyme. Additionally, I used these models to design experiments aimed at differentiating between these possibilities. Previously published measurements and the measurements that I performed are more consistent with autophosphorylation occurring within pairs.

In chapter 5, I constructed a detailed model for simultaneous interactions among Ca^{2+}, calmodulin and CaMKII. I used my experimental results, several other reported experimental results, and an automatic parameter search algorithm to fit the parameters for this model. This model can be used to explain quantitatively why CaMKII activation occurs in Ca^{2+} concentrations smaller than previously expected (Shifman et al., 2006). I used this model to characterize which of the parameters of Ca^{2+} transients are critical for CaMKII activation.

This modeling work can be continued to be used to design experiments focused at further narrowing down some of the parameters in the model. It can be integrated into more realistic models of dendritic spines in which both spatial and temporal aspects of Ca^{2+} second messenger signaling may be explored in greater detail.

Bibliography

T. Andersson, T. Drakenberg, S. Forsn, and E. Thulin. Characterization of the Ca2+ binding sites of calmodulin from bovine testis using 43Ca and 113Cd NMR. *Eur J Biochem*, 126(3):501–505, Sep 1982.

Y. S. Babu, J. S. Sack, T. J. Greenhough, C. E. Bugg, A. R. Means, and W. J. Cook. Three-dimensional structure of calmodulin. *Nature*, 315(6014):37–40, 1985.

S. E. Brown, S. R. Martin, and P. M. Bayley. Kinetic control of the dissociation pathway of calmodulin-peptide complexes. *J Biol Chem*, 272(6):3389–3397, Feb 1997.

P. Cohen and C. B. Klee. *Calmodulin*. Elsevier, 1988.

Tara R Gaertner, Steven J Kolodziej, Dan Wang, Ryuji Kobayashi, John M Koomen, James K Stoops, and M. Neal Waxham. Comparative analyses of the three-dimensional structures and enzymatic properties of alpha, beta, gamma and delta isoforms of Ca2+-calmodulin-dependent protein kinase II. *J Biol Chem*, 279(13):12484–12494, Mar 2004a. doi: 10.1074/jbc.M313597200. URL `http://dx.doi.org/10.1074/jbc.M313597200`.

Tara R Gaertner, John A Putkey, and M. Neal Waxham. RC3/Neurogranin and Ca2+/calmodulin-dependent protein kinase II produce opposing effects on the affinity of calmodulin for calcium. *J Biol Chem*, 279 (38):39374–39382, Sep 2004b. doi: 10.1074/jbc.M405352200. URL `http://dx.doi.org/10.1074/jbc.M405352200`.

D. B. Heidorn and J. Trewhella. Comparison of the crystal and solution structures of calmodulin and troponin C. *Biochemistry*, 27(3):909–915, Feb 1988.

M. Ikura, T. Hiraoki, K. Hikichi, T. Mikuni, M. Yazawa, and K. Yagi. Nuclear magnetic resonance studies on calmodulin: calcium-induced conformational change. *Biochemistry*, 22(10):2573–2579, May 1983.

S. Linse, A. Helmersson, and S. Forsn. Calcium binding to calmodulin and its globular domains. *J Biol Chem*, 266(13):8050–8054, May 1991.

T. Meyer, P. I. Hanson, L. Stryer, and H. Schulman. Calmodulin trapping by calcium-calmodulin-dependent protein kinase. *Science*, 256(5060):1199–1202, May 1992.

O. B. Peersen, T. S. Madsen, and J. J. Falke. Intermolecular tuning of calmodulin by target peptides and proteins: differential effects on Ca2+ binding and implications for kinase activation. *Protein Sci*, 6(4):794–807, Apr 1997.

A. Persechini, H. D. White, and K. J. Gansz. Different mechanisms for Ca2+ dissociation from complexes of calmodulin with nitric oxide synthase or myosin light chain kinase. *J Biol Chem*, 271(1):62–67, Jan 1996.

Oren S Rosenberg, Sebastian Deindl, Rou-Jia Sung, Angus C Nairn, and John Kuriyan. Structure of the autoinhibited kinase domain of CaMKII and SAXS analysis of the holoenzyme. *Cell*, 123(5):849–860, Dec 2005. doi: 10.029. URL `http://dx.doi.org/10.029`.

Bernardo L Sabatini, Thomas G Oertner, and Karel Svoboda. The life cycle of Ca(2+) ions in dendritic spines. *Neuron*, 33(3):439–452, Jan 2002.

J. M. Shifman, M. H. Choi, S. Mihalas, S. L. Mayo, and M. B. Kennedy. Activation of Ca2+ /calmodulin-dependent protein kinase II by computationally designed mutant calmodulins. *in press*, .:., 2006.

S. I. Singla, A. Hudmon, J. M. Goldberg, J. L. Smith, and H. Schulman. Molecular characterization of calmodulin trapping by calcium/calmodulin-dependent

protein kinase II. *J Biol Chem*, 276(31):29353–29360, Aug 2001. doi: 10.1074/jbc.M101744200. URL http://dx.doi.org/10.1074/jbc.M101744200.